UNIVERSITÀ
DEGLI STUDI
DI PADOVA

Sede Amministrativa: Università degli Studi di Padova

Dipartimento di Scienze Biomediche

CORSO DI DOTTORATO DI RICERCA IN: SCIENZE BIOMEDICHE SPERIMENTALI
CICLO XXX

Relationships between mitochondrial [Ca^{2+}] and ROS in experimental model of cardiac disease

Coordinatore: Ch.mo Prof. Paolo Bernardi
Supervisore: Ch.mo Prof. Fabio Di Lisa
Co-Supervisore: Dr. Nina Kaludercic

Dottorando: Salvatore Antonucci

INDEX

1 ABBREVIATIONS

$[Ca^{2+}]_I$	Intracellular Ca^{2+}
2-DG	2-deoxy-D-glucose
A/R	Anoxia/Reoxygenation
AKT (PKB)	Protein Kinase B
AlClPc	Aluminium Phthalocyanine Chloride
AP	Action Potential
ATP	Adenosine Triphosphate
BrdU	5-Bromo-2-Deoxyuridine
CaM	Calmodulin
CaMKII	Ca^{2+}/CaM-dependent protein kinase II
CASQ2	Calsequestrin-2
CDI	Ca^{2+}-dependent Inactivation
CICR	Ca^{2+}-induced Ca^{2+} release
CsA/H	Cyclosporin A / Cyclosporin H
CypD	Cyclophilin D
DCM	Diabetic Cardiomyopathy
DMEM	Dulbecco's modified Eagle's medium
DMSO	Dimethyl Sulfoxide
ECC	Excitation-Contraction Coupling
ETC	Electron Transport Chain
FAD	Flavin Adenine Dinucleotide
FBS	Fetal Bovine Serum
FCCP	Carbonyl cyanide-p-trifluoromethoxyphenylhydrazone
Glut II	Glucose Transporter Type II
Gpx1-4	Glutathione Peroxidase 1-4
GSIS	Glucose Stimulated Insulin Secretion
GSK-3β	Glycogen Synthase Kinase-3β
H_2O_2	Hydrogen Peroxide
HBSS	Hank's Balanced Salt Solution
HIF	Hypoxia-Inducible Factor
HLA	Human Leukocyte Antigen
HNE	Hydroxynonenal
I/R	Ischemia/Reperfusion

IL-1β	Interleukin-1β
IMM/OMM	Inner/Outer Mitochondrial Membrane
iPC	Ischemic Preconditioning
K_{ATP}	ATP-sensitive K^+ channels
LDH	Lactate Dehydrogenase
LTCCs	L-Type Ca^{2+} Channels
LV	Left Ventricle
MAOs	Monoamine Oxidases
MCU	Mitochondrial Calcium Uniporter
MCU OE	MCU Overexpression
MDR	Multidrug Resistance
MEM	Minimum Essential Medium
MFRTA	Mitochondrial Free Radical Theory of Aging
Mito/CytoHyPer	p-HyPer-dMito / p-HyPer-dCyto
MitoPQ	Mitochondrial Paraquat
MnSOD	Mn^{2+}-Superoxide Dismutase
MPG	N-(2-Mercaptoproprionyl)glycine
MsrA	Methionine Sulfoxide Reductase A
MTR	MitoTracker Red CM-H_2XRos
NCXs	Na^+/Ca^{2+} exchangers
NEAA	Non-Essential Amino Acids
NG/HG/HM	Normal Glucose / High Glucose / High Mannitol
NOX	NADPH Oxidase
Nrf2	Nuclear Factor Erythroid-2
NRVMs	Neonatal Rat Ventricular Myocytes
OxPhox	Oxidative Phosphorylation
P/S	Penicillin/Streptomycin
PI3K	Phosphatidylinositol 3-Kinase
PKA/PKC	Protein Kinase A / Protein Kinase C
PKC-ε	Ca^{2+}-dependent Protein Kinase C ε
PLN	Phospholamban
PMCAs	Plasma Membrane Ca^{2+} ATPases
Prx3	Peroxiredoxin3
PTEN	Phosphatase and Tensin Homolog
PTMs	Post Translational Modifications

PTP	Permeability Transition Pore
RISK	Reperfusion Injury Salvage Pathway
ROI	Region of Interest
ROS	Reactive Oxygen Species
RyRs	Ryanodine Receptors
SERCAs	Sarcoplasmic/Endoplasmic Reticulum Ca^{2+} ATPases
SR/ER	Sarcoplasmic Reticulum / Endoplasmic Reticulum
T1D/T2D	Type 1 diabetes / Type 2 diabetes
TAC	Transverse Aortic Constriction
TEA	Tetra Ethyl Ammonium chloride
Tg	Thapsigargin
TMRM	Tetramethylrhodamine
TnC/I	Troponin C / Troponin I
TPP	Triphenylphosphonium
Trx	Thioredoxin
T-tubules	Transverse Tubules
UCP2	Mitochondrial Uncoupling Protein 2
VDCCs	Voltage-Gated Ca^{2+} Channels
WT	Wild Type
$\Delta\Psi m$	Mitochondrial Membrane Potential

2 SOMMARIO

Variazioni dell'omeostasi del $[Ca^{2+}]$ ($[Ca^{2+}]_I$) intracellulare, disfunzione mitocondriale e specie reattive dell'ossigeno (ROS) sono generalmente interconnessi. Di conseguenza, è difficile stabilire una sequenza di eventi e relazioni di causa ed effetto. Per esempio, un aumento di $[Ca^{2+}]_I$ influenza il $[Ca^{2+}]$ mitocondriale e, in molti casi, è associato con un aumento di ROS mitocondriali che portano all'apertura del poro di transizione mitocondriale (PTP), disfunzione mitocondriale e morte cellulare. D'altro canto, i ROS modificano l'omeostasi del $[Ca^{2+}]_I$ interagendo con vari siti coinvolti nei flussi di Ca^{2+} intracellulari. I cambiamenti indotti dal $[Ca^{2+}]_I$ sulla formazione dei ROS e viceversa sono molto rapidi, rendendo difficile definire l'evento primario sia in seguito sia ad un evento fisiologico che ad un evento patologico.

I ROS sono prodotti in vari siti intracellulari e nei cardiomiociti i mitocondri sono il compartimento a più alto potenziale ossidoriduttivo. I mitocondri sono molto sensibili all'ossidazione, rappresentando sia una fonte che un bersaglio dei ROS. Tuttavia gli enzimi responsabili per la formazione dei ROS mitocondriali in condizioni patofisiologiche sono ancora motivo di discussione. Un'ulteriore complicazione è legata alle tecniche disponibili. Mentre esistono vari metodi per indurre un aumento primario e diretto di $[Ca^{2+}]_I$, i protocolli esistenti per innescare una produzione di ROS sono tutt'altro che specifici. Un aumento di ROS è in genere ottenuto come conseguenza della somministrazione di un ossidante esogeno (soprattutto H_2O_2) o applicando stimoli patologici (i.e. inibizione della catena respiratoria) che innescano inevitabilmente diversi altri effetti, incluse alterazioni nell'omeostasi del $[Ca^{2+}]_I$. In questo lavoro ci poniamo come obiettivo la risoluzione di questi problemi valutando gli effetti di un aumento primario dose-dipendente dei livelli di ROS mitocondriali sulla fisiologia cellulare, specialmente in cardiomiociti neonatali di ratto (NRVMs).

Per indurre un aumento primario dei livelli di ROS mitocondriali, abbiamo trattato i NRVMs con un analogo del paraquat diretto ai mitocondri (Mitochondrial Paraquat, MitoPQ). Questo composto si accumula selettivamente nella matrice mitocondriale e provoca la formazione di ROS per mezzo di un meccanismo ossidoriduttivo che coinvolge il complesso flavinico del complesso I della catena di trasporto degli elettroni (ETC). Inizialmente, abbiamo stabilito una curva dose-risposta con dosi diverse di

MitoPQ valutando la formazione di ROS, la funzione mitocondriale e la funzione della cellula. Abbiamo osservato che cellule trattate con alte dosi di MitoPQ mostravano un aumento dose-dipendente dei livelli di ROS mitocondriali. Alti dosaggi hanno portato ad una diminuzione del potenziale di membrana mitocondriale ($\Delta\Psi m$), apertura del PTP, omeostasi citosolica del [Ca^{2+}] compromessa e morte cellulare.

Successivamente, ci siamo chiesti se alte dosi di MitoPQ potessero innescare vie di segnalazione mitocondriali coinvolte nella formazione dei ROS. Ci siamo focalizzati sull'attività delle monoammino ossidasi (MAOs) che sono state recentemente identificate come contribuenti dello stress ossidativo nelle patologie cardiache. L'inibizione della MAO ha prevenuto la formazione di ROS indotta dal MitoPQ, così come la disfunzione mitocondriale e la morte cellulare. Oltre a questa via di amplificazione, questi risultati forniscono la prova diretta che i ROS prodotti nei mitocondri possono influenzare i processi citosolici, specialmente l'omeostasi del $[Ca^{2+}]_I$.

L'interazione tra Ca^{2+}, ROS e funzione mitocondriale ha un ruolo essenziale nella cardiomiopatia diabetica (DCM). Pertanto abbiamo esteso i risultati ottenuti con il MitoPQ, specialmente l'amplificazione indotta dalla MAO e l'alterazione dell'omeostasi del $[Ca^{2+}]_I$ indotta dai ROS mitocondriali, a un modello cellulare di DCM. NRVMs trattati con alti livelli di glucosio (HG) e interleuchina-1β (IL-1β) hanno manifestato un aumento significativo di livelli di H_2O_2 mitocondriale, sia dopo un trattamento prolungato (48 h) che breve (1 h). L'inibitore della MAO pargilina ha prevenuto questo aumento dei livelli di ROS. Quindi, abbiamo testato l'effetto dell'inibizione della MAO sull'omeostasi del [Ca^{2+}] citosolico in cellule trattate con il protocollo diabetico. Sorprendentemente, HG e IL-1β non hanno modificato significativamente i parametri oscillatori del Ca^{2+} (i.e. ampiezza, frequenza, area sotto la curva), mentre il pretrattamento con la pargilina o con la N-(2-Mercaptopropionil)glicina (MPG) ha peggiorato il difetto di contrattilità indotto da HG e IL-1β, compromettendo le oscillazioni. Questo risultato inaspettato suggerisce che un tono ossidativo di base sia necessario per un appropriato riciclo del Ca^{2+} in cardiomiociti trattati con HG e IL-1β.

Bisogna sottolineare che il diabete è correlato alla disfunzione delle β cellule pancreatiche. Nelle β cellule pancreatiche è stato dimostrato che lievi scariche di ROS contribuiscono all'omeostasi del $[Ca^{2+}]_I$ e la secrezione di insulina dipendente dal Ca^{2+}.

Nonostante nel diabete un marcato stress ossidativo conduca alla disfunzione delle β cellule, un aumento primario e moderato di ROS potrebbero modulare i transienti di Ca^{2+} promuovendo la secrezione di insulina. Abbiamo testato quest'ipotesi sulle β cellule Min6, una linea cellulare di insulinoma che può essere usata come modello di diabete applicato alle β cellule pancreatiche. Abbiamo innescato un aumento di livello di ROS intracellulari trattando le Min6 con alluminio ftalocianina cloruro (AlClPc), un fotosensitizzatore comunemente usato in terapia fotodinamica. La fotoattivazione dell'AlClPc induce cambiamenti chimici nelle molecole circostanti inducendo la produzione di ROS in quantità dipendente dall'intensità dell'illuminazione del LED. I risultati ottenuti hanno evidenziato che la modulazione dei ROS indotta dalla fotoattivazione dell'AlClPc o l'inibizione della pompa Calcio/ATPasi del reticolo endoplasmico (SERCA) per mezzo della tapsigargina (Tg) hanno indotto una simile accelerazione delle oscillazioni di Ca^{2+}, suggerendo che un aumento primario e controllato dei livelli di ROS citosolici modificano ma non bloccano le oscillazioni di Ca^{2+} modulando la SERCA.

I nostri dati mostrano che bassi livelli di ROS mitocondriali modulano leggermente l'omeostasi di $[Ca^{2+}]_I$ senza interferire con la funzione mitocondriale e citosolica. Abbiamo usato quest'informazione per studiare se la sovraespressione del trasportatore di Ca^{2+} mitocondriale (MCU) potesse modificare la formazione di ROS mitocondriali e conseguentemente la sopravvivenza mitocondriale e cellulare dei cardiomiociti. Cellule sovraesprimenti MCU hanno mostrato un aumento nei livelli di ROS che era correlato causalmente ad un aumento della tolleranza al danno da anossia/riossigenazione (A/R) in un processo che ha coinvolto l'attivazione di AKT. Queste scoperte dimostrano che un leggero aumento della formazione di ROS mitocondriali produce un effetto protettivo. Per testare quest'ipotesi, abbiamo studiato se i ROS mitocondriali indotti da basse dosi di MitoPQ potessero diminuire la suscettibilità al danno da A/R. Non solo quest'ipotesi è stata verificata, ma anche in questo caso la protezione è stata attribuita all'attivazione di AKT.

I dati di questo lavoro dimostrano che la formazione di ROS mitocondriali può innescare un ampio spettro di risposte con una chiara separazione tra livelli di ROS richiesti per evocare effetti benefici o dannosi. Cambiamenti nell'omeostasi del $[Ca^{2+}]_I$ possono essere a monte ma anche a valle della formazione dei ROS mitocondriali e

l'effetto cardioprotettivo collegato al leggero aumento dei livelli di ROS mitocondriali sembra dipendere dall'attivazione di AKT.

3 SUMMARY

Changes in intracellular [Ca^{2+}] ([Ca^{2+}]$_I$) homeostasis, mitochondrial dysfunction and reactive oxygen species (ROS) are generally intertwined. Therefore, it is difficult to establish sequence of events and causal relationships. For instance, an increase in [Ca^{2+}]$_I$ affects mitochondrial [Ca^{2+}] and in most cases it is associated with an increased mitochondrial ROS formation, leading to the opening of the permeability transition pore (PTP), mitochondrial dysfunction and cell death. On the other hand, ROS modify [Ca^{2+}]$_I$ homeostasis by acting at various sites involved in intracellular Ca^{2+} fluxes. The changes induced by [Ca^{2+}]$_I$ on ROS generation and vice versa are very rapid, making it difficult to elucidate the primary event under both physiological and pathological conditions.

ROS are produced at several intracellular sites, and in cardiac myocytes mitochondria are the most redox-active compartment. Mitochondria are very susceptible to oxidation, representing both a source and a target of ROS. Although the enzymes responsible for mitochondrial ROS formation under physiopathological conditions are still a matter of investigation. An additional matter of complexity is related to available techniques. While various methods are available to induce a primary and direct rise in [Ca^{2+}]$_I$, the existing protocols to trigger ROS production are far from being specific. An increase in ROS is generally obtained as a consequence of the exogenous administration of an oxidant (mostly H_2O_2) or by applying pathological stimuli (i.e., respiratory chain inhibition) that inevitably trigger several other effects, including alterations in [Ca^{2+}]$_I$ homeostasis. Here we aimed at solving these issues by evaluating the effects of a primary dose-dependent increase in mitochondrial ROS levels on cell physiology, especially in neonatal rat ventricular myocytes (NRVMs).

In order to induce a primary increase in mitochondrial ROS levels, we treated NRVMs with a paraquat analogue targeted to mitochondria (Mitochondrial Paraquat, MitoPQ). This compound accumulates selectively in the mitochondrial matrix and elicits ROS formation by means of redox cycling at the flavin site of Complex I of the electron transport chain (ETC). Initially, we established a dose-response curve with different doses

of MitoPQ by evaluating ROS formation, mitochondrial function and cell function. We observed that cells exposed to high doses of MitoPQ displayed a dose-dependent increase in mitochondrial ROS levels. High doses led to decreased mitochondrial membrane potential ($\Delta\Psi m$), PTP opening, impaired cytosolic [Ca^{2+}] homeostasis and cell death.

Subsequently, we wondered whether high doses of MitoPQ could trigger mitochondrial pathway involved in ROS formation. We focused our attention on the activity of monoamine oxidases (MAOs) that have been recently shown to contribute to oxidative stress in cardiac diseases. MAO inhibition prevented MitoPQ-induced ROS formation along with mitochondrial dysfunction and cell death. Besides this amplification pathway, these findings provide the direct evidence that ROS produced within mitochondria can affect cytosolic processes and especially $[Ca^{2+}]_I$.

The cross-talk between Ca^{2+}, ROS and mitochondrial function plays an essential role in diabetic cardiomyopathy (DCM). Therefore we extended the results obtained with MitoPQ, and especially MAO-induced amplification and alterations in $[Ca^{2+}]_I$ homeostasis induced by mitochondrial ROS to a cellular model of DCM. NRVMs treated with high glucose (HG) and interleukin-1β (IL-1β) displayed a significant increase in mitochondrial H_2O_2 levels, both after prolonged (48 h) and short (1 h) treatment. MAO inhibitor pargyline prevented this observed increase in ROS levels. Hence, we tested the effect of MAO inhibition on cytosolic [Ca^{2+}] homeostasis in cells exposed to the diabetes-like protocol. Surprisingly, HG and IL-1β did not perturb significantly Ca^{2+} oscillatory parameters (i.e. amplitude, frequency and area under curve), while pretreatment with pargyline or N-(2-Mercaptopropionyl)glycine (MPG) worsened contractility defects induced by HG and IL-1β, compromising the oscillatory pattern. These unexpected findings suggest that a basal oxidative tone is necessary for a proper Ca^{2+} cycling in cardiomyocytes exposed to HG and IL-1β.

Noteworthy, diabetes is related to pancreatic β-cells dysfunction. In pancreatic β-cell, short bursts of ROS have been shown to contribute to $[Ca^{2+}]_I$ homeostasis and Ca^{2+}-dependent insulin secretion. Although in diabetes a sustained oxidative stress leads to β-cell dysfunction, a primary and moderate increase in ROS levels could shape Ca^{2+} transients promoting insulin secretion. We tested this hypothesis on Min6 β-cells, an insulinoma cell line that can be used as a model of diabetes applied to pancreatic β-cells.

We evoked a primary increase in intracellular ROS levels by treating Min6 β-cells with aluminium phthalocyanine chloride (AlClPc), a photosensitizer commonly used in photodynamic therapy. Photoactivation of AlClPc induces chemical changes into neighboring molecules leading to ROS production in amount depending on the intensity of the LED illumination. Results obtained showed that modulation of ROS induced by photoactivation of AlClPc or Sarco/Endoplasmic Reticulum Ca^{2+} ATPases (SERCA) inhibition by thapsigargin (Tg) resulted in acceleration of Ca^{2+} to a similar degree, indicating that a primary and controlled increase in cytosolic ROS levels modifies but not abolishes Ca^{2+} oscillation via a modulation of SERCA.

Overall, our data showed that low levels of mitochondrial ROS slightly modulate $[Ca^{2+}]_I$ homeostasis without affecting mitochondrial and cell function. On the other hand, mitochondrial ROS can be elevated by increase in mitochondrial Ca^{2+} uptake. We used this notion to investigate whether mitochondrial Ca^{2+} uniporter (MCU) overexpression could modify mitochondrial ROS formation and consequently mitochondrial and cardiomyocyte viability. Cells overexpressing MCU displayed an increase in ROS levels that was causally related to an increased tolerance to anoxia/reoxygenation (A/R) injury in a process that involved AKT activation. These findings demonstrate that a slight increase in mitochondrial ROS formation exerts a protective effect. To test this hypothesis, we investigated whether mitochondrial ROS induced by low doses of MitoPQ could decrease the susceptibility to A/R injury. Not only this hypothesis was verified, but also in this case protection was due to AKT activation.

The data from this work demonstrate that mitochondrial ROS formation can trigger a wide array of responses with a clear separation between ROS levels required to elicit beneficial or detrimental effects. Changes in $[Ca^{2+}]_I$ homeostasis can be upstream but also downstream of mitochondrial ROS formation and the cardioprotective effect linked to a slight increase in mitochondrial ROS levels appears to depend on AKT activation.

4 INTRODUCTION

4.1 The role of Ca^{2+} in the excitation-contraction coupling in cardiac myocytes

Ca^{2+} is an ubiquitous second messenger of the cell and it is directly involved in the cardiac excitation-contraction coupling (ECC). This process links the electrical excitation of cardiomyocytes to the contraction of the heart and depends on peculiar properties and spatial arrangement of Ca^{2+} channels and pumps. Intracellular [Ca^{2+}] must be sufficiently high during the contraction (*systole*) and must decrease during the relaxation (*diastole*).[1, 2] Indeed, the amount of [Ca^{2+}] extruded from the cytosol during the diastole must be equal to the amount of [Ca^{2+}] required for systole.[3]

- **Systole:** the action potential (AP) induces an initial membrane depolarization that opens the L-Type Ca^{2+} channels (LTCCs) located on the sarcolemma in the transverse tubule (T-tubules). Ventricular myocytes display a complex network of T-tubules diving into the cell. Their role is to synchronize the AP within the cell network. A reduction in T-tubules organization reduces ECC efficacy.[4, 5] LTCCs opening results in the influx of a small amount of [Ca^{2+}] in the dyadic space, the region comprised between the T-tubule and the sarcoplasmic reticulum (SR).[2] Ca^{2+} enters in the cell according to its electrochemical driving force (2 mM outside, 100 nM inside, -80 mV plasma membrane potential). Calmodulin (CaM) is constitutively bound to LTCCs to sense local [Ca^{2+}] elevations and to induce LTCCs inactivation (Ca^{2+}-dependent inactivation, CDI).[6] CDI is the dominant physiologic mode of LTCCs inactivation. When CDI is abrogated experimentally, Ca^{2+} tends to overload in cells.[7] In each dyadic space there are clusters of ~20 LTCCs on the sarcolemma opposed to clusters ~200 ryanodine receptors (RyRs) on the SR membrane, and they evoke synergistically a local Ca^{2+} transient. RyR2 is the main RyR isoform expressed in the heart and it is involved in the SR Ca^{2+} release.[8] When LTCCs open, local [Ca^{2+}] in the *cleft* between the sarcolemma and the SR rises in < 1 ms to ~10-20 µM. This rise activates the Ca^{2+}-induced Ca^{2+} release (CICR) mechanism that evokes an efflux of Ca^{2+} from RyRs. CICR

elevates the [Ca^{2+}] in the cleft to 200-400 µM.[9] Noteworthy, the majority of [Ca^{2+}]$_I$ is bound to proteins (i.e. ratio free/bound Ca^{2+} ~1/200), meaning that during each systole the amount of free Ca^{2+} in the cytosol is ~1 µM.[10] Eventually [Ca^{2+}] binds to troponin C (TnC), a component of the myofilaments. The interaction between Ca^{2+} and TnC induces a conformational change that eventually allows the head of myosin to bind to actin. The myosin head uses adenosine triphosphate (ATP) to tilt causing sarcomere shortening, leading to the contraction.[11]

- **Diastole:** Ca^{2+} removal from the cytosol is at the expense of both SR uptake (i.e. via Sarco/Endoplasmic Reticulum Ca^{2+} ATPases activity, SERCA activity), and sarcolemmal extrusion (i.e. via Na^{+}/Ca^{2+} exchanger activity, NCXs), with a minor contribution (~1%, the so called "slow system") by the Plasma Membrane Ca^{2+} ATPases (PMCA) activity. SERCA plays the major role. The fraction of [Ca^{2+}]$_I$ taken up in the SR displays species variations (e.g. ~85-90% in rats and mice, ~70% in humans).[7] SERCA2a is the main SERCA isoform expressed in the heart.[12] The synergistic activity of SERCA2a and calsequestrin-2 (CASQ2) is very important. CASQ2 acts as a luminal [Ca^{2+}] sensor. Indeed, Ca^{2+} binding to CASQ2 reduces the relative high amount of [Ca^{2+}] inside the SR, allowing SERCA2a to move Ca^{2+} from the cytosol to the SR lumen at the expense of ATP.[13] Alterations in SERCA2a expression levels [14, 15] or in SERCA2a activity have been shown to be involved in heart failure.[16, 17] The principal regulator of SERCA2a activity is phospholamban (PLB). PLB is a 52 amino acid protein that can be phosphorylated at Ser16 and Thr17 by protein kinase A (PKA) and Ca^{2+}/CaM-dependent protein kinase II (CaMKII). PLB inhibits SERCA2a activity by physical interaction. Phosphorylation of PLB prevents the inhibition leading to an increase in Ca^{2+} transport inside the SR.[18] Moreover, PKA activity facilitates Ca^{2+} dissociation from myofilaments by phosphorylation of troponin I (TnI), thus reducing the affinity between TnC and Ca^{2+}.[19] The net result is the cardiac myocytes relaxation.

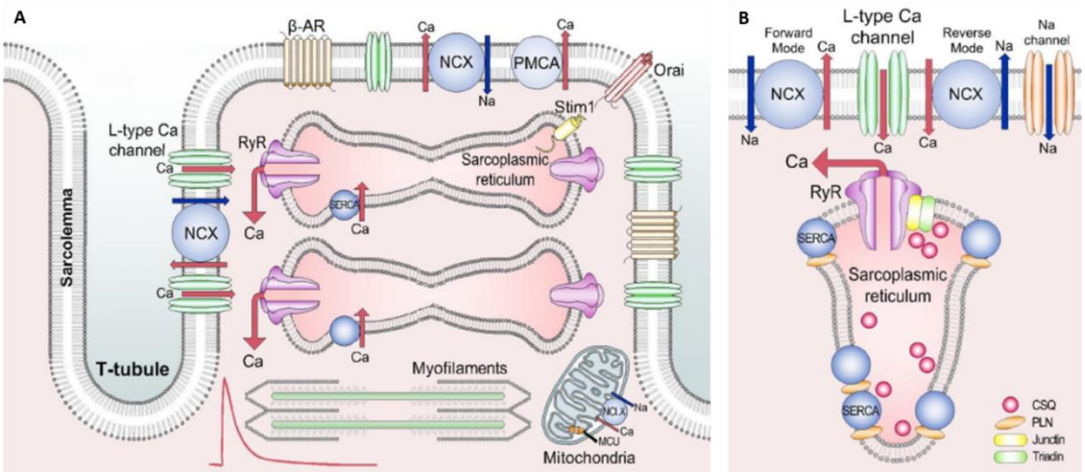

Figure 1. <u>Ca^{2+} cycling in ventricular myocytes.</u> A) Schematic cartoon representing T-tubule, sarcolemma, sarcoplasmic reticulum, mitochondria, myofilaments and proteins involved in the ECC. **B)** Schematic cartoon representing the dyadic space and proteins involved in CICR. *β-AR*: adrenoreceptor, *CSQ*: calsequestrin, *MCU*: mitochondrial Ca^{2+} uniporter, *PLN*: phospholamban, *PMCA*: plasma membrane Ca^{2+} ATPase, *NCX*: Na^{+}/Ca^{2+} exchanger, *NCLX*: mitochondrial Na^{+}/Ca^{2+} exchanger, *RyR*: ryanodine receptor, *SERCA*: sarco/endoplasmic reticulum Ca^{2+} ATPase. (*Adapted from Eisner, D.A., et al., 2017, [2]*)

4.1.1 Intracellular [Ca^{2+}] homeostasis: the role of mitochondria

Mitochondria are the main producers of cardiomyocyte ATP. ATP is required for both the contraction event (i.e. myosin ATPase) and ion transport ATPases (i.e. SERCA).[9] Mitochondrial [Ca^{2+}] can modulate the oxidative phosphorylation (OxPhox) [20], thus representing a crucial link between energy supply and demand. Mitochondrial Ca^{2+} uptake depends on the activity of the selective mitochondrial Ca^{2+} uniporter (MCU).[21, 22] MCU oligomerizes in the inner mitochondrial membrane (IMM) and it is part of a larger complex that finely regulates mitochondrial Ca^{2+} uptake.[23] However, the rate of Ca^{2+} influx is extremely low under physiological conditions. The contribution of mitochondrial and MCU Ca^{2+} uptake to Ca^{2+} buffering within cardiac myocytes has been matter of debate. During a cytosolic [Ca^{2+}] transient only ~1% of the Ca^{2+} removed from the cytosol is buffered by mitochondria.[24] Notably, there are ~200 MCU channels per mitochondrion, and when MCU is knocked down the cytosolic [Ca^{2+}] transients increase by ~1/3.[25, 26] Indeed, mitochondrial Ca^{2+} uptake via MCU can drastically be increased when $[Ca^{2+}]_I$ levels are chronically elevated. One explanation for this process is that mitochondria and SR are in close proximity, so that frequent and sustained release of Ca^{2+} by means of RyRs might be sensed by mitochondria.[24, 27-29] The contribution of

mitochondrial Ca^{2+} uptake to beat to beat variations of cytosolic [Ca^{2+}] has been questioned by Lederer.[25, 30] Studying the influence of Ca^{2+} sparks and $[Ca^{2+}]_I$ transients on mitochondrial Ca^{2+} uptake, the conclusion was drawn that mitochondrial Ca^{2+} uptake did not alter cytosolic Ca^{2+} signaling under physiological conditions.[30] Besides MCU, the mitochondrial [Ca^{2+}] depends also on the activity of the mitochondrial Na^{+}/Ca^{2+} exchangers (NCLX).[31] However, the extrusion mechanism is kinetically slow and can hardly participate to the phasic changes of cytosolic [Ca^{2+}].[9] Finally, the permeability transition pore (PTP) has been proposed as a pathway for releasing large amounts of Ca^{2+} accumulated within the mitochondrial matrix.[32, 33]

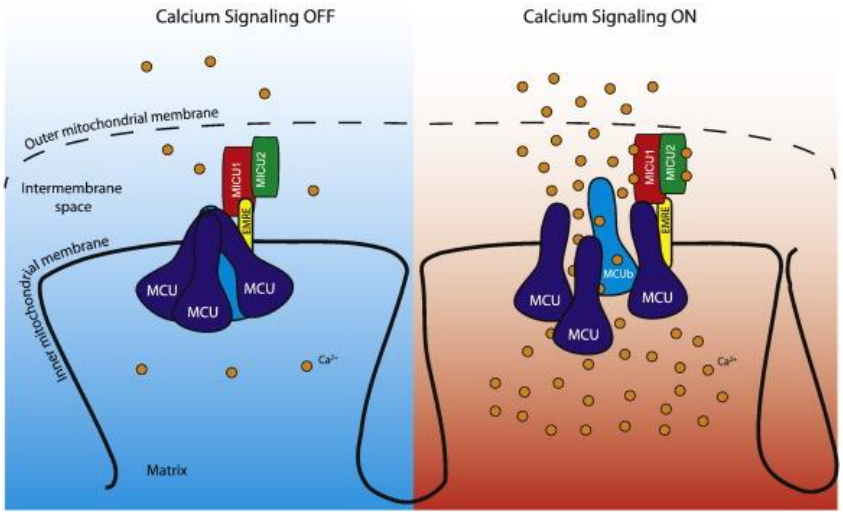

Figure 2. Schematic representation of the MCU Complex. The channel forming subunit MCU and MCUb are colored in blue and light blue respectively. The gatekeeping subunits MICU1 and MICU2 are colored in red and green respectively. The EMRE subunit is colored in yellow. (*Adapted from De Stefani, D., et al., 2015, [34]*)

4.2 Mitochondria as source of reactive oxygen species (ROS)

Mitochondria are the most redox-active compartment within the cell, and several studies showed that these organelles are the major contributor to reactive oxygen species (ROS) production in cardiomyocytes.[35-37] High levels of ROS lead to critical damage to mitochondria and cells. Indeed, ROS are described as the main contributor to cardiovascular diseases.[38] To counterbalance dysfunctions deriving from an oxidative stress, mitochondria have a well characterized antioxidant defense mechanism. Mn^{2+}-superoxide dismutase (MnSOD) rapidly converts superoxide deriving from the electron

transport chain (ETC) into hydrogen peroxide (H_2O_2), the main ROS produced within mitochondria.[37]. Besides MnSOD, peroxide handling is carried out by a thiol redox system based on glutathione (the reduced GSH and the oxidized GSSG) and thioredoxin (Trx).[39, 40] H_2O_2 is reduced to water by glutathione peroxidases (Gpx1 and 4) and peroxiredoxin 3 (Prx3), whose reduction depends on Trx activity.[41] The oxidized forms of glutathione and Trx are reduced by the corresponding reductases at the expense of $NADP(H^+)$. Prx3 removes > 90% of H_2O_2 in mitochondria. Nevertheless, under severe oxidative stress (i.e. Ischemia/Reperfusion injury, I/R) Prx3 is highly susceptible to oxidation and Gpx1 might become the major sink for H_2O_2.[41, 42]

ETC, $p66^{Shc}$ and monoamine oxidase (MAO) are the major sources of ROS formation in mitochondria (see also [43-45] and section 4.2.2). The list of ROS producers within mitochondria might include also NADPH oxidase 4 (Nox4, [46]). Unlike other NOX isoforms, Nox4 displays a preferential localization to intracellular sites, appears to be constitutively active, and generates H_2O_2.[47] On the other hand, a recent study argued against its mitochondrial localization and its role in the normoxic heart.[48]

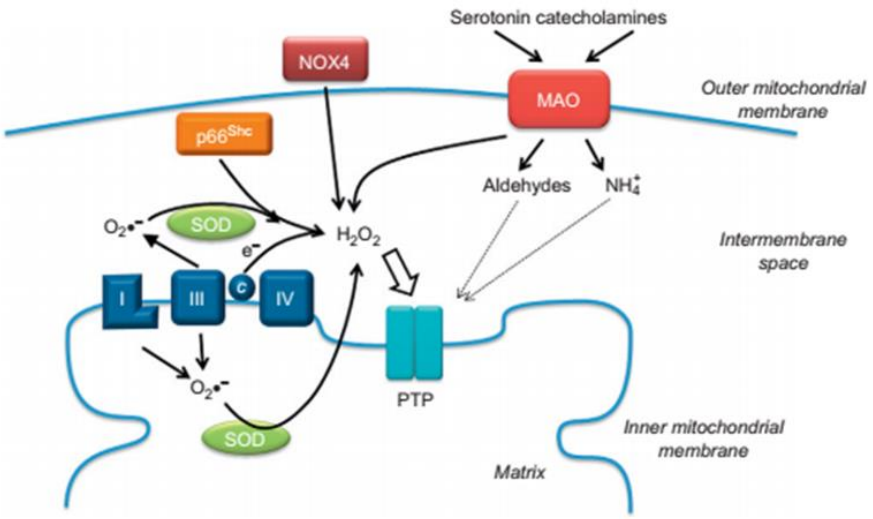

Figure 3. Schematic representation of principal mitochondrial sources of ROS. *c:* Cytochrome C, *I, II, IV*: Complexes I/II/IV, *MAO*: Monoamine Oxidase, *NOX4*: NADPH Oxidase, *PTP*: Permeability Transition Pore, *SOD*: Superoxide Dismutase. (*Adapted from Di Lisa, F. & Scorrano, L., 2012, [49]*)

4.2.1 Electron transport chain (ETC)

ETC is located in the IMM and it is composed by four complexes that reduce oxygen to water by the transfer of electrons from NADH and $FADH_2$ to oxygen. The flow of electrons drives the movement of protons into the intermembrane space. The resulting electrochemical gradient drives the translocations of protons from the intermembrane space back into the mitochondrial matrix by means of the F_0F_1-ATP synthase activity.[50] This proton translocation is coupled to the phosphorylation of ADP to generate ATP.[37] At the level of the first three complexes, oxygen is partially reduced into superoxide, especially under conditions that decrease the flow of electrons towards complex IV. This is caused by the leak of a minor fraction of electrons (~0.1%) from the ETC or by the reverse electron flow.[51] The relevance of reverse electron flow has been recently supported by a study that demonstrates that succinate accumulates during ischemia and it is oxidized during reperfusion *in vivo*, causing ROS formation at complex I by means of reverse electron flow.[52] Superoxide that does not cross the IMM is rapidly dismutated into H_2O_2 by MnSOD.[53] Cardiac dysfunction induced by I/R injury can alter mitochondrial structure and function, compromising ETC activity during the ischemia and inducing an increased ROS generation during reperfusion. Indeed, the whole ETC has been proposed to be both target and source of ROS in I/R.[54, 55]

Although ETC is considered as an important source of ROS formation, recent studies revealed that NOXs and MAOs generate 10-fold higher levels of ROS in human atrial myocardium.[43, 45, 56]

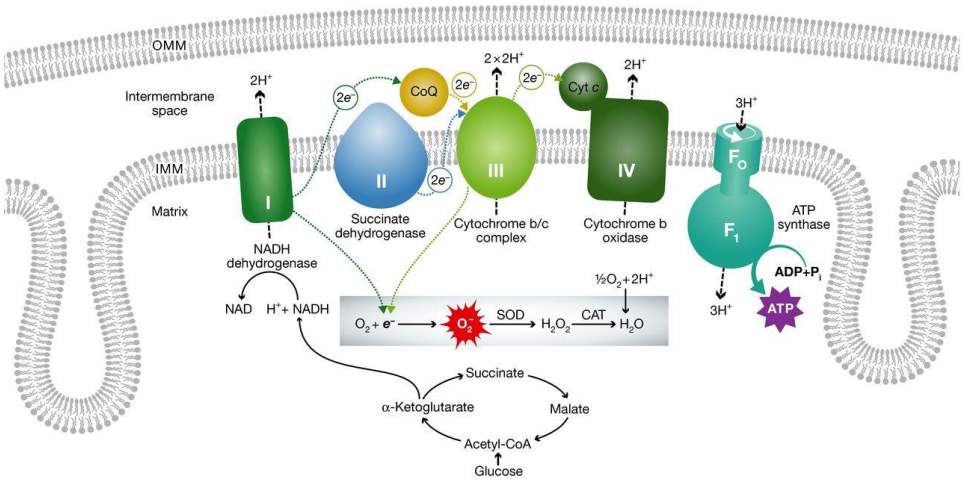

Figure 4. Schematic structure of the electron transport chain. ETC complexes are indicated by their respective roman numerals. ROS deriving from the electron leak are reported. (*Adapted from Dorn, G.W., 2015, [57]*)

4.2.2 Monoamine oxidases (MAOs)

Monoamine Oxidases (MAO-A and B) are flavoenzymes located at the OMM that catalyze the oxidative deamination of catecholamines and biogenic amines, resulting in the formation of H_2O_2, aldehydes and ammonia [58] according to the following reaction:

$$RCH_2NR´R´´ + O_2 + H_2O \rightarrow RCHO + N\,R´R´´ + H_2O_2$$

This reaction occurs in two steps. In the first step, the cofactor of MAO flavin adenine dinucleotide (FAD) is reduced to an aldehyde intermediate and ammonia, while in the second step FAD is re-oxidized and H_2O_2 is produced. Aldehyde dehydrogenase metabolizes the reactive aldehyde into the corresponding acid.[58] MAO-A and MAO-B are distinguished by different substrate specificity and inhibitor sensitivity. MAO-A and MAO-B present 70% homology in their primary sequence and both of them contain the obligatory cofactor FAD, necessary for catalysis. Although human MAO-A is monomeric and MAO-B is dimeric, both isoforms display a dimerization in their membrane-bound forms.[59, 60]

MAO is prevalent in the nervous system, where it has been extensively studied. However, MAO is also expressed in peripheral tissues (e.g. heart, liver), and its role in cardiac oxidative stress was recently elucidated.[58, 61] MAO-A is the predominant isoform in human cardiomyocytes and it exerts a role both in physiological and in

pathological conditions. Mice lacking MAO-A activity display accumulation of catecholamines, cardiomyocyte hypertrophy and left ventricle (LV) dilation at baseline.[62] On the other hand, MAO-A deficient mice are protected from cardiac injury induced by I/R.[63] Moreover, it was demonstrated that MAOs are highly involved in maladaptive hypertrophy in heart subjected to pressure overload.[64] Indeed, mice expressing a dominant-negative MAO-A and exposed to 9 weeks of transverse aortic constriction (TAC) displayed reduced impairment in LV function and reduced fibrosis when compared to WT mice along with a decrease in mitochondrial dysfunction, caspase activation and apoptosis.[44, 45, 64] Moreover, these data were confirmed by pharmacological treatment with clorgyline, a selective inhibitor of MAO-A.[45] Indeed, MAO inhibition with clorgyline and pargyline prevented I/R injury both in isolated Langendorff perfused mouse hearts[65] and in an *in vivo* rat model.[44] Lastly, the significant contribution of MAO activity to oxidative stress and cardiac dysfunction was elucidate by the overexpression of this flavoenzyme. These studies reported that overexpression of MAO in mice resulted in the loss of ~50% of cardiomyocytes, fibrosis and heart failure.[66, 67] The relevance of MAO as source of ROS in cardiomyocyte is linked to the availability of specific inhibitors.[68] Thus, MAO represents an attractive and important therapeutic target for the treatment of cardiovascular diseases.

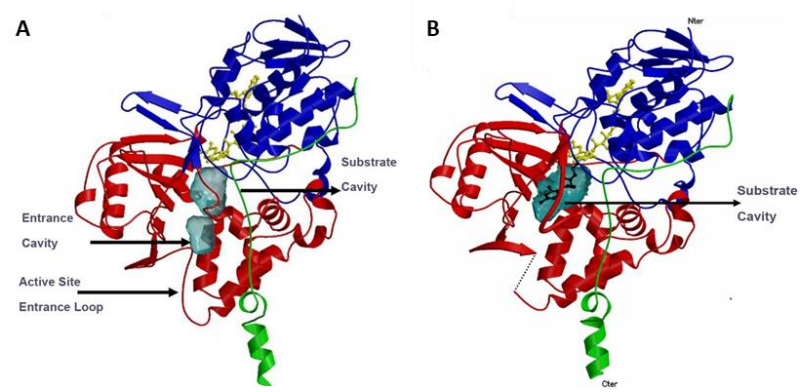

Figure 5. Ribbon structures of two isoforms of MAO. Structures of **A)** MAO-A and **B)** MAO-B. The covalent flavin moiety is shown in a ball and stick model in yellow. The flavin binding domain is in blue, the substrate domain is in red and the membrane binding domain is in green. (*Adapted from Edmondson, D.E., et al., 2004, [60]*)

4.2.3 p66^{shc}

p66^{Shc} is an important mitochondrial source of ROS. p66^{Shc} is a cytosolic adaptor protein that is ubiquitously expressed in vertebrates.[61, 69] Unlike its splicing variants (i.e. p46^{Shc}, p52^{Shc}), p66^{Shc} expression is restricted to certain cell types and depends on stimulatory conditions through epigenetic modifications of its distinct promoter.[70, 71] Cells and mice lacking p66^{Shc} show reduction in markers of oxidative stress [65]. Under basal conditions, p66^{Shc} is associated with a high molecular weight complex and to heat shock protein 70 [72] and components of the transporter of the outer and inner mitochondrial membrane.[70] Under stress conditions, the activity of kinases (i.e. protein kinase Cβ, PKCβ) phosphorylates p66^{Shc} on Ser36 inducing its translocation into the mitochondrial intermembrane space. Moreover, an oxidative stress (i.e. H_2O_2) induces the dissociation of these complexes and the release of p66^{Shc} that reacts with cytochrome c, resulting in H_2O_2 formation.[71-73]

p66^{Shc} expression appears to be low in cardiomyocytes under physiological conditions, yet it can be induced by various stimuli. p66^{Shc} is directly involved in several pathologies. Cardiac protection was demonstrated in mouse hearts exposed to I/R. Indeed, the cardiac deletion of p66^{Shc} resulted in increased viability and decreased oxidative stress.[65] In addition, it was demonstrated that PKCβ inhibition reduced p66^{Shc} translocation to mitochondria induced by I/R.[74] Although it is widely accepted that mice lacking p66^{Shc} display better functional recovery and less infarction during reperfusion, studies highlight the potential protective effect of ROS induced by p66^{Shc}. Indeed, p66^{Shc} might increase the resistance to short periods of ischemia by activating AKT. AKT (also known as protein kinase B, PKB) is a serine/threonine (Ser/Thr) protein kinase involved in several processes, such as glucose metabolism, apoptosis and cell proliferation.[75, 76] The proposed mechanism is that AKT phosphorylation can be enhanced by ROS-dependent inhibition of protein tyrosine phosphatases via oxidation of critical cysteine residues.[77] However, p66^{Shc}-dependent ROS would be detrimental after severe ischemia or in case of prolonged diseases, such as DCM. Despite the role of p66^{Shc} in severe oxidative stress in the heart is widely accepted, at the moment there are no drugs available that can prevent or modulate ROS forming activity of p66^{Shc}.

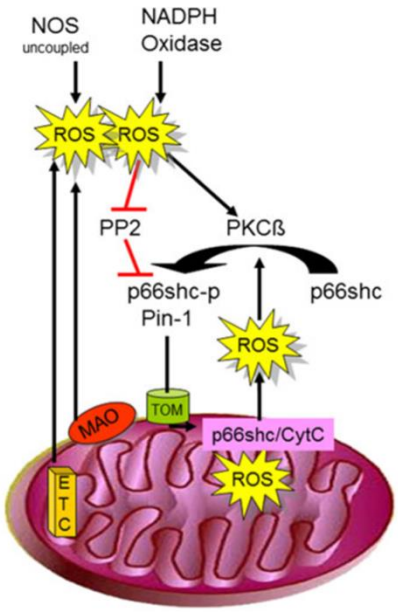

Figure 6. Schematic representation of p66^{Shc} activation pathway. ROS derived from uncoupled NOS, NOXs, MAOs or ETC activate PKCβ and inhibit protein phosphate 2 (PP2). The phosphorylation of p66^{Shc} increases and the protein translocates into the mitochondrial intermembrane space. p66^{Shc} then catalyzes electron transfer from cytochrome c to oxygen, increasing ROS formation. (*Adapted from Di Lisa, F., et al., 2016, [71]*)

4.3 Interplay between Ca^{2+} and ROS

Since Ca^{2+} can regulate ROS production and vice versa, in the last years the interplay between Ca^{2+} and ROS signaling has been subject of countless studies.[78, 79] The bidirectional communication between Ca^{2+} and ROS plays a pivotal role in many pathophysiological conditions, such as neurodegenerative diseases, inflammatory diseases and cardiovascular diseases.[80] Mitochondrial [Ca^{2+}] homeostasis is fundamental for the cellular physiology. Moreover, in cardiomyocytes mitochondrial-derived ROS have been found to be necessary to maintain [Ca^{2+}] homeostasis by interactions with SR Ca^{2+} components.[81]

In addition to mitochondria, NOXs are other ROS-generating enzymes that play a fundamental role in cardiomyocytes. The NOX family is composed by seven members (i.e. Nox1-5, Duox1-2) and its activity is to catalyze the reduction of oxygen to superoxide using NADPH as an electron donor, with the only exception of Nox4 that has been proposed to contribute also to H_2O_2 formation.[82] The activity of endogenous NOX in SR has been reported to increase RyR activity [83]. Moreover, studies demonstrated

the connection between NOX-derived ROS and SR [Ca^{2+}] homeostasis in a model of dystrophic cardiomyopathy.[84] On the other hand, preconditioning tachycardia induces translocation of cytosolic Nox subunits to a SR-enriched fraction isolated from dog ventricular muscle.[85]

4.3.1 Ca^{2+}-derived production of mitochondrial ROS

Ca^{2+} promotes ATP synthesis by stimulating the activity of crucial mitochondrial dehydrogenases involved in the Krebs cycle. As a consequence more electrons are available for the ETC activity. The increase in mitochondrial metabolism would consume more oxygen resulting in increasing ROS levels.[86] However, studies aimed to unravel the connection between mitochondrial [Ca^{2+}] and ROS reported controversial findings. An increase in mitochondrial Ca^{2+} uptake has been shown to promote or to decrease ROS generation and vice versa.[78, 86, 87]

Nevertheless, a general consensus exists that mitochondrial Ca^{2+} overload is associated with oxidative stress. This is especially the case with the I/R. At the onset of post-ischemic reperfusion, mitochondria are exposed to high levels of Ca^{2+}.[88] Since mitochondrial Ca^{2+} uptake and ATP synthesis utilize the same driving force (i.e. $\Delta\Psi m$), the uptake of Ca^{2+} by mitochondria is unavoidable.[88] The rise in mitochondrial [Ca^{2+}] promotes the PTP opening and it is associated with increased formation of ROS. Moreover, Ca^{2+} and ROS facilitate the opening of the PTP, establishing a vicious cycle that exacerbates mitochondrial dysfunction.[88]

4.3.2 ROS-derived regulation of Ca^{2+} homeostasis

While doubts exist about the mechanisms linking changes in [Ca^{2+}] with ROS production, the consequences of an increase of ROS on [Ca^{2+}] homeostasis have been investigated and clarified by many studies. The following list is made to provide only major examples.

- **LTCCs:** LTCCs are redox sensitive proteins due to the presence of two cysteine residues in the pore forming subunit.[89] Besides the direct

modulation by means of cysteine oxidation, ROS can modulate LTCC activity by interacting with signaling pathways.[90] As detailed in the following section, ROS generally inhibit the activity of protein phosphatases leading to the stimulation of protein kinases. Several protein kinases have been reported to target LTCC stimulating their activity. Therefore, LTCCs can be inhibited by a direct effect of ROS and activated by indirect consequence of kinases activation.[91]

- **RyRs:** RyR2 is the main isoform expressed in the cardiac tissue and it contains many cysteine residues that can be targeted by ROS.[92] ROS can directly oxidize redox-sensing thiol groups of RyR, thus enhancing channel activity, SR Ca^{2+} leak and spark frequency.[93, 94] Mild oxidative stress induced by I/R enhances RyR2 activity, and recently mitochondrial ROS have been associated with the oxidation of RyRs.[95, 96]

- **SERCAs:** SERCA2a is the main isoform expressed in the cardiac tissue. ROS inhibit SERCA activity by oxidation of specific cysteine residues.[94] Moreover, since SERCA is dependent on ATP hydrolysis, ROS have been suggested to prevent ATP binding to SERCA.[97] However, SERCA activity can be indirectly modulated by ROS. Indeed, ROS can oxidize and activate CaMKII, and inhibit SERCA activity by phosphorylation of PLB.[98]

- **Protein Kinases:** ROS are involved also in the oxidation of key kinases implicated in the phosphorylation of LTCCs, RyRs, and SERCAs, thus regulating their activity.[94] Indeed, ROS-induced activity of CaMKII, PKA and PKC results in an increase of Ca^{2+} influx through LTCCs.[99] In addition, among the kynases activated by ROS, it is worth mentioning CaMKII. This kinase can be oxidized at Met281/282, leading to a sustained CaMKII activity in the absence of Ca^{2+}/CaM. CaMKII oxidation can be reverted by methionine sulfoxide reductase A (MsrA).[100] This processes have been proposed to play a relevant role in cardiac dysfunction and arrhythmogenesis.[98]

4.3.3 ROS as signaling molecules

The detrimental impact of high levels of mitochondrial ROS on function and viability of any cell type is undeniable. Beneficial effects elicited by inhibition or deletion of mitochondrial sources and by preventing ROS accumulation [61, 101] in cardiovascular diseases, such as I/R injury, heart failure and DCM.[65, 102] On the other hand, mitochondrial ROS play a crucial role in signaling processes occurring within mitochondria or between mitochondria and other cellular sites.[103-105] Mitochondrial ROS interact with a variety of cardiomyocyte functions by means of post-translational modifications (PTMs) of proteins, especially at the level of cysteine residues.[106] ROS have been shown to exert both short term responses (i.e. oxidation of protein phosphatases, [107]) and long-lasting changes. Long-lasting changes are obtained by the effects of mitochondrial ROS on transcriptional factors, such as hypoxia-inducible factor (HIF) and nuclear factor erythroid-2 related factor 2 (Nrf2).[108-110]

In the last twenty years, mitochondrial ROS were associated with a variety of physiological pathways.[103, 111] Indeed, redox balance is a critical regulator of differentiation of embryonic stem cells to cardiomyocytes.[112] Moreover, ROS are required for induction of autophagy under starvation [113] and a transient increase in ROS levels is supposed to be protective against I/R injury.[114, 115] Indeed, deletion of $p66^{Shc}$ and ablation of Trx-interacting protein exacerbate the mild injury induced by the short-term I/R protocol.[116, 117] These paradoxical findings contrast with the protection elicited by antioxidant treatments in prolonged episodes of I/R, but support the concept that antioxidants abrogate protection induced by both ischemic pre- and post-conditioning, as discussed in section 4.5.2.[114, 118]

Overall, the non-linear response that ROS seem to have (i.e. low amounts versus high amounts), argued against *Mitochondrial Free Radical Theory of Aging* (MFRTA) exposed by Harman in 1972.[119] According to this theory, increased ROS formation causes an accumulation of cell damage with age. Accordingly, antioxidants were studied extensively as the most promising strategy to decrease ROS levels and to counteract aging. Not only most, if not the totality, of these studies were negative, but in some cases antioxidant treatment elicited detrimental consequences.[120] This is because although high levels of ROS are harmful, low levels of ROS are likely to exert beneficial effects on several cell functions.

This kind of non-linear response to potentially harmful substances was named *hormesis.* Subsequently, the term *mitohormesis* was coined to extend this concept to mitochondria.[121] Accordingly, a low level of oxidants is beneficial as opposed to the detrimental effect elicited by large amount of ROS. Therefore, antioxidants could cause harmful effects removing the ROS associated with endogenous protection.

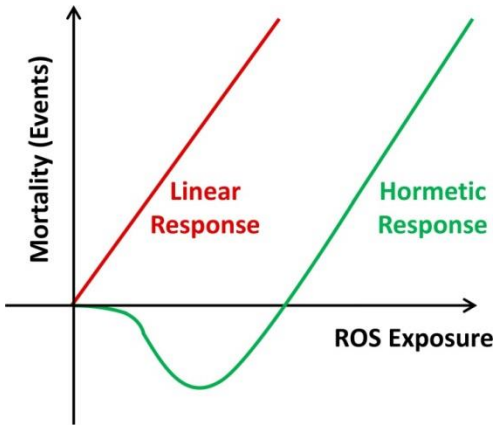

Figure 7. Mitochondrial Hormesis (*Mitohormesis*). The classical *Free Radical Theory of Aging* suggests a linear dose-response increase in ROS and oxidative stress related cell death (*Red Line*)**.** Mitohormesis indicates a non-linear dose-response relationship, where low doses of ROS decrease mortality. (*Adapted from Ristow, M., et al., 2014, [122]*)

4.4 Oxidative stress and diabetes related complications

Diabetes is a complex disease caused by a combination of alterations of multiple genes and environmental factors leading to loss of functional β-cell mass and hyperglycemia.[123] Type 1 diabetes (T1D) is characterized by a progressive β-cell mass reduction (~70-80%) that leads to insulin deficiency. It is caused by several environmental factors (i.e. dietary factors, viral infection) and by defective genes belonging to the human leukocyte antigen (HLA) family. Thus, in T1D, pancreatic β-cells become target of the immune system, with infiltration of mononuclear cells in an inflammatory reaction (*insulitis*).[124, 125] Type 2 diabetes (T2D) is characterized by hyperglycemia, insulin resistance and relative insulin deficiency. It is linked to a progressive decrease of β-cells function and reduction in β-cells mass (~25-50%) that lead to glucose intolerance.[126, 127] T2D is caused by environmental factors (i.e. augmented caloric intake, ageing) that increase the risk to develop the disease.[128]

Hyperglycemia is a common feature of both T1D and T2D. A large amount of data highlights the deterioration of pancreatic β-cells as concomitant with the elevation of blood glucose levels and rise of ROS accumulation.[129, 130] Oxidative stress is the result of the imbalance between the increased production of ROS and the decrease of the antioxidant defense capacity of the cell. Many metabolic pathways can be modulated by an overproduction of ROS, such as NF-κB pathway.[131] This is one the most important link between diabetes and inflammation. *In vivo* studies revealed that hyperglycemia-induced oxidative stress occurs before that diabetes becomes clinically evident.[132, 133]

Since mitochondria are the site of fatty acid and carbohydrates oxidation, impaired metabolism associated with diabetes inevitably impact on mitochondrial function. Besides metabolic abnormalities, respiratory complexes have been reported to be altered by H_2O_2.[134] In addition, impaired cardiac insulin signaling has been linked to abnormalities in mitochondrial bioenergetics.[135] The relationship between diabetes and mitochondrial dysfunction has been studied in animal models of diabetes. In a model of T1D, mitochondrial biogenesis is decreased along with mitochondrial function.[136] Similar defects in mitochondrial biogenesis has been described in T2D.[137]

4.4.1 Pancreatic β-cells dysfunction

Islets of Langherans are the main constituent of the endocrine pancreas. The islets of Langherans are cells aggregates included into the exocrine parenchyma and they are composed by glucagon releasing *α-cells* (~40-45%), insulin releasing *β-cells* (~55-60%), somatostatin-producing *δ-cells* (~3-10%), and pancreatic polypeptide-producing *PP-cells* (~1%).[138]

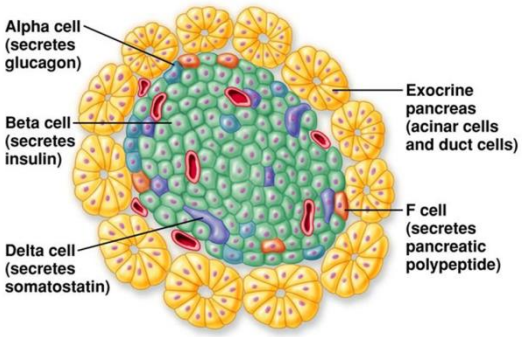

Figure 8. **Schematic Structure of pancreatic islet.** Representation of the distribution of various cell types within the islet of Langherans. (*Adapted from Stanfield, C.L. & Germann, W.J., 2006, [139]*)

Glucose stimulation of β-cells is coupled to insulin secretion through a sequence of events including depolarization of plasma membrane and exocytosis of insulin granules (Glucose Stimulated Insulin Secretion, GSIS).[139] Glucose is transported into the cell by the low affinity glucose transporter type II (Glut II). Within the cell glucose utilization results in ATP formation leading to an elevation of the ATP/ADP ratio that induces the closure of the plasma membrane ATP-sensitive K^+ channels (K_{ATP}).[140] The result is the depolarization of the plasma membrane leading to the opening of the voltage-gated Ca^{2+} channels (VDCCs). The consequent increase in $[Ca^{2+}]_I$ triggers the exocytosis of insulin containing granules.[141]

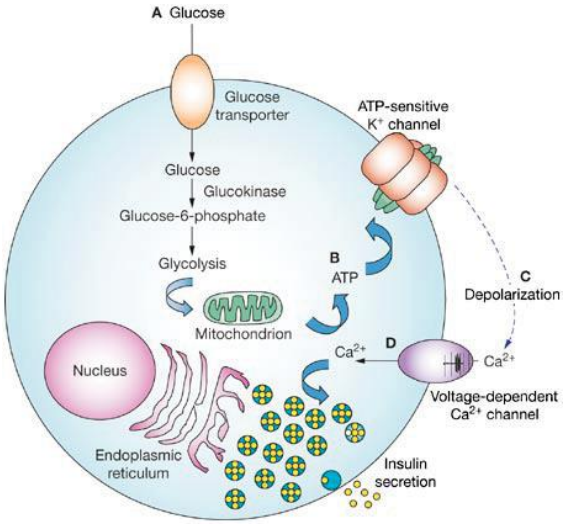

Figure 9. **GSIS in pancreatic β-cells.** **A)** The uptake and the metabolism of glucose induce **B)** an increase in the ATP/ADP ratio, resulting in the closure of the $K_{ATP,}$ **C)** membrane depolarization and **D)** opening of the VDCCs. The net result is an increase in $[Ca^{2+}]_I$ that triggers insulin release. (*Adapted from De Leon, D.D. & Stanley, C.A., 2007, [142]*)

Mitochondrial metabolism and Ca^{2+} in the mitochondrial matrix activates several dehydrogenases and enhances mitochondrial oxidative activity. MCU deletion impairs the rise in mitochondrial [Ca^{2+}] levels, thus inhibiting insulin exocytosis.[143] Generation of ATP is pivotal to induce membrane depolarization triggering cytosolic Ca^{2+} influx.[144] In addition, the inhibition of complex I is shown to abolish GSIS.[145]

The physiological production of ROS is normally counterbalanced by the endogenous antioxidant mechanism. However, ROS formation can be enhanced when mitochondrial respiration is stimulated under conditions of altered redox state due to hyperglycemia.[146] Different levels of ROS may exert both a positive and a negative effect in pancreatic β-cells. Indeed, recent studies showed that both H_2O_2 and superoxide can be one of the coupling factors involved in the stimulation of GSIS.[147] On the other hand, a severe oxidative stress can lead to β-cells dysfunction, disrupting the signaling pathways of GSIS. A defence mechanism has been described whereby an increase expression of uncoupling protein 2 (UCP2) might reduce the mitochondrial ROS formation.[148] The expression of UCP2 can increase in response to cytokines involved in cellular stress by reducing ROS and cell death.[149] Interestingly, in β cells, mitochondrial sub-lethal ROS levels can induce an up-regulation of UCP2, leading to the restoration and eventually amelioration of secretory β cell function.[150]

4.4.2 Diabetic cardiomyopathy (DCM)

Diabetic cardiomyopathy (DCM) is one of the major complications associated with diabetes. [131] Diabetic patients frequently displayed diastolic dysfunction at early stages and previous to manifest systolic dysfunction.[151-153] LV diastolic dysfunction is detected in almost 63% of the diabetic patients and it is associated with increase in ventricle stiffness and decrease in ventricle relaxation.[154, 155] Thus, the inability of the ventricle to accept an adequate amount of blood at normal diastolic pressure leads to diastolic heart failure.[156, 157]

Among many mechanisms involved in DCM, mitochondrial ROS and dysfunction appear to play a relevant role in the pathogenesis of diabetes.[102, 157-159] The increased oxidative stress in mitochondria from diabetic cardiomyocytes correlates with mitochondrial fatty acid oxidation and lipid overload.[160] Cardiac mitochondria from

diabetic patients display dysfunction, abnormal morphology of the cristae [136], increase in H_2O_2 levels [157], impaired and uncoupled respiration [157] and increased levels of hydroxynonenal (HNE) modified proteins.[134] Notably, overexpression of antioxidant enzymes (i.e. MnSOD) were sufficient to rescue mitochondrial function and morphology in diabetic mice without decreasing hyperglycemia.[161]

The changes observed in mitochondrial morphology and bioenergetics (e.g. mitochondrial uncoupling) might lead to decrease in cardiac ATP generation [102], impairment of $[Ca^{2+}]_I$ homeostasis [157] and ultimately to cardiac dysfunction.[162] Impaired mitochondrial Ca^{2+} handling may contribute to cardiac dysfunction. However, the existence and the relevance of alterations of mitochondrial Ca^{2+} dynamics in the development of contractile dysfunction is still matter of debate [157], even though studies demonstrated impaired mitochondrial $[Ca^{2+}]$ homeostasis in *ob/ob* mice.[163, 164]

It is worth to mention that diabetic heart mitochondria demonstrated an enhanced susceptibility to PTP opening.[165, 166] Since both ROS and Ca^{2+} are inducers of PTP [167, 168], a likely hypothesis is that the hyperglycemia-induced ROS and mitochondrial dysfunction augment PTP opening in diabetes.

4.5 Role of mitochondria in ischemia-reperfusion (I/R)

Ischemia is characterized by a lack of oxygen for mitochondrial oxidation that leads to a rapid depletion of creatine phosphate, with a concomitant rise in Pi and lactate formation.[88] The accumulation of lactate and the hydrolysis of ATP decrease intracellular pH. Thus, the fall in ATP that initially stimulates glycolysis, under severe ischemia is followed by the inhibition of glycolysis.[169] The decrease of mitochondrial-derived ATP is due to the arrest of the respiratory chain. However, $\Delta\Psi m$ does not collapse immediately. In fact, $\Delta\Psi m$ is maintained by the inverse rotation of F_0F_1-ATP Synthase at the expense of the ATP generated by glycolysis.[170] Thus, during ischemia mitochondria cease to be the major producer of ATP and become its major consumer. Myocardial tissue exhibits a transition from reversible to irreversible damage. The lack of ATP production results in a slow degenerative process that leads to loss of plasma membrane integrity and release of intracellular components. In this context, alterations of mitochondrial functions result in cell death.[88, 170]

The re-introduction of oxygen during reperfusion leads to sudden changes on myocardial viability. In this context, cardiomyocytes exhibit uncontrolled hypercontracture of myofilaments associated with a rapid increase in cell membrane permeability and in $[Ca^{2+}]_I$ leading to irreversible injury.[171] $[Ca^{2+}]_I$ overload is concomitant with massive accumulation of Ca^{2+} within mitochondrial matrix. Notably, $[Ca^{2+}]_I$ overload indicates that the rapid transition toward cell death requires a coupled mitochondrial respiration.[51, 170] Indeed, upon reperfusion mitochondria are exposed to high levels of cytosolic $[Ca^{2+}]$ due to both the failure of Ca^{2+} ATPases and to the uptake by means of NCXs. Since mitochondrial Ca^{2+} uptake and ATP synthesis utilize the same driving force, mitochondrial Ca^{2+} accumulation results in a decrease in ATP formation.[170]

In addition, the rise in mitochondrial $[Ca^{2+}]$ promotes the opening of the PTP and is associated with increased formation of ROS at the onset of reperfusion providing a great contribution to cell death.[172, 173] Alterations of mitochondrial respiration contribute largely to the ROS-induced damage, as well as other mitochondrial sources described in sections 4.2.2 and 4.2.3 (i.e. MAO, $p66^{Shc}$, [61]). On the other hand, the involvement of MCU and its role in post-ischemic injury are still debated since the results obtained with mice lacking MCU are controversial.[174, 175]

4.5.1 The permeability transition pore (PTP) and its role in I/R

The PTP molecular nature has been recently elucidated. Pharmacological and genetic evidences have been produced showing that PTP is formed from dimers of F_0F_1-ATP synthase.[176-180] PTP opening is generally considered a pathological phenomenon. Prolonged opening of the PTP results in dissipation of $\Delta\Psi m$ followed by ATP and NAD^+ depletion.[181] Thus, a cascade of catastrophic consequences occurs, such as impairment of ion homeostasis, matrix swelling and release of mitochondrial proteins that activate programmed cell death.[182, 183]

It is commonly accepted that PTP is a major factor in cell death occurring in I/R. During ischemia the rise in factors that sensitize PTP opening (e.g. membrane depolarization, increase in $[Ca^{2+}]_I$ and Pi) is balanced by PTP antagonists (i.e. intracellular acidosis, high levels of Mg^{2+}).[184] On the other hand, upon reperfusion

there is a recovery of the pH and a burst in ROS formation in the presence of high levels of Ca^{2+} and Pi. All these factors creates the perfect scenario for the opening of the PTP, despite the antagonizing effect of membrane potential recovery.[88, 184] Notably, severe oxidative stress promotes a prolonged PTP opening and vice versa, generating a feedback loop that contribute to the dysfunction. Cyclosporin A (CsA), the prototype desensitizer of the PTP, protects from myocardial I/R and this protection is connected to cyclophilin D (CyPD) inhibition.[185, 186] However, this kind of protection is dependent on animal species and on the duration of the ischemic event. Indeed, a paradoxical finding is that CyPD deletion has been shown to exacerbate myocardial injury after a short ischemic episode.[187] This paradox is explained by the hypothesis of transient and short openings of the PTP that elicits a mild ROS increase that could exert protection from I/R.[118] Nevertheless, today one of the therapeutic strategies is the inhibition of the PTP, also due to translation of experimental findings into clinical approaches.[183, 188] However, the initial positive results were not confirmed by a more recent clinical trial.[189] Unfortunately, the interventions to limit PTP opening that have been used so far, such as CsA, target CyPD that is a modulator but not a constituent of the PTP.[189]

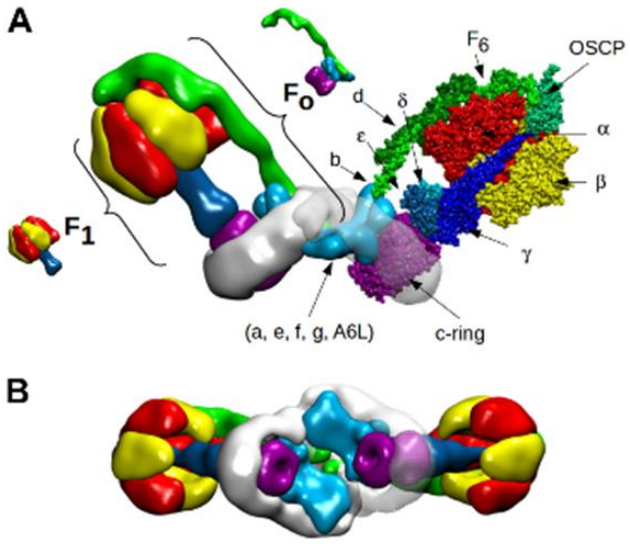

Figure 10. Model of F-ATP synthase dimer. A) The model is viewed from the lateral side. **B)** The model is viewed from the intermembrane space. The F_1 α and β subunits are colored in red and yellow respectively. The F_1 γ, δ and ε subunits are colored in shades of blue. The peripheral stalk subunits and OSCP are colored in shades of green. The c-ring is colored in purple. The remaining subunits are colored in light blue. The white part is detergent that surrounds the intermembrane F_0. (*Adapted from Bernardi, P., et al., 2015, [33]*)

4.5.2 Mechanisms of ischemic pre-conditioning (iPC)

Ischemic preconditioning (iPC) is a phenomenon discovered and described by Murry, Jennings and Reimer in 1986.[190] It consists of brief episodes of ischemia and reperfusion (5 min) followed by a sustained period of ischemia, resulting in reduced infarct size.[191] A general consensus exists that iPC results in a decrease occurrence of PTP opening during reperfusion. Indeed, cardioprotection elicited by iPC is similar to that obtained by the inhibition of the PTP.[181]

The molecular mechanism linking PTP opening to iPC remains to be elucidate. For instance a pathway termed as Reperfusion Injury Salvage Kinase (RISK) has been proposed. The RISK pathway comprises the PI3K-AKT-GSK3β pathway that has been reported to counteract PTP opening.[191-193] This pathway can be linked also to the protective role of mitochondrial Ca^{2+}-dependent protein kinase ε (PKC-ε) and stimulation of adenosine receptors.[194, 195]

The protective mechanism underling iPC appears to involve a mild generation of ROS. Indeed a relevant finding in the field was that antioxidants abolish iPC-induced cardioprotection.[118] Supporting this finding, other reports have shown that iPC-like protection can be induced by mild elevation in $[Ca^{2+}]_I$ and/or ROS.[196, 197] Also in this case, the RISK pathway, especially AKT, seems to represent the main mechanism.[192, 198] Indeed, most of the pathways involving mitochondria, Ca^{2+} and ROS seem to converge on cytosolic AKT.[75, 77, 199, 200] Up to date the link between ROS and AKT activation is not been yet clarified. Nevertheless, ROS although do not activate directly AKT or other kinases can stimulate their function indirectly through the inhibition of upstream phosphatases or activation of upstream kinases.[76, 77] In the case of AKT, ROS have been shown to directly activate phosphatidylinositol 3-kinase (PI3K) amplifying its downstream pathway and concurrently inactivate phosphatase and tensin homolog (PTEN), resulting in AKT activation.[201-203]

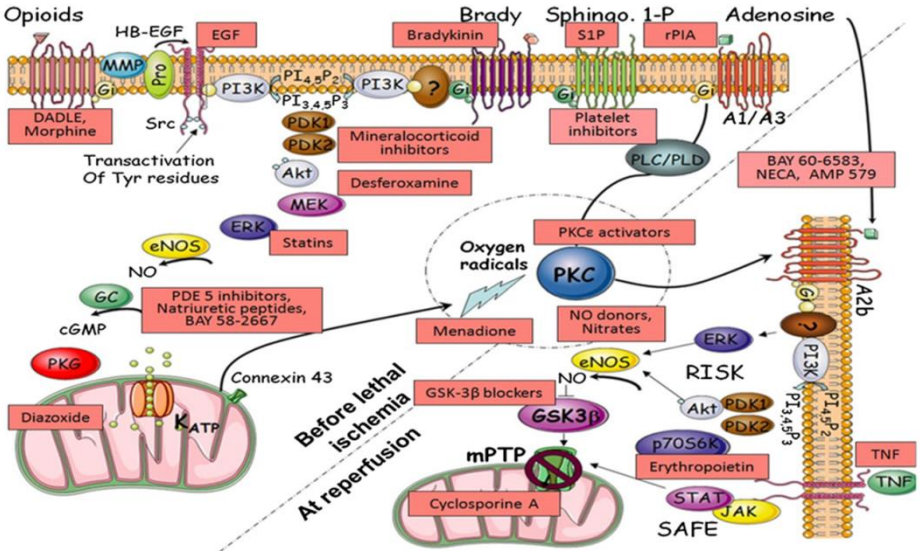

Figure 11. **Ischemic Preconditioning (iPC).** Summary map of proposed signaling pathways involved in iPC. Pink boxes indicate pharmacological intervention to reduce cardiac damage prior to reperfusion. (*Adapted from Hausenloy, D.J., et al., 2016, [191]*)

5 AIM OF THE WORK

This study aimed at characterizing the processes linking changes in mitochondrial ROS and Ca^{2+} homeostasis in the context of cardiac pathophysiology**.** In particular, we addressed the following points: (i) the effects of a primary increase in mitochondrial ROS formation; (ii) the role of MAO as a relevant source of ROS in mitochondria; (iii) the protective mechanisms triggered by a primary increase in either mitochondrial ROS or $[Ca^{2+}]$.

The attention was mostly focused on cardiac injury induced by ischemia and reperfusion (anoxia and reoxygenation in isolated cells). Diabetic cardiomyopathy was also investigated. In these pathological conditions a rise in mitochondrial $[Ca^{2+}]$ and ROS is usually considered a pivotal factor in determining cardiomyocyte dysfunction and loss of viability. On the other hand, a modest elevation in ROS is involved in endogenous protective mechanisms against cardiomyocyte injury. However, the direct contribution of ROS to injury and protection can hardly be singled out, since ROS elevation, especially in mitochondria, is invariably associated with or caused by other cellular events. To override this problem, we employed tools to cause a primary increase in mitochondrial ROS formation.

Regarding mitochondrial pathways involved in ROS formation, we evaluated the contribution of MAO that has been described as a powerful source of H_2O_2 formation in the heart. The characterization of MAO by means of specific substrates and inhibitors, as well as the use of agents causing a primary increase in mitochondrial ROS, allowed us to investigate whether ROS produced in mitochondria remained confined to these organelles or can modify cytosolic processes, such as cytosolic $[Ca^{2+}]$ homeostasis.

Finally, the effect of a primary increase in mitochondrial Ca^{2+} uptake or a mild elevation in ROS were used to investigate the interplay between mitochondrial $[Ca^{2+}]$ and ROS in cardiac protection. Besides characterizing the resulting protection, studies were carried out to clarify the signaling pathway leading from an increase of mitochondrial ROS and/or $[Ca^{2+}]$ to a decrease susceptibility to A/R injury.

6 MATERIALS AND METHODS

6.1 Cells cultures

6.1.1 Isolation and culture of neonatal rat ventricular myocytes (NRVMs)

Neonatal rat ventricular myocytes (NRVMs) were isolated from 1-3 days old Wistar rats as previously described.[56] Hearts were excised, cut into smaller pieces and left for overnight digestion with 2.5% trypsin 10X (Thermo Fisher Scientific) at 4°C in Hank's balanced salt solution (HBSS, Sigma). Next day, tissues were incubated with 0.75 mg/ml collagenase type II (Thermo Fisher Scientific) in HBSS for 10 min (at 2 min intervals) at 37°C and cells dissociated by pipetting. Following centrifugation at 1200 rpm for 7 min, cells were resuspended in minimum essential medium (MEM, Invitrogen) and pre-plated for 2 h, to let cardiac fibroblasts attach to the plastic surface. Plates/coverslips were coated with a solution of 0.1% porcine gelatin (Sigma) and incubated at 37°C for 1 h. The non-adherent myocytes were plated in gelatin coated plates at variable density (at least $1x10^5$ cells/ml) in MEM supplemented with 10% fetal bovine serum (FBS, Thermo Fisher Scientific), 1% penicillin/streptomycin (P/S, Thermo Fisher Scientific), 1% non-essential amino acids (NEAA, Thermo Fisher Scientific), 1 mM 5-Bromo-2-Deoxyuridine (BrdU, Sigma). Cells were maintained at 37°C in presence of 5% CO_2. The medium was changed to MEM supplemented with 1% FBS, 1% P/S and 1% NEAA after 24 h of plating.

6.1.2 Culture of Min6 β-cells

Min6 β-cells, an insulinoma transformed cell line [204], were grown in Dulbecco's modified Eagle's medium (DMEM, Thermo Fisher Scientific) high glucose (4 g/L – 23 mM), supplemented with 15% FBS, 1% P/S and maintained at 37°C in presence of 5% CO_2. Medium was changed every 2-3 days and cells were splitted every 5-7 days when they reached ~60% confluency.[204, 205]

6.2 Cells treatments

6.2.1 Treatment of NRVMs

To evoke a primary increase in mitochondrial ROS, NRVMs were treated in culture medium with different concentrations of MitoPQ [206], from 0.01 to 1 µM for 2 h, unless specified in results.

To mimic diabetes, NRVMs were treated in culture media with following additions: normal glucose (NG, 5 mM), high glucose (HG, 25 mM) or high mannitol (HM 25 mM, osmotic control), in presence or absence of interleukin-1β (IL-1β, 25 ng/ml, Sigma). ROS formation were measured after 48 h for pro-longed treatment and after 1 h for short treatment, with or without 30 min of pretreatment with HG to avoid an osmotic effect. Ca^{2+} transients were analyzed before and after 1 h of treatment with HG and IL-1β as described in results.

To inhibit MAO activity, cells were pretreated with 100 µM pargyline (Sigma), a specific and irreversible inhibitor of both MAO isoforms [207], for 30 min. To scavenge ROS, cells were pretreated with 500 µM N-(2-Mercaptoproprionyl)glycine (MPG, Sigma) [171] for 30 min. To prevent PTP opening, cells were pretreated with 0.5 or 1 µM Cyclosporin A (CsA, Sigma) [208] for 30 min.

6.2.2 Treatment of Min6 β-cells

To evoke a primary increase in cytosolic ROS levels, Min6 β-cells were cultured on 0.1% poly-L-lysine (Sigma) treated coverslips (2 h) and incubated at 37°C in DMEM high glucose for a total time of 1 h in presence of 10 µM AlClPc.[209] Photoactivation of AlClPc was triggered by means of 660 nm LED, that was activated in a pulsed-light fashion for 100 ms/pulse and 1 pulse/second, filtering the light through a pair of polarizers to modulate LED intensity.[210]

6.3 Amplification and purification of DNA plasmids

Competent DH10B E. Coli cells were mixed with 100 ng of DNA plasmid, incubated on ice for 5 min, and then heat shocked by keeping them at 42°C in a termoblock for 30 sec. The aliquot was immediately returned to ice for 2 min. Cells were then distributed in previously prepared LB agar plates containing ampicillin (100 µg/ml)

or kanamycin (100 µg/ml), according to the plasmid resistance. The plates were incubated in a stationary 37°C incubator to grow the bacterial colonies.

One colony from LB agar plate seeded with transformed DH10B E. coli was collected and inoculated in a 250 ml overnight culture of LB medium at 37°C. On the following morning, the bacteria culture was centrifuged at 4000 rpm for 10 min and DNA plasmid was extracted and purified following the manufacturer's instructions of a commercial kit (PureLink HiPure Plasmid Maxiprep Kit, Life technologies).

6.4 Fluorescence microscopy

- **NRVMs:** Experiments were carried out at 37°C and cells maintained in HBSS at pH 7.4 (adjusted with NaOH). The HBSS was composed of 137 mM NaCl, 5 mM KCl, 0.4 mM $MgSO_4$, 0.4 mM $MgCl_2$, 0.4 mM KH_2PO_4, 0.4 mM Na_2HPO_4, 0.4 mM $NaHCO_3$, 2 mM $CaCl_2$, 5.5 mM D-glucose.

  Images were acquired using an inverted fluorescence microscope (Leica DMI6000B equipped with DFC365FX camera). Fluorescence intensity was quantified using the Fiji distribution of the Java-based image processing program ImageJ (NIH, [211]), and background signal was subtracted from all analyzed regions of interest (ROIs). For Ca^{2+} imaging, traces were analyzed using the "Peak Analyzer" tool of Origin Pro 9.1.

- **Min6 β-cells**: Experiments were conducted at room temperature under constant flow perfusion with a saline buffer at pH 7.4 (adjusted with NaOH). The saline buffer was composed of 150 mM NaCl, 5 mM KCl, 1 mM MgCl, 10 mM Hepes, 2 mM NaPyr, 2 mM $CaCl_2$, and either 3 or 25 mM D-glucose. 15 mM Tetra Ethyl Ammonium (TEA, a K^+ channel blocker) chloride was added to the saline buffer containing 25 mM D-glucose.[205, 210] Where indicated, SERCA were inhibited by the addition of 0.2 µM thapsigargin (Tg, SIGMA).

  Images were acquired using an upright fluorescence microscope equipped with a complementary metal-oxide semiconductor (CMOS) cooled camera (Pco.Edge). Fluorescence intensity was quantified with software developed using the Matlab platform (Release 14, MathWorks, Inc., Natick, Ma, USA), and background signal

was subtracted from all analyzed ROIs. For Ca^{2+} imaging, traces were analyzed using an ad-hoc developed Matlab function that identified local maxima.

6.5 Measurement of mitochondrial ROS formation

6.5.1 Assessment of ROS formation with MitoTracker Red in NRVMs

To monitor mitochondrial ROS formation, cells were incubated with 25 nM MitoTracker Red CM-H_2XRos (**Figure 12**, MTR, Thermo Fisher Scientific, excitation/emission 579/599 nm) for 30 min at 37°C in a humidified incubator. MTR is a reduced dye that fluoresces upon oxidation and accumulates inside the mitochondria depending on the ΔΨm. Results were normalized to the control value (DMSO vehicle), and were expressed as % vs control.

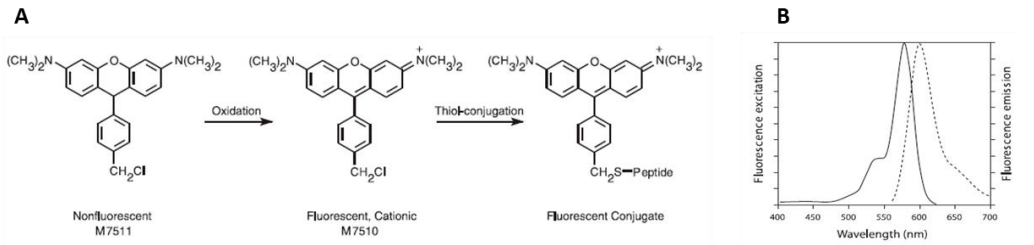

Figure 12. A) MitoTracker Red CM-H_2XRos intracellular reaction. **B)** MitoTracker Red CM-H_2XRos fluorescence spectra. (*Adapted from MitoTracker manuals and protocols, Thermo Fisher Scientific*)

6.5.2 Assessment of superoxide formation with MitoSOX in Min6 β-cells

To measure mitochondrial superoxide formation, cells were incubated with 2.5 µM MitoSOX (**Figure 13**, Thermo Fisher Scientific, excitation/emission 510/580 nm) for 15 min at 37°C in a humidified incubator. MitoSOX is a reduced dye that fluoresces upon oxidation and accumulates inside mitochondria depending on ΔΨm. Results were expressed as $\Delta F/F_0$, where ΔF is MitoSOX emission intensity excited at 510 nm divided by F_0, that indicates pre-stimulus intensity average.

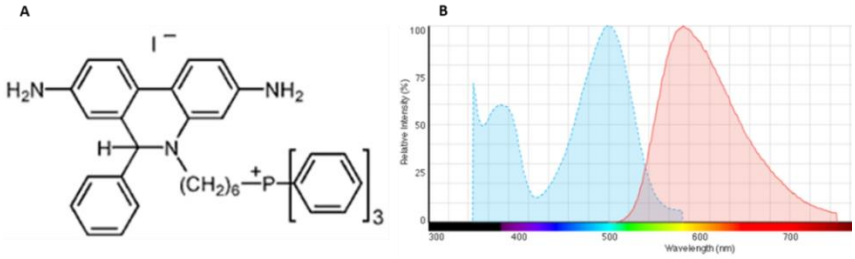

Figure 13. A) MitoSOX molecular structure. **B)** MitoSOX fluorescence spectra. (*Adapted from MitoSOX manuals and protocols, Thermo Fisher Scientific*)

6.5.3 Transfection of cells and assessment of H_2O_2 formation with HyPer

H_2O_2 formation in NRVMs and Min6 β-cells was measured using genetically encoded H_2O_2 sensors p-HyPer-dMito and p-HyPer-dCyto (MitoHyPer, CytoHyPer, Evrogen) [212], targeted either to mitochondria or cytosol. HyPer is a ratiometric sensor with two excitation maxima (420/500 nm), and one emission maximum (516 nm).[213] Upon exposure to H_2O_2, the intensity of the 420 nm peak decreases proportionally to the increase of the intensity of the 500 nm peak. An increase in H_2O_2 levels is directly proportional to the increase in fluorescence ratio F500/F420 (**Figure 14**).[214]

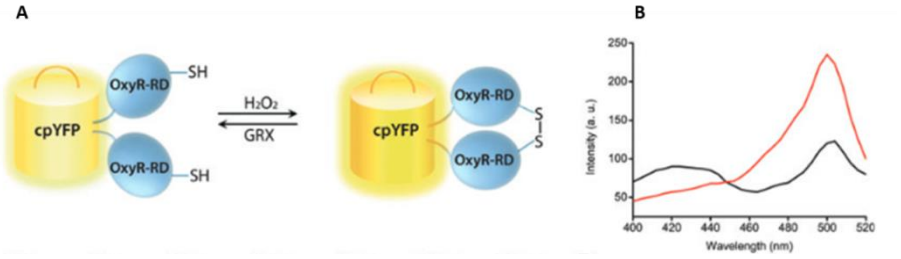

Figure 14. A) Scheme of HyPer structure and its oxidation and reduction reaction. **B)** Excitation spectra of reduced (*black line)* and full oxidized (*red line*) HyPer. (*Adapted from Bilan, D.S. & Belousov, V.V., 2016, [214]*)

NRVMs were plated in 6-well plates at a density of $3x10^5$ cells/well and transfected with two methods:

- **Calcium Phosphate**: for each transfection, 2 µg of plasmid (MitoHyPer or CytoHyPer) were rapidly mixed with ice cold 0.25 M $CaCl_2$ in HBS 2X (274 mM NaCl, 10 mM KCl and 1.4 mM Na_2HPO_4) and left for 4 min to precipitate. The mixture was added to the cells, and after 4 h of incubation cells were rinsed with PBS and new MEM was added. Transfected cells were used for experiments after 48 h.

- **Lipofectamine 3000**: for each transfection, 2.5 µg of MitoHyPer were rapidly mixed with 5 µl of P3000™ reagent in 125 µl of Opti-MEM medium (Thermo Fisher Scientific). Subsequently 4 µl of Lipofectamine™ 3000 (Sigma) were diluted in 125 µl of Opti-MEM medium, and both aliquots were left for 5 min at room temperature. The diluted DNA was added to the diluted Lipofectamine™ 3000, mixed well and incubated for 15 min at room temperature. The DNA-lipid complexes were added to the cells and incubated overnight. The day after, cells were rinsed with PBS and new MEM was added. Transfected cells were used for experiments after 48 h.

Min6 β-cells were plated in 24-well plates at density of 10^5 cells/well and transfected with the **Lipofectamine 3000** method as described.

Results were expressed as intensity of fluorescence ratio (500/420, NRVMs) or as $\Delta R = R - R_0$ (Min6 β-cells), where R represents fluorescence ratio, and R_0 represents average ratio at baseline.

6.6 Assessment of mitochondrial membrane potential (ΔΨm) in NRVMs

Cells were incubated with 25 nM tetramethylrhodamine (TMRM, Thermo Fisher Scientific) in presence of 1.6 µM cyclosporin H (CsH) for 30 min at 37°C in presence of 5% CO_2. TMRM (**Figure 15**, Thermo Fisher Scientific, excitation/emission 535/660) is a lipophilic rhodamine dye that accumulates into the mitochondria of live cells depending on their ΔΨm. Since a defective ETC may not lead to a detectable decrease in ΔΨm in case of compensation by the reverse activity of F_0F_1 ATP Synthase [215], TMRM fluorescence intensity was monitored following addition of 4 µM oligomycin (Sigma). After incubation, images were acquired before and after the addition of 4 µM carbonyl cyanide-p-trifluoromethoxyphenylhydrazone (FCCP, Sigma), a protonophore (H^+ ionophore) and a potent mitochondrial OxPhox uncoupler, to completely abolish ΔΨm. In order to exclude artifacts due to different TMRM loading in various cells, and to avoid erroneous interpretation of TMRM fluorescence, results were expressed ΔF according to the following formula: $\Delta F = F_0/F_{FCCP}$, where F_0 = TMRM fluorescence intensity at baseline; F_{FCCP} = fluorescence after addition of FCCP.[216] TMRM fluorescence

intensity was quantified as described and data were expressed as % vs control initial value.

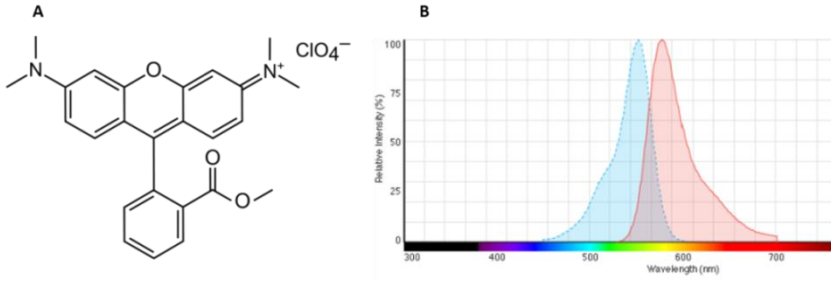

Figure 15. A) TMRM molecular structure. **B)** TMRM fluorescence spectra (*Adapted from TMRM manuals and protocols, Thermo Fisher Scientific*)

6.7 Assessment of PTP opening in NRVMs

NRVMs cells were incubated with 1 µM Calcein acetoxymethyl (AM) ester (Thermo Fisher Scientific) in presence of 1 mM Cobalt Chloride ($CoCl_2$) for 15 min at 37°C in a humidified incubator.[217] The slow mitochondrial uptake of cobalt prevents this cation to quench calcein accumulated in mitochondria. In this way, upon cobalt addition calcein fluorescence is quenched. In addition, cobalt does not promote PTP opening, such as other metal ions with the same quenching property (i.e. Cu^{2+}, Mn^{2+}).[218] After incubation, cells were washed and external Co^{2+} was removed. PTP opening was expressed as the decrease in calcein fluorescence. In fact, when the PTP opens it permits the efflux of molecules up to 1.5 kDa.[33] PTP inducers cause the efflux of calcein (622 Da) from the mitochondria, leading to a decrease in mitochondrial fluorescence. In addition, calcein is an hydrophilic molecule that does not bind membranes (i.e. mitochondrial membranes) and does not interact with Ca^{2+}, resulting in no changes in fluorescence intensity.[217] Data are expressed as % of initial value.

6.8 Assessment of Ca^{2+} homeostasis

6.8.1 NRVMs

NRVMs were incubated with 5 µM Fluo-4 acetoxymethyl (AM) ester (**Figure 16**, Thermo Fisher Scientific, excitation/emission 494/506), 0.01% w/v Pluronic F-127 (Sigma) and 250 µM Sulfinpyrazone (Sigma), for 20 min at 37°C in MEM followed by 20 min of de-esterification. Pluronic and Sulfinpyrazone were used to prevent the

complexation and secretion of the dye. Images were acquired continuously at 1 frame/second. Results are calculated according to the ratio $\Delta F/F_0$, where ΔF = Fluorescence – F_0 and F_0 = average of fluorescence at baseline. Amplitude, area under curve and frequency are expressed as % vs DMSO.

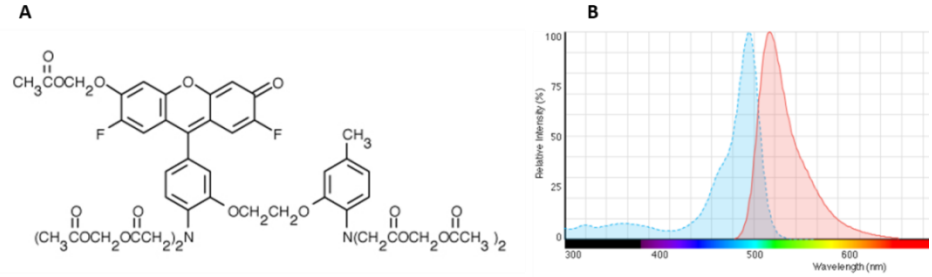

Figure 16. A) Fluo-4 AM molecular structure. **B)** Fluo-4 AM fluorescence spectra. (*Adapted from Fluo-4 manuals and protocols, Thermo Fisher Scientific*)

6.8.2 Mitochondrial Ca^{2+} imaging in NRVMs

NRVMs were plated in 6-well plates at a density of $3x10^5$ cells/well and transfected with Lipofectamine™ 3000. Cells were co-transfected with MCU plasmid DNA and mitochondrial targeted 4mt-GCaMP6f plasmid DNA. Transfections were performed delayed of 1 h each other. For each transfection, 2.5 µg of plasmid were rapidly mixed with 5 µl of P3000™ reagent in 125 µl of Opti-MEM medium (Thermo Fisher Scientific). Subsequently 4 µl of Lipofectamine™ 3000 (Sigma) were diluted in 125 µl of Opti-MEM medium, and both aliquots were left for 5 min at ambient temperature. The diluted DNA was added to the diluted Lipofectamine™ 3000 and incubated for 15 minutes at room temperature. The DNA-lipid complexes were added to the cells and incubated overnight. On the day after, cells were rinsed with PBS and new MEM was added. Transfected cells were used for experiments after 48 h.

Mitochondrial Ca^{2+} levels were measured using genetically encoded Ca^{2+} sensor 4mt-GCaMP6f (a kind gift of Professor Rizzuto's Laboratory).[219] 4mt-GCaMP6f is a ratiometric sensor with two excitation maxima (410/474 nm), and one emission maximum collected through a 515/530 nm band pass filter. Upon exposure to Ca^{2+}, the intensity of the 410 nm wavelenght does not change, while 474 nm peak displays a Ca^{2+}-dependent increase of the intensity. Thus, the ratio between the two wavelengths (F474/F410) will always be independent of sensor expression. Images were acquired continuously at 1

frame/second. Results are expressed as $\Delta R/R_0$, where $\Delta R = R - R_0$, R = fluorescence Ratio, and R_0 represents average ratio at baseline. In addition, in order to compare results, data were expressed also as % vs Control Normoxia.

6.8.3 Min6 β-cells

Min6 β-cells were incubated with 5 µM Fura-2 acetoxymethyl (AM) ester (**Figure 17**, Thermo Fisher Scientific, excitation ratio 340/380, emission 510), 0.01% w/v Pluronic F-127 (Sigma) and 250 µM Sulfinpyrazone (Sigma), for 20 min at 37°C in DMEM followed by 20 min of de-esterification. Pluronic and Sulfinpyrazone were used to prevent the complexation and secretion of the dye. Images were acquired continuously at 1 frame/second. Results are expressed as $\Delta R = R - R_0$, where R represents fluorescence Ratio, and R_0 represents average ratio at baseline.

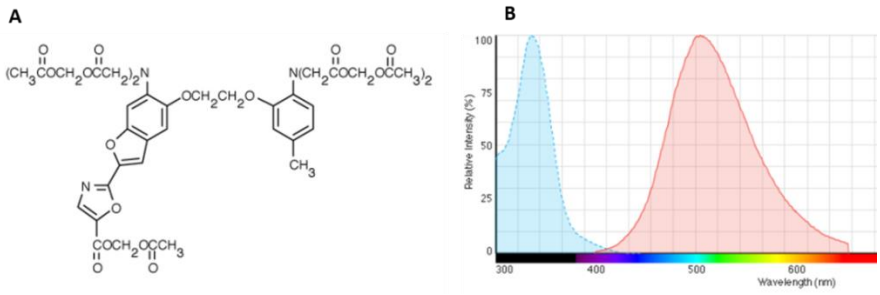

Figure 17. A) Fura-2 AM molecular structure. **B)** Fura-2 AM fluorescence spectra. (*Adapted from Fura-2 manuals and protocols, Thermo Fisher Scientific*)

6.9 Protein analysis by gel electrophoresis and western blot

NRVMs were plated in 6w plates at density of $4x10^5$ cells/well. Cells were lysates in 80 µl RIPA lysis buffer (Sigma) containing proteases (cOmplete mini protease inhibitor cocktail, Roche) and phosphatases (PhosSTOP, Roche) inhibitors. Samples were sonicated, centrifuged at 12000 x g for 15 min at 4°C and then the pellet was discarded. Protein concentration was determined using BCA Protein Assay Kit (Pierce) following the manufacturer's protocol. Samples were mixed with 1X NuPage sample buffer (Novex) and β-mercaptoethanol (3%) in order to denature and solubilize the proteins. Samples were boiled at 100°C for 10 minutes and then they were loaded on the gel or aliquoted and stored at -20°C.

Proteins were separated on 4-12% gradient SDS-PAGE (NuPage) using running buffer (50 mM MES, 50 mM Tris Base, 0.1% SDS, 1 mM EDTA, pH 7.3) at 150 V and transferred to the nitrocellulose membrane (Bio-rad) overnight using transfer buffer (25 mM Tris, 192 mM glycine, 10% methanol, pH 8.0) at 150 mA. The next day, the membrane was incubated with Red Ponceau dye (EuroClone) to stain all the proteins on the membrane, de-stained with NaOH, washed and saturated using 5% BSA dissolved in TBST (Tris buffered saline solution, 0.1% Tween 20), composed of 50 mM Tris-HCl, 85 mM NaCl, pH 7.4. After 1 h of blocking at room temperature, membranes were incubated at 4°C overnight with primary antibody diluted in BSA.

Following incubation with primary antibodies, membranes were washed three times for 10 min with the washing buffer TBST and incubated with secondary antibodies diluted in BSA for 1 h at room temperature. The following primary and secondary antibodies were used:

Rabbit Anti AKT total	Cell Signaling #9272	Dilution 1:1000
Rabbit Anti Phospho-AKT (Ser473)	Cell Signaling #9271	Dilution 1:1000
Anti Rabbit	Santa Cruz	Dilution 1:3000

6.10 Normoxia and Anoxia/Reoxygenation treatments protocols

- **Normoxia:** NRVMs were seeded in 24-well plates at density of 10^5 cells/well and cultured in MEM supplemented with 1% FBS, 1% P/S and 1% NEAA. Cells were incubated with different concentrations of MitoPQ (0.1 – 0.5 – 1 µM), with or without 100 µM pargyline, 500 µM MPG or 0.5 µM CsA for 24 h at 37°C in a humidified incubator.

- **Anoxia/Reoxygenation:** NRVMs were seeded in 24-well plates at density of 10^5 cells/well and incubated in 118 mM NaCl, 5 mM KCl, 1.2 KH_2PO_4, 1.2 mM $MgSO_4$, 2 mM $CaCl_2$, 25 mM MOPS pH 6.4 (anoxia) or 7.4 (reoxygenation).[220] Anoxia was induced adding 20 mM 2-deoxy-D-glucose (2-DG) and by incubation in a BD GasPak™ EZ Anaerobe Gas-generating Pouch System with an indicator (BD Biosciences) at 37°C for 12 h.[221] To induce reoxygenation, plates were removed from the GasPak™

pouch, 2-DG was replaced with 10 mM D-glucose, the pH was restored at 7.4 and the plates were incubated at 37°C in a humidified incubator for 1 h.

6.10.1 Assessment of cell death

The release of lactate dehydrogenase (LDH) from NRVMs was measured to evaluate cell death occurring in anoxia and reperfusion as described before.[208, 222] Supernatant aliquots were collected after 12 h of anoxia and 1 h of reoxygenation. At the end of the experiments, intact cells were lysed by means 1% Triton X-100 (Sigma) for 30 min and supernatant were collected to evaluate the total amount of LDH. LDH enzymatic activity was measured by spectrophotometrically measuring the absorbance of NADH (Roche) at 340 nm (reduction of pyruvate to lactate) as described in the following reaction.

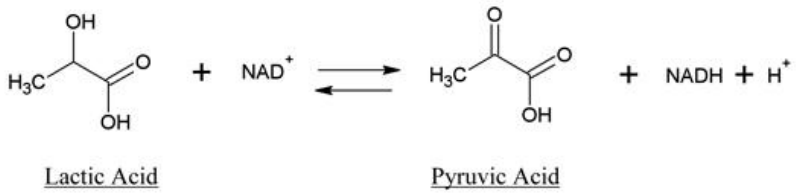

Data were expressed as % of LDH release compared to the % of total LDH (i.e. Anoxia + Reoxygenation + Lysate). Preliminary experiments were carried out to define the proper duration of anoxia and reoxygenation. Conditions were selected to obtain at least 50% decrease in cell viability. The reliability of the A/R protocol, as well as the involvement of the PTP, were assessed as illustrated in **Figure 18**.

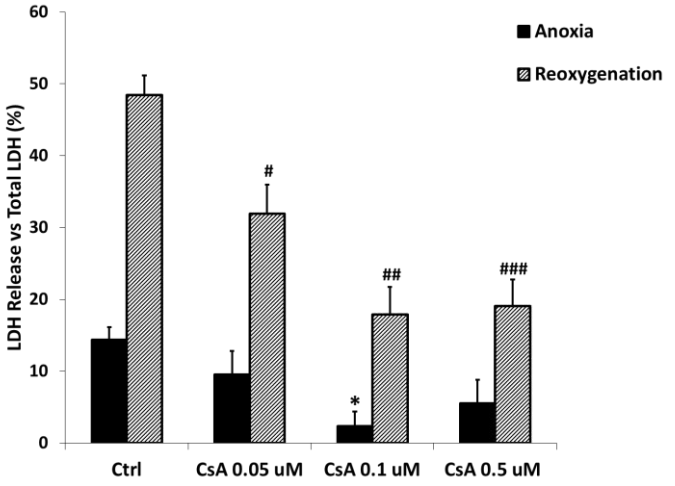

Figure 18. <u>NRVMs exposed to Anoxia/Reoxygenation protocol.</u> NRVMs were exposed to 12 h of anoxia and 1 h of reoxygenation and cell death was measured as the release of LDH. Treatment with different concentrations of CsA (10 min of pretreatment and treatment for the entire anoxia phase) reduces PTP-dependent cell death in a dose dependent manner, validating the reliability of the protocol. *p < 0.05 vs Ctrl Anoxia, #p < 0.05, ##p < 0.01, ###p < 0.001 vs Ctrl Reoxygenation. *CsA*: Cyclosporin A, *LDH*: Lactate Dehydrogenase, *NRVM*: Neonatal Rat Ventricular Myocytes

6.11 Mathematical modeling

We used a mathematical model of oscillatory behavior in β-cells [223] to investigate the effects of modifications in endoplasmic reticulum (ER) Ca^{2+} handling and Ca^{2+} oscillations. The model includes 4 voltage-gated currents: (i) a Ca^{2+} current (I_{Ca}), (ii) a delayed rectifier K^+ current (I_k), (iii) a Ca^{2+}-dependent K^+ current ($I_{k(Ca)}$), and (iv) an ATP-sensitive K^+ current ($I_{k(ATP)}$). All currents were modeled as reported.[223] The ratio ATP/ADP is allowed to vary according to evidence of ATP oscillations in Min6 β-cells.[224] The model also includes Ca^{2+} dynamics in the cytosol and in the ER. Influx into the ER, via SERCA, and ER efflux are modeled and CICR mechanism were simulated.[225] The main mechanism resulting in oscillatory behavior in the model is negative feedback of Ca^{2+} onto the ATP concentrations.[210] Simulations were performed in the XPPAUT software [226] using the cvode solver.

6.12 Statistical analysis

All values are expressed as mean ± S.E.M. Comparison between groups was performed by one-way ANOVA, followed by a Tukey's post hoc multiple comparison for normally distributed. Data that did not follow the normal distribution were statistically analyzed by the non-parametric Kolgomorov-Smirnov's test. Comparisons between two

groups were performed using non paired two-tailed Student's t-test. Statistical comparisons for experiments performed with Min6 β-cells were done with unpaired t test for samples with unequal variance. A value of $p < 0.05$ was considered significant.

7 RESULTS

7.1 MitoPQ induces a primary increase in mitochondrial ROS levels in a dose-dependent manner in NRVMs by means of MAO activation

The protocols available for increasing ROS are far from being specific, since they trigger several other effects making difficult the interpretation of the result. For instance, it is possible to increase mitochondrial superoxide production by treatment with respiratory complexes inhibitors (i.e. rotenone, antimycin) [227], but the main result is the disruption of ΔΨm and the decrease of ATP levels. Moreover, it is possible to decrease mitochondrial ROS using antioxidants or by means of the modulation of expression of endogenous MnSOD. Anyway, the total deletion of ROS could be detrimental for the physiological cell signaling.[228] In order to investigate the consequences of a primary increase in mitochondrial ROS on cell physiology, we selectively increased mitochondrial ROS treating NRVMs with the mitochondria-targeted compound MitoPQ (**Figure 19**).[206] MitoPQ is an analogue of the viologen paraquat (PQ, 1,1'-dimethyl-4,4'-bipyridinium dichloride), an herbicide commonly used to increase and study ROS production *in vitro* and *in vivo* [229], conjugated with a triphenylphosphonium (TPP) group. MitoPQ is a redox cycler at the level of the flavin site of complex I of the ETC, generating radical monocations that react rapidly with oxygen to generate superoxide.[230]

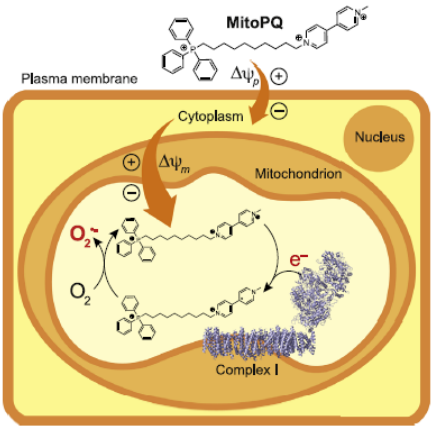

Figure 19. <u>Structure of MitoPQ and accumulation inside mitochondrial matrix</u>. MitoParaquat (MitoPQ) is composed by a paraquat molecule, an hydrophobic carbon chain and a mitochondria-targeting triphenylphosphonium cation. MitoPQ accumulates in mitochondrial matrix driven by the plasma and the mitochondrial membrane potentials. MitoPQ works as a redox cycler at the flavin site of complex I of the electron transport chain and reacts with O_2 to generate superoxide. (*Adapted from Robb, E.L., et al., 2015, [206]*)

Thus, NRVMs were treated for 2 h with different doses of MitoPQ. ROS levels were initially assessed with MTR.

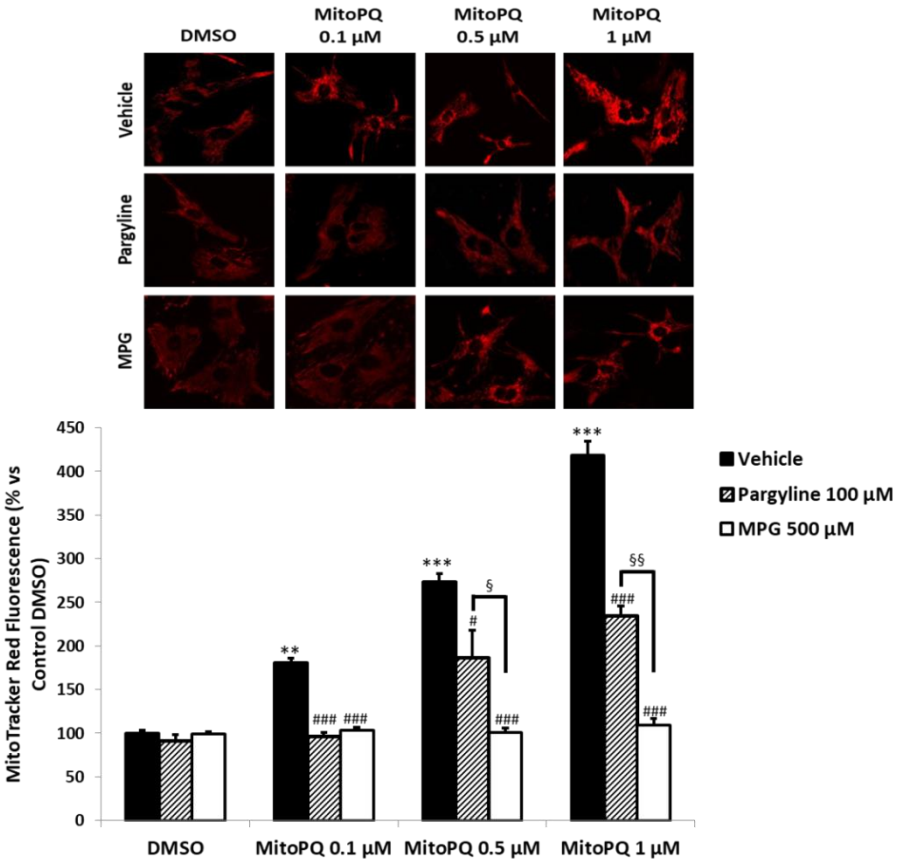

Figure 20. <u>Effects of MitoPQ on ROS formation</u>. Mitochondrial ROS formation monitored by MTR in isolated NRVMs treated for 2 h with different concentrations of MitoPQ (0.1 – 0.5 – 1 µM), with or without 30 min of pretreatment with 100 µM pargyline or 500 µM MPG. **p < 0.01, ***p < 0.001 vs DMSO vehicle; #p < 0.05, ###p < 0.001 vs MitoPQ; §p < 0.05, §§p < 0.01 pargyline vs MPG. *DMSO*: Dimethyl Sulfoxide, *MitoPQ*: Mitochondrial Paraquat, *MPG*: N-(2-Mercaptoproprionyl)glycine, *MTR*: MitoTracker Red CMH_2X-ROS, *NRVMs*: Neonatal Rat Ventricular Myocytes, *ROS*: Reactive Oxygen Species

MitoPQ caused a dose-dependent increase in mitochondrial ROS levels, that was not observed when cells were pretreated for 30 min with the antioxidant MPG (**Figure 20**).

However, MTR presents also some limitations: (i) it is not very sensitive, (ii) it is not specific for oxidant species, (ii) its accumulation depends on cell and mitochondrial membrane potential, that can be affected by different treatments independently of ROS formation, (iv) its emission fluorescence depends on the amount of the probe that accumulates in the mitochondrial matrix.[231] To investigate whether MitoPQ induced

ROS formation at low doses, we used the genetically encoded sensor MitoHyPer that detects submicromolar concentrations of H_2O_2.

MitoPQ doses ≤ 0.1 µM induced a significant increase in mitochondrial H_2O_2 levels in a dose-dependent manner (**Figure 21A-C**). In addition, cells were treated with an identical concentration of a MitoPQ analogue that does not undergo redox cycling (MitoPQ-Control 2). NRVMs treated with MitoPQ-Control 2 did not show any increase in mitochondrial H_2O_2 levels (**Figure 21B**).

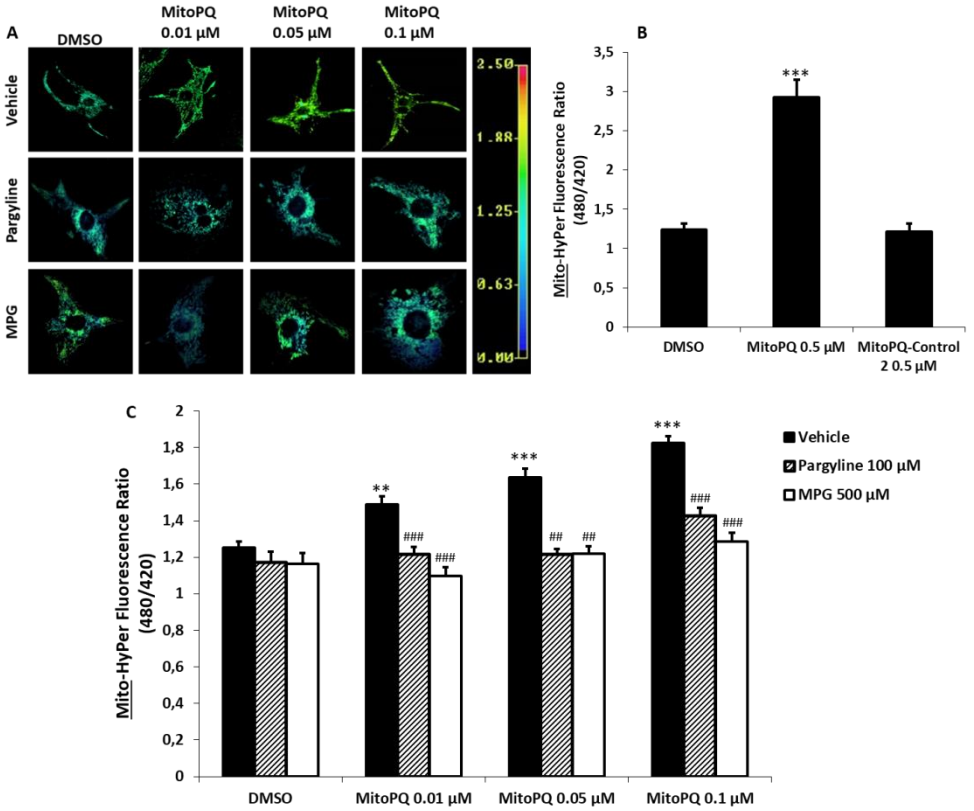

Figure 21. <u>Effects of MitoPQ on H_2O_2 formation</u>. A-C) Mitochondrial H_2O_2 formation measured by MitoHyPer in isolated NRVMs treated for 2 h with different concentrations of MitoPQ (0.01 – 0.05 – 0.1 µM), with or without 30 min of pretreatment with 100 µM pargyline or 500 µM MPG. **p < 0.01, ***p < 0.001 vs DMSO vehicle; ##p < 0.01, ###p < 0.001 vs MitoPQ. **B)** Mitochondrial H_2O_2 formation measured by MitoHyPer in isolated NRVMs treated for 2 h with 0.5 µM MitoPQ or with 0.5 µM MitoPQ-Control 2. ***p < 0.001 vs DMSO. *DMSO*: Dimethyl Sulfoxide, *MitoHyPer*: p-mito-dHyPer, *MitoPQ*: Mitochondrial Paraquat, *MitoPQ-Control 2*: Mitochondrial Paraquat Control compound 2, *MPG*: N-(2-Mercaptoproprionyl)glycine, *NRVMs*: neonatal rat ventricular myocytes, *ROS*: Reactive Oxygen Species

Next step was to investigate whether the measured H_2O_2 could be contributed by sources other than the ETC. In this respect, the attention was focused on MAOs that have

been shown to provide the relevant contribution to oxidative stress in the heart.[45, 58] In particular, we tested the possibility that MitoPQ-derived ROS could trigger an amplification pathway involving MAO activation. NRVMs were pretreated for 30 min with the MAO inhibitor pargyline [45] and then treated for 2 h with increasing doses of MitoPQ. Pargyline decreased significantly mitochondrial ROS accumulation induced by MitoPQ. This finding was obtained by using either MTR or MitoHyPer (**Figure 20**, **Figure 21**). However, pargyline was not able to counteract the increase in ROS induced by MitoPQ doses ≥ 0.5 μM.

Taken together, these results confirm that MitoPQ is an useful tool to induce a primary and dose-dependent increase in mitochondrial ROS levels in NRVMs. Moreover, results suggest that MAO can be triggered by low levels of ROS, leading to a further increase in ROS production.[232] In addition, data obtained with the MitoPQ-Control 2 indicate that mitochondrial ROS formation is due to the redox cycling property of MitoPQ.

7.2 A primary increase in mitochondrial ROS levels affects mitochondrial function in NRVMs

7.2.1 MitoPQ-induced ROS reduce mitochondrial membrane potential (ΔΨm) in a dose-dependent manner

Cardiac diseases involve oxidative stress and various alterations of mitochondrial functions, such as impaired OxPhos, decrease in ΔΨm, and PTP opening.[80, 233, 234] ROS increase and membrane potential impairment are tightly connected. For instance, an increase in mitochondrial ROS production has been reported to induce a decrease of ΔΨm, preceded or followed by PTP opening.[235, 236] Therefore, to investigate whether MitoPQ-induced ROS affect mitochondrial function, we monitored ΔΨm using TMRM fluorescence.

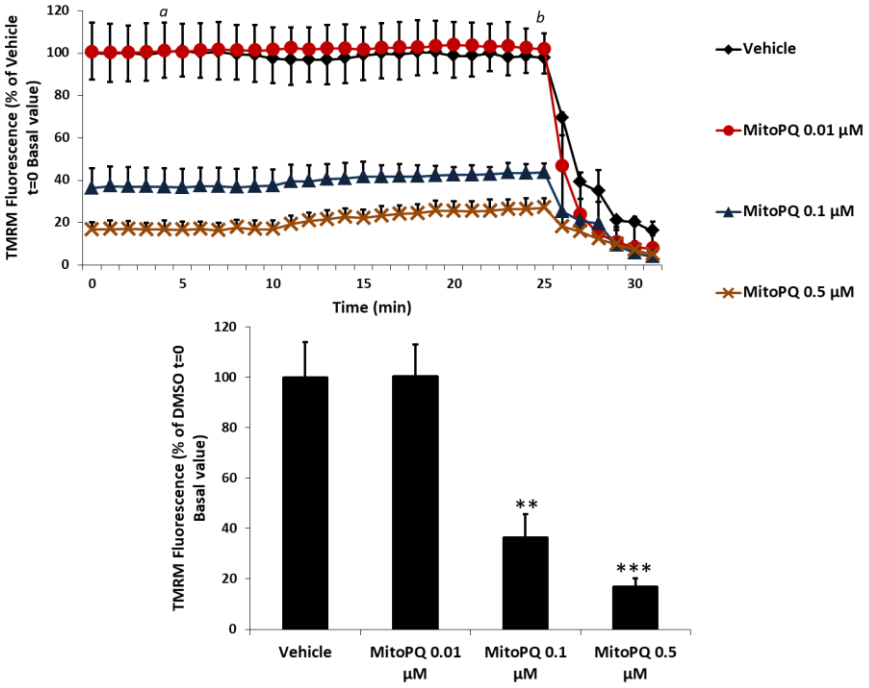

Figure 22. **Effects of MitoPQ on mitochondrial membrane potential**. Mitochondrial membrane potential (ΔΨm) monitored by TMRM fluorescence in isolated NRVMs treated for 2 h with different concentrations of MitoPQ (0.01 – 0.1 – 0.5 µM). *a*: 4 µM Oligomycin, *b*: 4 µM FCCP. **p < 0.01, ***p < 0.001 vs vehicle. *FCCP*: Carbonyl cyanide-p-trifluoromethoxyphenylhydrazone, *MitoPQ*: Mitochondrial Paraquat, *NRVMs*: Neonatal Rat Ventricular Myocytes, *ROS*: Reactive Oxygen Species, *TMRM*: tetramethylrhodamine,

NRVMs treated with different doses of MitoPQ displayed a dose-dependent decrease of ΔΨm (**Figure 22**). Notably, although promoting H_2O_2 formation (**Figure 21**) 0.01 µM MitoPQ did not affect ΔΨm. Since oligomycin [215] was present in all the experiments, the lack of ΔΨm variations at low MitoPQ doses suggests that a mild ROS formation is not likely to alter the ETC function.

Since pargyline reduced ROS induced by MitoPQ (**Figure 20**, **Figure 21**), we checked whether also mitochondrial dysfunction could be prevented by MAO inhibition.

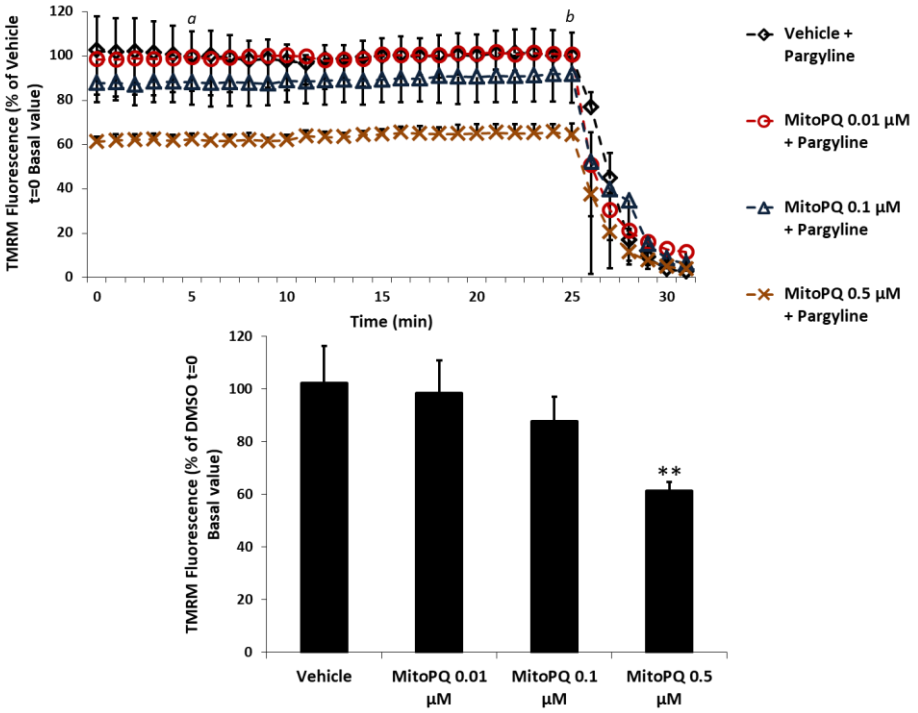

Figure 23. <u>Effects of MitoPQ and MAO inhibition on mitochondrial membrane potential</u>. Mitochondrial membrane potential (ΔΨm) monitored by TMRM fluorescence in isolated NRVMs treated for 2 h with different concentrations of MitoPQ (0.01 – 0.1 – 0.5 µM) with 30 min of pretreatment with 100 µM pargyine. *a*: 4 µM Oligomycin, *b*: 4 µM FCCP. **p < 0.01, vs vehicle. *FCCP*: Carbonyl cyanide-p-trifluoromethoxyphenylhydrazone, *MitoPQ*: Mitochondrial Paraquat, *NRVMs*: Neonatal Rat Ventricular Myocytes, *ROS*: Reactive Oxygen Species, *TMRM*: tetramethylrhodamine,

A 30 min pretreatment with pargyline, prevented completely the decrease of ΔΨm in cells treated with 0.1 µM MitoPQ. MAO inhibition could counteract only partially the large fall of ΔΨm induced by 0.5 µM MitoPQ (**Figure 23**).

Taken together, these results show that mitochondrial ROS formation induced by MitoPQ doses ≥ 0.1 µM decreases ΔΨm in a dose-dependent manner. Therefore, a primary mitochondrial oxidative stress alters mitochondrial function, although this does not occur at low ROS levels. In addition, MitoPQ appears to trigger MAO activity that provides relevant contribution to ROS formation and ΔΨm fall at MitoPQ doses ≥ 0.1 µM.

7.2.2 MitoPQ-induced ROS formation causes PTP opening

Several studies show that ROS facilitate PTP opening by means of several mechanisms including modulation of CyPD binding to the IMM [184], direct oxidation of

crucial CyPD cysteine (Cys 203) [237], and redox modulation of F_0F_1-ATP synthase.[238] The study of the causal relationship between PTP, ROS formation and mitochondrial dysfunction is complicated by the fact that PTP opening is both a cause and a consequence ΔΨm fall and mitochondrial ROS generation.[183, 239, 240] In this respect, MitoPQ represents a unique tool to determine the degree of oxidative stress necessary to induce PTP opening.[73, 184, 241]

PTP opening was assessed by monitoring calcein fluorescence.[217, 242] NRVMs were pretreated with or without CsA, a desensitizer of the PTP. Since CsA is also an inhibitor of the multidrug resistance (MDR) P-glycoprotein, cells were pretreated also with cyclosporine H (CsH) which inhibits MDR but does not affect PTP opening.[243]

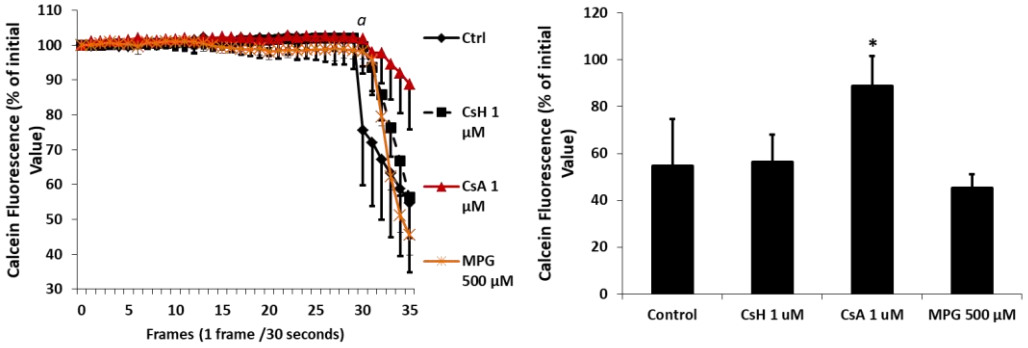

Figure 24. **Effect of calcimycin on PTP opening.** PTP opening monitored by decrease of calcein fluorescence in isolated NRVMs pretreated for 30 min with or without 1 µM CsH, 1 µM CsA or 500 µM MPG. *a*: 5 µM Calcimycin. *p < 0.05 vs Ctrl. *Ctrl*: Control untreated, *CsA*: Cyclosporin A, *CsH*: Cyclosporin H, *MPG*: N-(2-Mercaptoproprionyl)glycine, *NRVMs*: Neonatal Rat Ventricular Myocytes.

Initially we tested the reliability of this procedure in NRVMs. Cells were treated with the Ca^{2+} ionophore calcimycin that resulted in decrease in calcein fluorescence. The inhibition afforded by CsA allowed the attribution of the fluorescence decrease to PTP opening, that was further supported by the lack of effect of CsH (**Figure 24**).

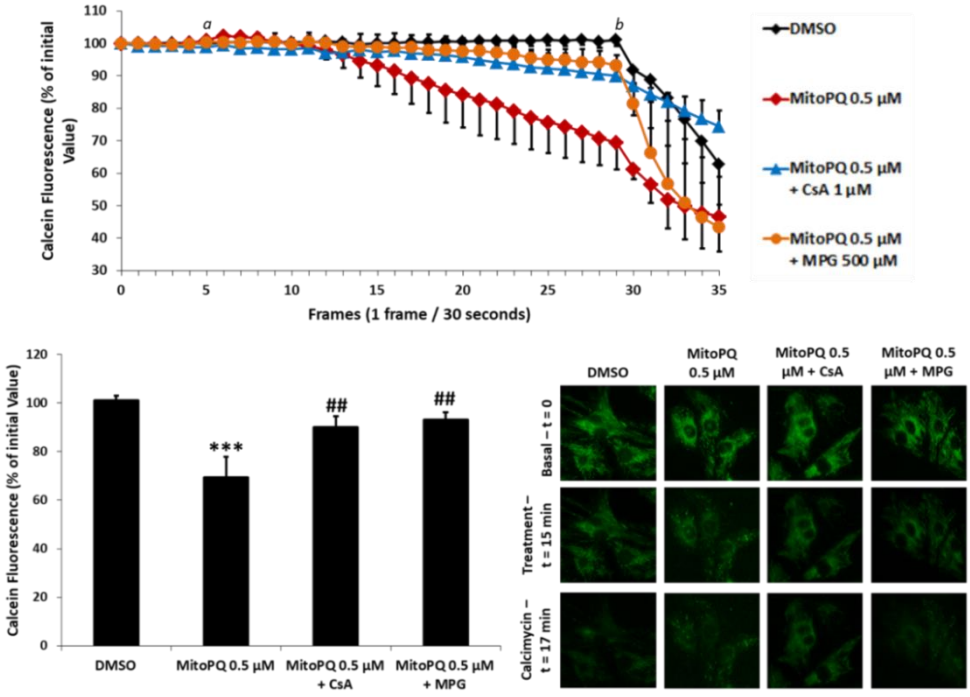

Figure 25. <u>Effects of MitoPQ on PTP opening.</u> PTP opening monitored by decrease of calcein fluorescence in isolated NRVMs pretreated for 30 min with or without 1 µM CsA or 500 µM MPG. *a*: treatment with DMSO as control or 0.5 µM MitoPQ; *b*: 5 µM Calcimycin. ***p < 0.001 vs DMSO; ##p < 0.01 vs MitoPQ. *CsA*: Cyclosporin A, *DMSO*: Dimethyl Sulfoxide, *MitoPQ*: Mitochondrial Paraquat, *MPG*: N-(2-Mercaptoproprionyl)glycine, *NRVMs*: Neonatal Rat Ventricular Cardiomyocytes

Treatment with 0.5 µM MitoPQ induced a rapid decrease in calcein fluorescence (~30%) that was prevented by CsA. MitoPQ-induced PTP opening was dependent on ROS formation since it was abolished by MPG. Notably, MPG did not display any effect when PTP opening was induced by calcimycin (**Figure 25**).

Taken together, these results indicate that ROS induced by 0.5 µM MitoPQ induce PTP opening in NRVMs.

7.3 A primary increase in mitochondrial ROS levels affects NRVMs function and viability

7.3.1 MitoPQ-induced ROS formation impairs $[Ca^{2+}]_I$ homeostasis in a dose-dependent manner

We hypothesized that mitochondrial-derived ROS could interact with cellular sites and functions other than mitochondria. Therefore we evaluated whether mitochondrial ROS could interfere with cytosolic processes. In particular, since the objects of our investigation were cardiomyocytes, the attention was focused on $[Ca^{2+}]_I$ homeostasis.[244, 245] $[Ca^{2+}]$ homeostasis was monitored with Fluo-4 AM in NRVMs pretreated with different concentrations of MitoPQ.

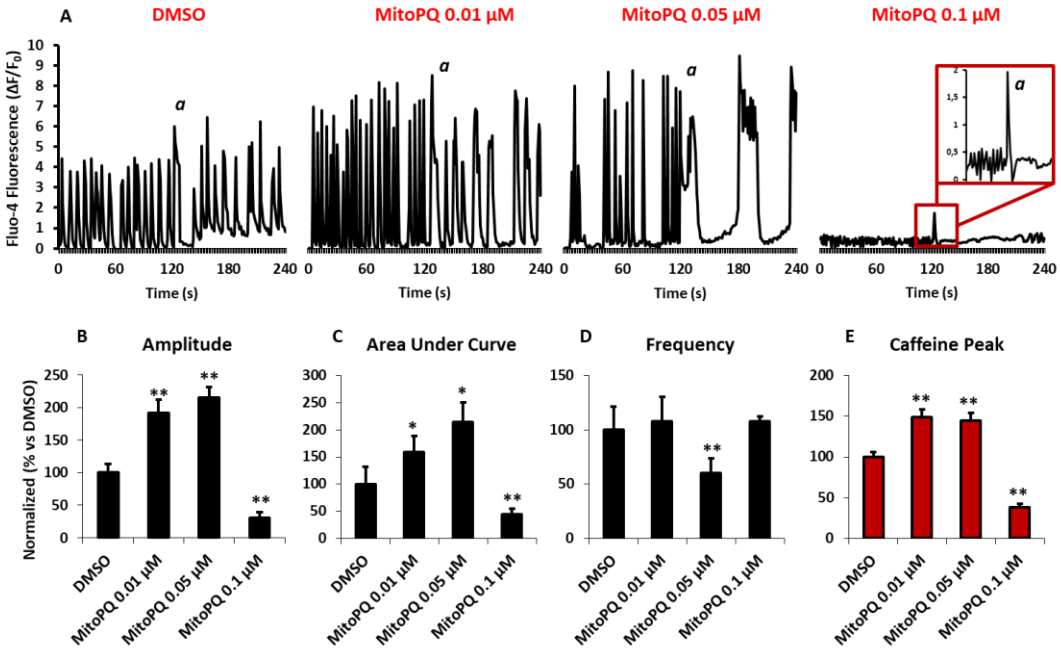

Figure 26. <u>Effects of MitoPQ on intracellular $[Ca^{2+}]$ homeostasis.</u> Intracellular $[Ca^{2+}]$ homeostasis monitored by Fluo-4 AM in isolated NRVMs treated for 2 h with different concentrations of MitoPQ (0.01 – 0.05 – 0.1 µM). **A**) Comparison between intracellular Ca^{2+} oscillatory patterns. *a*: 10 mM Caffeine. **B**) Peak amplitude average; **p < 0.01 vs DMSO; **C**) Area Under Curve (AUC) average; *p < 0.05, **p < 0.01 vs DMSO; **D**) Peaks Frequency average; **p < 0.01 vs DMSO; **E**) Caffeine Peak average; **p < 0.01 vs DMSO. *DMSO*: Dimethyl Sulfoxide, *MitoPQ*: Mitochondrial Paraquat, *NRVMs*: Neonatal Rat Ventricular Myocytes

Treatment with 0.01 µM MitoPQ caused a significant increase in both amplitude (**Figure 26B**) and caffeine peak (**Figure 26E**), without affecting the oscillatory pattern or the frequency (**Figure 26A-D**). Doses of MitoPQ > 0.01 µM induced dose-dependent alterations in all the oscillatory parameters (**Figure 26**). In particular, at 0.1 µM MitoPQ,

$[Ca^{2+}]_I$ homeostasis was disrupted and cells became unexcitable (**Figure 26**). Higher doses could not be tested because of loss of viability described below.

Overall, these findings demonstrate that ROS produced within mitochondria can travel to the cytosol altering $[Ca^{2+}]_I$ homeostasis and mechanical activity. We think that this is the first direct evidence of the alterations of cytosolic processes induced by a primary mitochondrial ROS formation. Nevertheless, it is worth pointing out that the alteration of cytosolic processes requires a burst of mitochondrial ROS and that it is not detectable at low MitoPQ doses.

7.3.2 MitoPQ-induced ROS formation reduces cell viability in a dose-dependent manner by means of PTP opening

Oxidative stress related to mitochondrial dysfunction is known to jeopardize cell viability.[65, 246] Thus, we investigated whether MitoPQ-induced oxidative stress could lead to cell death in NRVMs. The loss of cell viability was measured as LDH release in NRVMs treated for 24 h with increasing doses of MitoPQ.

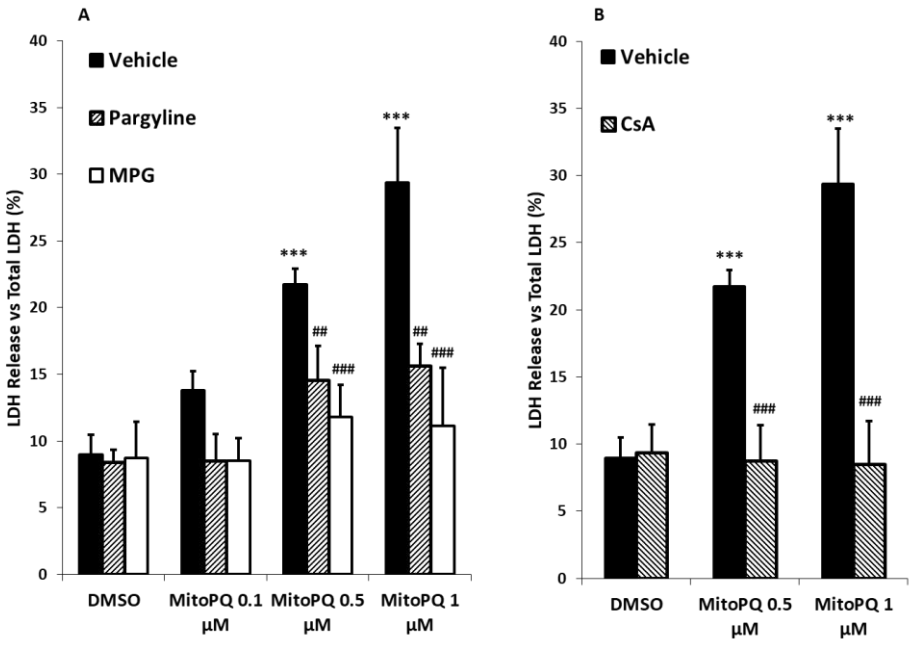

Figure 27. <u>Effects of MitoPQ on cell viability</u>. Cell death monitored by LDH release released from isolated NRVMs treated for 24 h with different concentrations of MitoPQ (0.1 – 0.5 – 1 µM). **A**) NRVMs pretreated with or without 100 µM pargyilne or 500 µM MPG. ***p < 0.001 vs DMSO vehicle, ## p < 0.01, ###p < 0.001 vs MitoPQ. **B**) NRVMs pretreated with or without 0.5 µM CsA. ***p < 0.001 vs DMSO vehicle, ###p < 0.001 vs MitoPQ. *CsA*: Cyclosporin A, *DMSO*: Dimethyl Sulfoxide, *LDH*: lactate dehydrogenase, *MitoPQ*: Mitochondrial Paraquat, *MPG*: N-(2-Mercaptoproprionyl)glycine, *NRVMs*: Neonatal Rat Ventricular Myocytes

MitoPQ doses ≥ 0.5 μM induced a significant increase in cell death (~30%), that was not observed at 0.1 μM MitoPQ (**Figure 27A**). It is worth pointing out that this latter dose of MitoPQ induces ROS formation, mitochondrial dysfunction and $[Ca^{2+}]_I$ dyshomeostasis without causing cell death. Therefore, we hypothesized that decrease in cell viability was related to PTP opening.[247, 248] Indeed, CsA treatment prevented significantly the occurrence of cell death induced by MitoPQ doses ≥ 0.5 uM (**Figure 27B**).

Similar protection was obtained by pretreating the cells with the MPG or pargyline (**Figure 27A**), indicating the causal relationship between MitoPQ-induced ROS formation and PTP opening. Regarding pargyline cell viability was not maintained at MitoPQ doses ≥ 0.5 μM that is when MAO inhibition was without effect against MitoPQ-induced mitochondrial ROS formation. This observation suggests that (i) the amplification pathway involving MAO is crucial for causing cell death at intermediate MitoPQ doses, and that (ii) a severe oxidative stress hampers cell viability independently of MAO activity, as shown by the protection afforded by MPG (**Figure 27A**).

7.4 Mitochondrial ROS in a model of diabetes

7.4.1 High glucose and interleukin-1β induce mitochondrial and cytosolic H_2O_2 formation by means of MAO activation in NRVMs

It is widely accepted that hyperglycemia is associated with oxidative stress and mitochondrial dysfunction, which are both involved in DCM.[249, 250] Nevertheless, the sources of ROS formation that are more relevant in diabetes-induced oxidative stress and the mechanism underling mitochondrial dysfunction are still matter of debate.[130, 251] Recently, the contribution of MAO-induced oxidative stress was described in cardiac pathology.[45, 58] Thus, we investigated the involvement of MAOs in oxidative stress in NRVMs exposed to a diabetes-like protocol. To this aim, high glucose (HG) was added with interleukin-1β (IL-1β) to mimic inflammation that is frequently associated with diabetes and metabolic syndrome. Indeed, patients with DCM display elevated levels of inflammatory cytokines in circulating blood, such as TNF-α and interleukins.[252, 253]

NRMVs were treated with HG and IL-1β with or without pargyline, and ROS formation was monitored by means of HyPer constructs targeted either to mitochondria or cytosol.

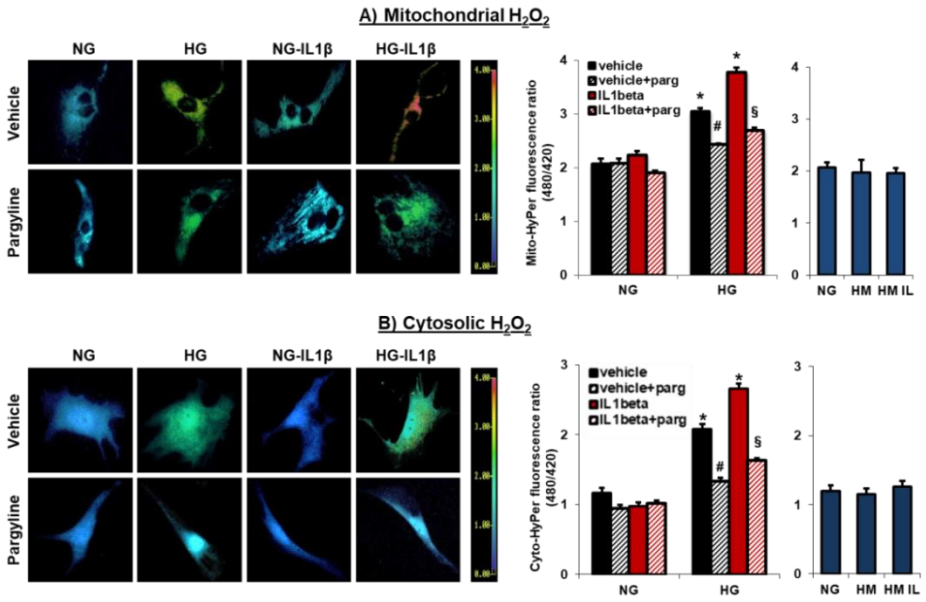

Figure 28. Effects of High Glucose and IL-1β on H_2O_2 formation. **A**) Mitochondrial and **B**) cytosolic H_2O_2 formation monitored by HyPer constructs after 48 h of treatment with NG (5 mM), HG (25 mM) and HM (25 mM) in presence or absence of 25 ng/ml IL-1β, with or without 100 µM pargyline. *p < 0.05 vs NG vehicle, #p < 0.05 vs HG vehicle, §p < 0.05 vs HG + IL-1β. *NG*: Normal Glucose, *HG*: High Glucose, *HM*: High Mannitol *IL-1β*: Interleukin-1β, *NRVMs*: Neonatal Rat Ventricular Myocytes.

HG induced a significant increase in both mitochondrial (**Figure 28A**) and cytosolic (**Figure 28B**) H_2O_2 formation. The H_2O_2 elevation obtained with HG was further enhanced by co-treatment with IL-1β. In any case, pargyline significantly prevented the increase in H_2O_2 formation both in mitochondria and in cytosol. To rule out the possibility that the increase in HyPer fluorescence was not due to an osmotic effect, incubation with HG was compared to incubation with high mannitol (HM). This latter treatment did not cause any change in HyPer fluorescence (**Figure 28A-B**).

Since HG has been reported to induce phasic changes in mitochondrial ROS levels [254], we investigated whether HG and IL-1β could induce also a rapid increase in H_2O_2 levels in cardiomyocytes.

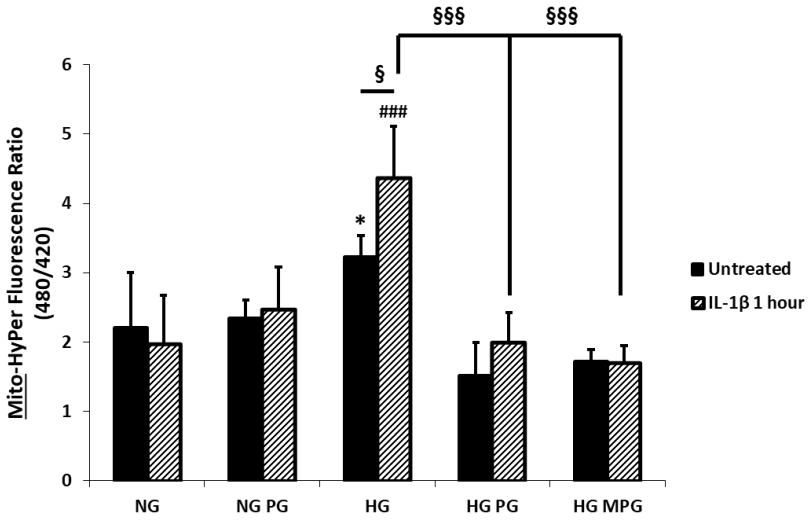

Figure 29. Mitochondrial H_2O_2 elevation induced by short-term treatments with HG and IL-1β. Mitochondrial H_2O_2 formation monitored by MitoHyPer after 30 min of treatment with NG (5 mM) and HG (25 mM Untreated), and 1 h after the treatment with 25 ng/ml IL-1β, pretreated for 30 min with or without 100 µM pargyline or 500 µM MPG. *p < 0.05 vs NG untreated, ###p < 0.001 vs HG untreated, §p < 0.05 HG untreated vs HG + IL-1β, §§§p < 0.001 vs HG + IL-1β. *NG*: Normal Glucose, *HG*: High Glucose, *IL-1β*: Interleukin-1β, *MPG*: N-(2-Mercaptoproprionyl)glycine, *NRVMs*: Neonatal Rat Ventricular Myocytes, *PG*: Pargyline.

NRVMs treated with HG displayed a significant increase in mitochondrial H_2O_2 levels prevented by both pargyline and MPG (**Figure 29**). Moreover, co-treatment with IL-1β induced a further increase in ROS levels as soon as 1 h after the treatment (**Figure 29**).

Overall, these data show that HG induces both a rapid and a pro-longed increase in H_2O_2. Since IL-1β alone does not induce an increase in ROS levels both after pro-longed and acute treatments, our interpretation is that HG is essential to trigger the oxidative stress induced by IL-1β. Notably, pargyline prevents H_2O_2 formation both with HG and IL-1β, indicating the crucial role of MAO in hyperglycemia-induced ROS formation.

7.4.2 Effects of high glucoses and IL-1β on cytosolic [Ca^{2+}] homeostasis in NRVMs

Besides mitochondrial dysfunction and oxidative stress, diabetes affects normal cardiac myocyte functions, contractility and $[Ca^{2+}]_I$ homeostasis.[162, 255] Data obtained with MitoPQ show that a primary increase in mitochondrial ROS interferes with cytosolic $[Ca^{2+}]$ homeostasis in NRVMs only when oxidative stress is severe. Therefore we investigated whether the co-treatment with HG and IL-1β altered cytosolic $[Ca^{2+}]$

homeostasis in NRVMs, in presence or absence of either pargyline or MPG. Ca^{2+} transients were monitored with Fluo-4 and analyzed before and after 1 h of co-treatment.

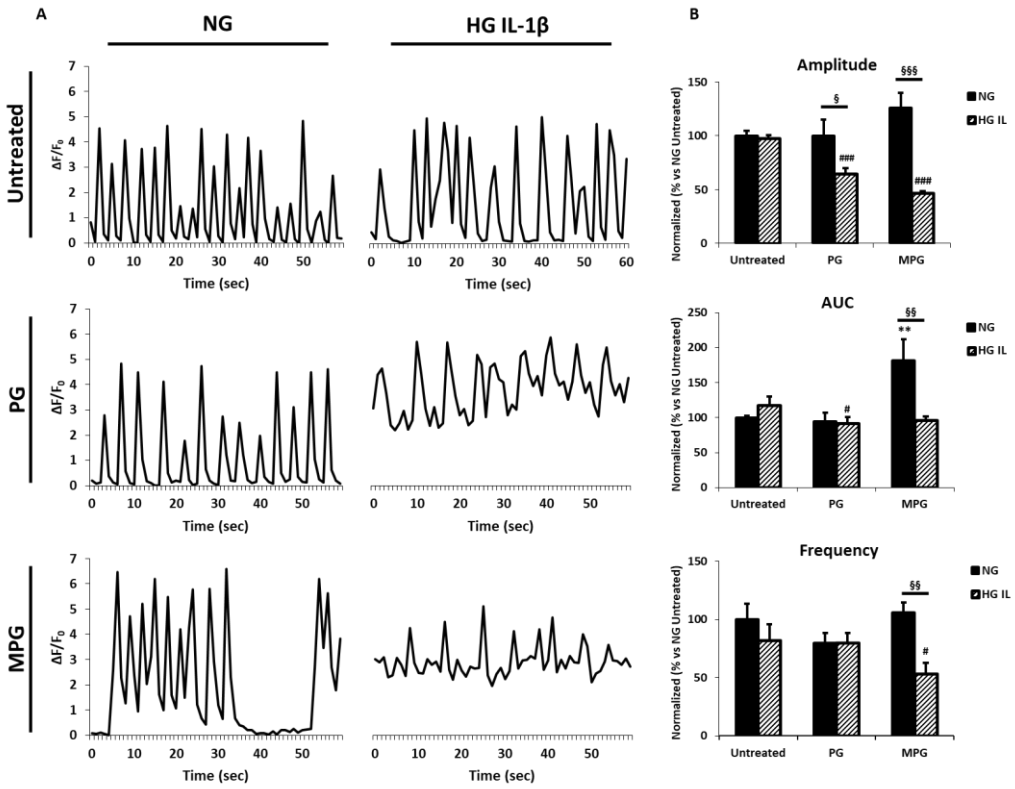

Figure 30. <u>Effects of High Glucose and IL-1β on cytosolic [Ca^{2+}] homeostasis.</u> Cytosolic [Ca^{2+}] homeostasis monitored by Fluo-4 AM in isolated NRVMs treated with NG (5 mM) or co-treated for 1 h with HG (25 mM) and 25 ng/ml IL-1β, in presence or absence of 100 µM pargyline or 500 µM MPG. **A**) Comparison between oscillatory patterns in different conditions. **B**) Comparison between cytosolic [Ca^{2+}] homeostasis parameters. **p < 0.01 vs NG untreated; #p < 0.05, ###p < 0.001 vs HG IL untreated; §p < 0.05, §§p < 0.01, §§§p < 0.001 NG vs HG IL. *NG*: Normal Glucose, *HG*: High Glucose, *IL-1β*: Interleukin-1β, *MPG*: N-(2-Mercaptoproprionyl)glycine**,** *NRVMs*: Neonatal Rat Ventricular Myocytes, *PG*: Pargyline

(i) HG and IL-1β did not cause any significant change of Ca^{2+} oscillatory parameters (**Figure 30B**). Compared to NG, the amplitude was constant while the increase in the AUC and the decrease in frequency were not significant.

(ii) Pretreatment with pargyline did not affect cytosolic [Ca^{2+}] homeostasis in NG, but it significantly altered Ca^{2+} oscillatory parameters in the presence of HG and IL-1β. In particular, the net result was a ~40% decrease in the amplitude and a ~15% decrease in the total amount of Ca^{2+} cycling in the cytosolic compartment (**Figure 30B**).

(iii) MPG was used to reduce ROS formation. Cells incubated in NG displayed a severe increase in both peak amplitude (~30%) and AUC (~60%), indicating an increase in cytosolic Ca^{2+} levels. On the other hand, in NRVMs treated with HG and IL-1β, MPG impaired cytosolic [Ca^{2+}] homeostasis inducing a severe decrease in both peak amplitude (~60%) and frequency (~50%) (**Figure 30B**).

The lack of effect of HG and IL-1β *per se* appears to support the evidence obtained with MitoPQ that cytosolic [Ca^{2+}] homeostasis is disturbed only in the presence of a relevant formation of mitochondrial ROS. Surprisingly, cytosolic [Ca^{2+}] homeostasis becomes impaired when ROS formation is decreased. To the base of our knowledge, these unexpected and novel observation can hardly been explained by any available information. Future studies are necessarily to elucidate the mechanisms underlying this potentially interesting phenomenon. It is tempting to suggest that a basal oxidative tone is required for the maintenance of proper $[Ca^{2+}]_I$ homeostasis in this experimental model of cardiomyocyte injury.

7.4.3 A primary increase in cytosolic ROS perturbs $[Ca^{2+}]_I$ homeostasis in pancreatic Min6 β-cells in a dose-dependent manner

We showed that in NRVMs a dose-dependent increase in mitochondrial ROS levels can modulate cytosolic [Ca^{2+}] homeostasis (see 7.3.1) and that mitochondrial ROS formation induced by a short-term diabetes-like protocol is not sufficient to alter cytosolic [Ca^{2+}] transients (see 7.4.2). However, it is likely that a cytosolic increase of ROS alters $[Ca^{2+}]_I$ homeostasis. This possibility was investigated in another experimental model related to diabetes. Hallmark of diabetes is insulin deficiency (T1D, [256]) or insulin resistance (T2D, [257]). Insulin is secreted from the pancreatic β-cells and bursts of insulin are driven by underlying oscillations in cytosolic Ca^{2+} levels, which periodically trigger Ca^{2+}-regulated exocytosis.[258]

Thus, we investigated if a primary increase in cytosolic ROS could interfere with $[Ca^{2+}]_I$ homeostasis in Min6 β-cells, an insulinoma cell line. To this aim, cells were treated with aluminium phthalocyanine chloride (AlClPc), a photosensitizer commonly used in photodynamic therapy.[209] Photoactivation of AlClPc induces chemical changes into neighboring molecules leading to ROS production by means of Fenton reaction.[259]

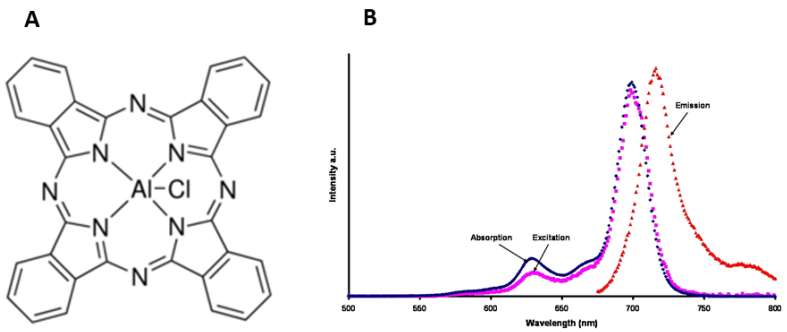

Figure 31. A) Aluminium Phthalocyanine Chloride molecular structure. **B)** Aluminium Phthalocyanine Chloride fluorescence spectra. (*Adapted from Aluminium Phthalocyanine Chloride manuals and protocols, Sigma*)

ROS levels were monitored by means of MitoSOX fluorescence. When photoexcited at 660 nm, AlClPc induces ROS production in amounts depending on the intensity of the LED illumination that was calibrated in order to avoid an increase of MitoSOX signal in the absence of AlClPc (**Figure 32A**). The data obtained with MitoSOX were confirmed by using MitoHyPer (**Figure 32B**).

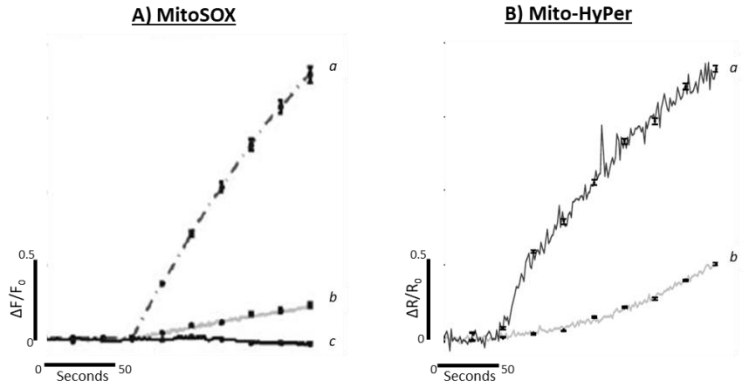

Figure 32. <u>Effects of AlClPc photoactivation on ROS production</u>. ROS production was monitored by MitoSOX and MitoHyPer in Min6 β-cells incubated for 1 hour with 10 µM AlClPc. *a*) 100% LED intensity, *b*) 10% LED intensity. *c*) 100% LED intensity in absence of AlClPc. Illumination from t = 60 s.

Subsequently we investigated whether an increase in cytosolic ROS levels could disturb cytosolic [Ca^{2+}] homeostasis by altering ER Ca^{2+} cycling. Fura-2 fluorescence was used to assess Ca^{2+} transients in Min6 β-cells.

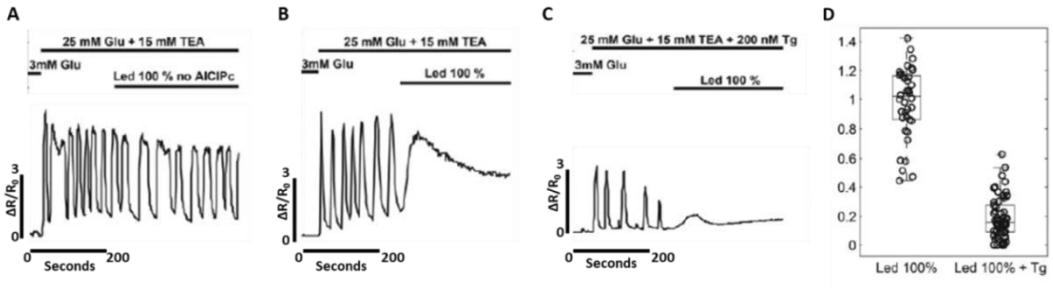

Figure 33. <u>Effects of AlClPc photoactivation on $[Ca^{2+}]_I$ homeostasis</u>. Ca^{2+} oscillations monitored with Fura-2 AM in Min6 β-cells before and after photoactivation of AlClPc. **A**) 100% LED intensity in absence of AlClPc. **B**) Photoactivation of AlClPc with 100% LED intensity. **C**) Photoactivation of AlClPc with 100% LED intensity in the presence of 0.2 μM thapsigargin. **D**) Summary of the Fura-2 averaged ROS-induced peaks normalized to oscillation amplitude in the respective cells. Ratio, arbitrary unit. (*LED 100%*: 0.98 ± 0.04, *LED 100% + Tg*: 0.19 ± 0.02, $p < 0.001$). *AlClPc*: Aluminium Phthalocyanine Chloride, *Glu*: Glucose, *TEA*: Tetra Ethyl Ammonium Chloride, *Tg*: Thapsigargin.

Min6 β-cells display regular and large-amplitude oscillations if exposed to high glucose (25 mM) and to K^+ channel antagonist tetraethylammonium (15 mM, TEA) [205, 210], consisting of a 1st phase with rapid oscillations followed by a 2nd phase typically with slower oscillations. For experiments carried out at highest led intensity, the attention was focused on the 1st phase since decrease in frequency was hypothesized. Indeed, we found that ROS production resulting from photoactivation of AlClPc at maximal (100%) LED intensity abolished Ca^{2+} oscillations in Min6 β-cells that displayed a single peak and Ca^{2+} accumulation (**Figure 33B**). Tg, that inhibits SERCA preventing ER Ca^{2+} filling, significantly reduced the large Ca^{2+} peak induced by ROS (**Figure 33C**). The ROS-induced peak was normalized to oscillation amplitude of the same cell (ratio to peaks). The obtained value displayed a significant reduction of the ROS-induced peak in cells treated with Tg if compared to untreated cells (**Figure 33D**). Control experiments in the absence of AlClPc showed that maximal LED illumination did not influence $[Ca^{2+}]_I$ homeostasis *per se* (**Figure 33A**).

The decrease in ROS-induced elevation of $[Ca^{2+}]_I$ peak elicited by Tg, suggests that the release of Ca^{2+} induced by ROS derives primarily from the ER.

Having established that high levels of ROS produced by AlClPc abolish Ca^{2+} transients in Min6 β-cells, next step was to check the effect of moderate ROS levels induced by AlClPc photoactivation.

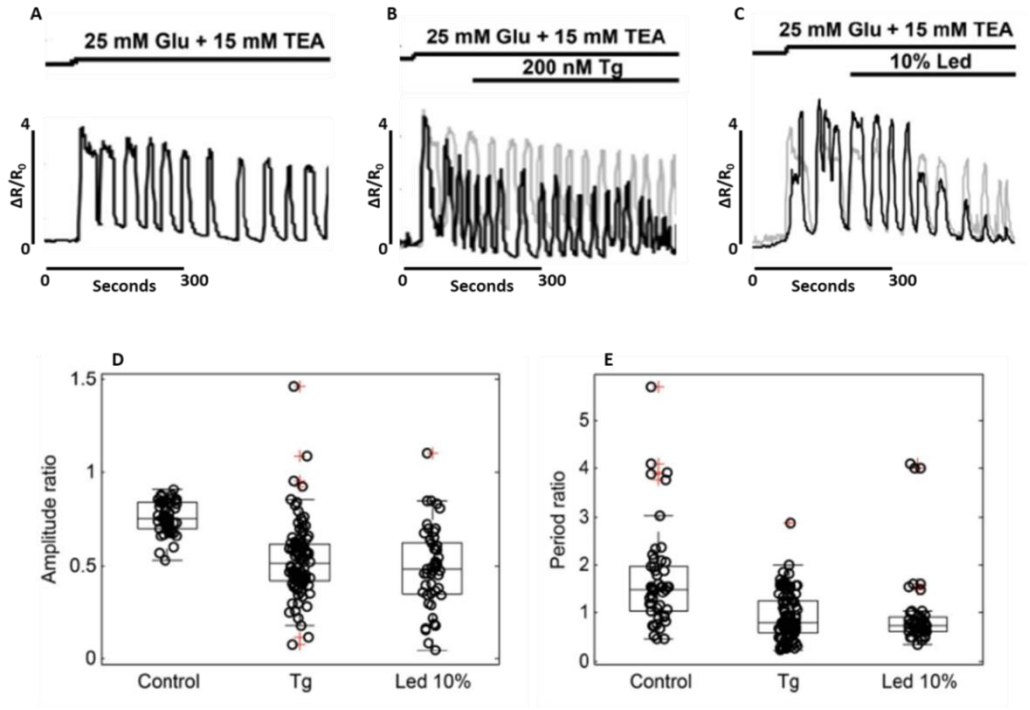

Figure 34. <u>Effects of Tg and moderate AlClPc photoactivation on $[Ca^{2+}]_i$ homeostasis</u>. Ca^{2+} oscillations monitored with Fura-2 AM in Min6 β-cells before and after photoactivation of AlClPc. **A**) example of Ca^{2+} trace in a Min6 β-cell exposed to 25mM glucose and 15 mM TEA. **B**) Cells treated with 0.2 μM Tg after 4 min from the beginning of the acquisition. Two cells of the same experiments are shown. **C**) Photoactivation of AlClPc with 10% LED intensity. Two cells of the same experiments are shown. **D**) Summary of 2nd phase averaged peak amplitude **E**) and 2nd phase averaged period normalized to 1st phase amplitudes and periods respectively, in presence or absence of 0.2 μM Tg and moderate AlClPc photoactivation. *AMPLITUDE*: Control: 0.76 ± 0.12, Tg: 0.53 ± 0.02, Led 10%: 0.49 ± 0.03, in both cases $p < 0.001$ vs control, $p = 0.20$ tg vs 10% LED. *PERIOD*: Control: 1.69 ± 0.14, Tg: 0.93 ± 0.05, Led 10%: 0.99 ± 0.12, in both cases $p < 0.001$ vs control, $p = 0.22$ tg vs 10% LED. *AlClPc*: Aluminium Phthalocyanine Chloride, *Glu*: Glucose, *TEA*: Tetra Ethyl Ammonium Chloride, *Tg*: Thapsigargin.

For experiments at the lower LED intensity, the 2nd phase was considered. Photoactivation of AlClPc at 10% led intensity increased the frequency of oscillation of the second phase (**Figure 34B**), as well as treatment with Tg (**Figure 34C**). Both Treatments resulted in a heterogeneous population of Ca^{2+} oscillations. To handle cell heterogeneity, we normalized the single-cell 2nd phase to the 1st phase. This analysis revealed that cells exposed to ROS or treated with Tg displayed a reduction both of the amplitude and of the period (**Figure 34D-E**).

Taken together, these findings indicate that (i) the presence of Tg results in a reduction in the Ca^{2+} peak elicited by high ROS levels, (ii) ROS modify Ca^{2+} oscillations via a reduction of ER Ca^{2+} levels, (iii) moderate ROS production by AlClPc and SERCA inhibition by Tg accelerate Ca^{2+} oscillations of the 2nd phase to a similar degree,

suggesting that SERCA inhibition is the common denominator of Tg and low levels of ROS induced by AlClPC.

To test whether this interpretation is compatible with Ca^{2+} handling mechanisms of β-cells, a mathematical model was implemented.

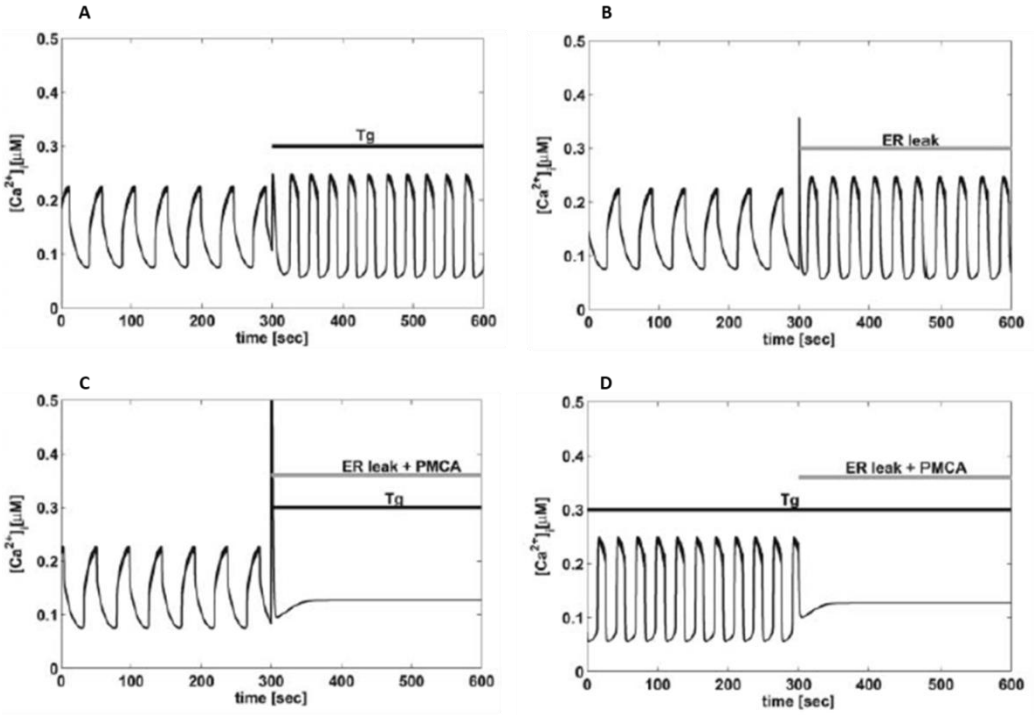

Figure 35. <u>Mathematical modeling supports the experimental findings</u>. **A**) Model simulation showing acceleration of Ca^{2+} oscillations in response to Tg (k_{SERCA} = 0 ms^{-1}) **B**) As in panel A but with increased ER Ca^{2+} release (p_{leak} multiplied by a factor 10). **C**) Simulation of the combined effect of inhibition of PMCAs (k_{pmca} lowered from 0.20 to 0.12 ms^{-1}), Tg application (as in panel A) and increased ER leak (as in panel B), which abolish Ca^{2+} oscillations as seen experimentally. **D**) As in panel C) but with Tg present throughout as in experimental data, which removes the Ca^{2+} peak when ER leak and PMCA inhibition is simulated. *ER*: Endoplasmic Reticulum, *PMCA*: Plasma Membrane Ca^{2+} ATPase, *Tg*: Thapsigargin

Consistent with our working hypothesis, the oscillatory behavior of the mathematical model accelerated when SERCA activity was lowered (**Figure 35A**). Similarly, increasing Ca^{2+} release from the ER in the model (mimicking ROS interaction with e.g. RyRs and IP_3Rs) increased the frequency of the Ca^{2+} oscillations (**Figure 35B**). Notably, the simulated modifications of ER Ca^{2+} handling were insufficient to abolish Ca^{2+} oscillations in the model, suggesting that high levels of ROS also act on other components involved in cytosolic [Ca^{2+}] homeostasis. For example, ROS are known to inhibit not only SERCAs, but also PMCAs.[260] The simulations confirmed that a

reduction in the PMCA rate, together with reduced SERCA activity and increased ER Ca^{2+} leak, could abolish Ca^{2+} oscillations (**Figure 35C**). According with the experimental findings, the mathematical model showed that the addition of Tg before the increase in ROS levels, reduced the Ca^{2+} peak (**Figure 35D**).

Both the model and the experimental data suggest that moderate ROS levels mainly act on ER Ca^{2+} handling, while high ROS concentrations might also inhibit PMCAs and thus abolish Ca^{2+} oscillations.

7.5 A primary increase in mitochondrial Ca^{2+} levels influences mitochondrial ROS and cellular function in NRVMs

7.5.1 MCU overexpression induces an increase in ROS levels and AKT activation in NRVMs

Overall, the data described above show that a primary increase in either mitochondrial or cytosolic ROS is linked to $[Ca^{2+}]_I$ homeostasis regulating both mitochondrial and cell function. This concept is based mostly on results obtained in models of cell injury. However, both ROS and Ca^{2+} are involved in physiological responses as well as in defense mechanisms.[228, 260, 261] Regarding mitochondria, mitochondrial Ca^{2+} uptake is involved in the modulation of ATP synthesis and ROS metabolism.[86, 87] Recent (unpublished) results obtained in Professor Di Lisa's laboratory pointed out the link between mitochondrial Ca^{2+} uptake, mitochondrial ROS formation and AKT activation resulting in cardioprotection against I/R injury. Indeed MCU overexpression (MCU OE) in NRVMs resulted in slight increase of mitochondrial H_2O_2 formation and in a ROS-dependent increase in activated AKT under normoxia. Moreover, MCU OE prevented cell death induced by the ischemic insult.

7.5.2 MCU overexpression protects from A/R injury my means of AKT activation

This interesting set of data lacked the necessary assessment of mitochondrial Ca^{2+} levels, especially during post-anoxic injury. To this aim we investigated if MCU OE could influence mitochondrial Ca^{2+} uptake. MCU uptake was evaluated during normoxia and during post-anoxic reperfusion phase. NRVMs were co-transfected with MCU and 4mt-GCaMP6f, a ratiometric Ca^{2+} sensor targeted to mitochondria, and mitochondrial

Ca^{2+} uptake was induced increasing cytosolic [Ca^{2+}] by stimulation of RyRs with caffeine.

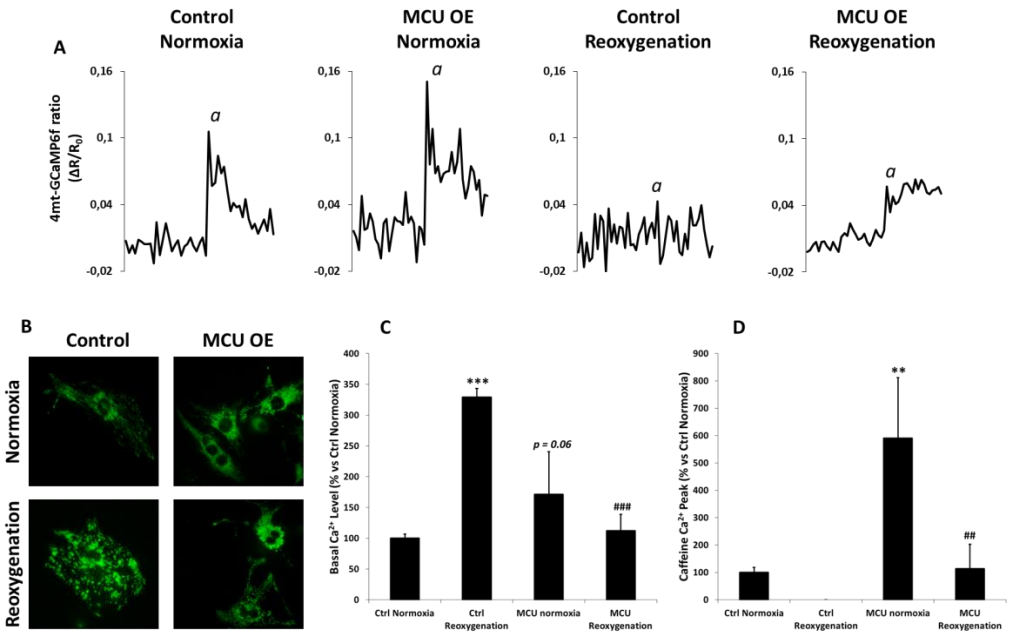

Figure 36. <u>Effects of MCU OE on mitochondrial [Ca^{2+}] in normoxia and post-anoxic reperfusion</u>. A) Mitochondrial Ca^{2+} uptake monitored by 4mt-GCaMP6f in isolated NRVMs in normoxia and post-anoxic reoxygenation, with or without overexpression of MCU. *a)* 10 mM Caffeine. **B)** Comparison between mitochondria of NRVMs exposed to normoxia and post-anoxic reoxygenation, with or without overexpression of MCU. **C)** Comparison between mitochondrial basal [Ca^{2+}] levels and **D)** response to caffeine in NRVMs exposed to normoxia and post-anoxic reoxygenation, with or without overexpression of MCU. **p < 0.01, ***p < 0.001 vs Ctrl Normoxia, ##p < 0.01, ###p < 0.001 vs Ctrl Reoxygenation. *Ctrl*: Control cells, *MCU OE*: Mitochondrial Ca^{2+} Uniporter Overexpression, *NRVMs*: Neonatal Rat Ventricular Myocytes

Under normoxia, MCU OE induced a significant increase in the response to caffeine (**Figure 36D**), with no major changes in basal [Ca^{2+}] levels (**Figure 36C**). On the other hand, MCU OE prevented the increase in mitochondrial [Ca^{2+}] levels occurring during reoxygenation (**Figure 36C**) and preserved the response to caffeine that was completely lost in control cells (**Figure 36D**). In addition, MCU OE prevented the disruption of mitochondrial network induced by post-anoxic reoxygenation (**Figure 36B**).

Another information missing in the previous work was the evaluation of the contribution of AKT activation to MCU OE-induced protection in the I/R. This issue was addressed by treating NRVMs overexpressing MCU with an A/R protocol, with or without a pretreatment with the pan-AKT allosteric inhibitor MK-2206.[262]

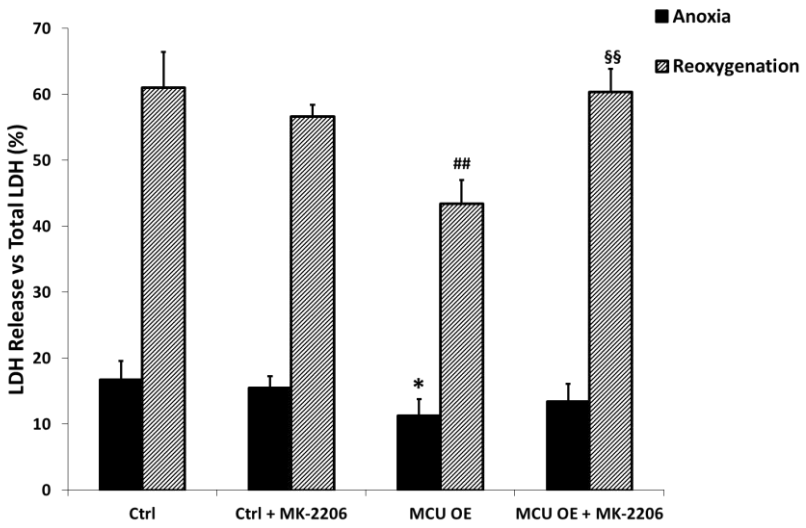

Figure 37. <u>NRVMs overexpressing MCU exposed to Anoxia/Reoxygenation protocol</u>. NRVMs were exposed to 12 h of anoxia and 1 h of reoxygenation and cell death were measured as the release of LDH. MCU overexpressing cells were compared with control cells, with or without 30 min of pretreatment with 0.05 µM MK-2206. *p < 0.05 vs Ctrl Anoxia, ##p < 0.01 vs Ctrl Reoxygenation, §§p < 0.01 vs MCU OE Reoxygenation. *Ctrl*: Control Cells, *LDH*: Lactate Dehydrogenase, *MCU OE*: Mitochondrial Ca^{2+} Uniporter Overexpression, *NRVMs*: Neonatal Rat Ventricular Myocytes

NRVMs overexpressing MCU displayed a significant decrease in cell death both after anoxia and after reperfusion, measured as LDH release. The protection induced by MCU OE (LDH release ~40%) was abolished by the pretreatment of cells with the AKT inhibitor MK-2206 (LDH release ~60%) (**Figure 37**), indicating the crucial role of AKT activation in MCU OE-induced protection.

Taken together, on one hand these findings clarify the sequence of events linking MCU OE with cardiac protection and highlight the relevance of AKT. On the other hand, a clear evidence is provided that besides the damages induced by mitochondrial ROS formation investigated in the first part of this work, ROS generated within mitochondria play a relevant role in protective mechanisms. This concept is further supported by low doses of MitoPQ as described in the following section.

7.6 Low levels of MitoPQ-induced ROS reduce post-anoxic reperfusion cell death by means of AKT activation

We demonstrated that low doses of MitoPQ (0.01 µM MitoPQ, **Figure 21**) did not alter mitochondrial function, $[Ca^{2+}]_I$ homeostasis and cell viability (**Figure 22**, **Figure 26**).

Based on the result obtained with MCU OE, we hypothesized that the slight increase in mitochondrial ROS levels elicited by 0.01 µM MitoPQ could trigger AKT activation eventually increasing the tolerance to post-anoxic injury. To this aim, cells were pretreated with 0.01 µM MitoPQ, with or without the antioxidant MPG.

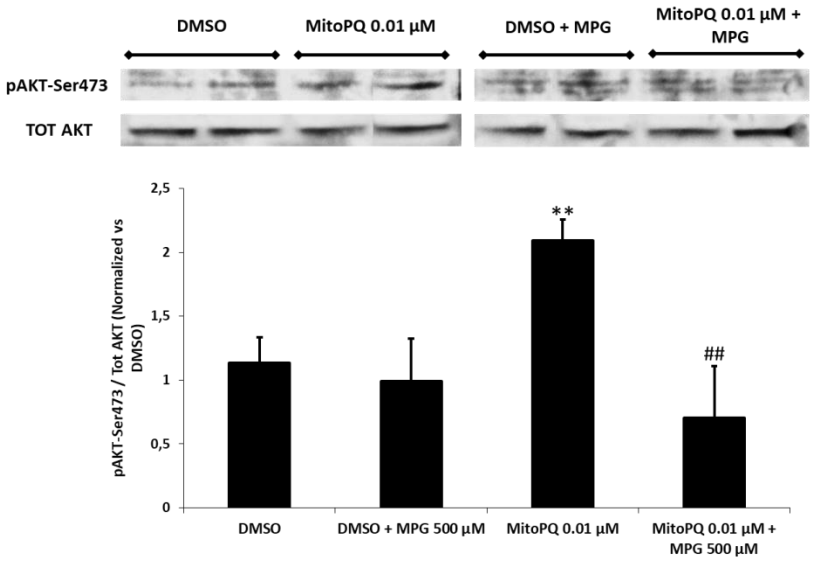

Figure 38. **AKT Ser 473 protein phosphorylation in NRVMs lysates**. Phosphorylation level of AKT at Ser473 in NRVMs lysates of cells treated for 2 h with either DMSO or 0.01 µM MitoPQ, with or without 500 µM MPG. **p < 0.01 vs DMSO, ##p < 0.01 vs MitoPQ. *DMSO*: Dimethyl Sulfoxide, *MitoPQ*: Mitochondrial Paraquat, *MPG*: N-(2-Mercaptoproprionyl)glycine, *pAKT*: phosphorylated AKT, *NRVMs*: Neonatal Rat Ventricular Myocytes

The results obtained confirm our hypothesis. Indeed, MitoPQ treatment increases the phosphorylated levels of AKT at Ser473 without modifying total AKT content. This increase was prevented by MPG indicating the causal role of mitochondrial ROS generation induced by MitoPQ (**Figure 38**).

The next step was to assess whether the low dose of MitoPQ elicited protection against A/R injury mimicking iPC. Cells pretreated with 0.01 µM MitoPQ, with or without the antioxidant MPG, were exposed to 12 h of anoxia followed by 1 h of reoxygenation.

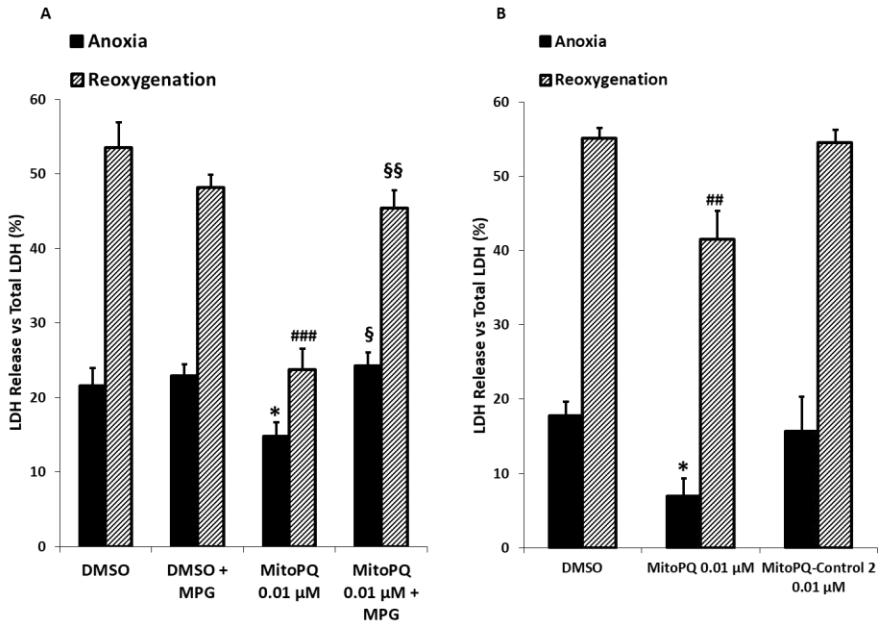

Figure 39. <u>Effects of MitoPQ on NRVMs viability exposed to Anoxia/Reoxygenation protocol</u>. Cells were exposed to 12 h of Anoxia and 1 h of reoxygenation. **A)** Cell death measured by LDH release from isolated NRVMs treated for 2 hours with 0.01 µM MitoPQ, with or without 500 µM MPG. **B)** Cell death measured by LDH release from isolated NRVMs treated for 2 hours with 0.01 µM MitoPQ or with 0.01 µM MitoPQ-Control 2. *p < 0.05 vs DMSO Anoxia, ##p < 0.01, ###p < 0.001 vs DMSO Reoxygenation, §p < 0.05, §§p < 0.01 vs MitoPQ. *DMSO*: Dimethyl Sulfoxide, *LDH*: Lactate Dehydrogenase, *MitoPQ*: Mitochondrial Paraquat, *MPG*: N-(2-Mercaptoproprionyl)glycine, *NRVMs*: Neonatal Rat Ventricular Myocytes

MitoPQ treatment resulted in a significant decrease in the occurrence of cell death at the end of anoxia but even more after reoxygenation. The cardioprotective effect of MitoPQ was completely lost when cells were treated with MPG (**Figure 39A**). In addition, cells were treated with an identical concentration of MitoPQ-Control 2. NRVMs treated with MitoPQ-Control 2 did not show any protection (**Figure 39B**), indicating that the increase in cell viability is due to MitoPQ-induced ROS.

The different extent of cell death in treated cells (**Figure 39**) is likely due to changes in the susceptibility to A/R injury in different cells preparations. We preferred to show the actual data rather than normalize to control. In any case, it is worth pointing out that MitoPQ-induced protection was always observed.

Finally the involvement of AKT activation was investigated by using the AKT inhibitor MK-2206.

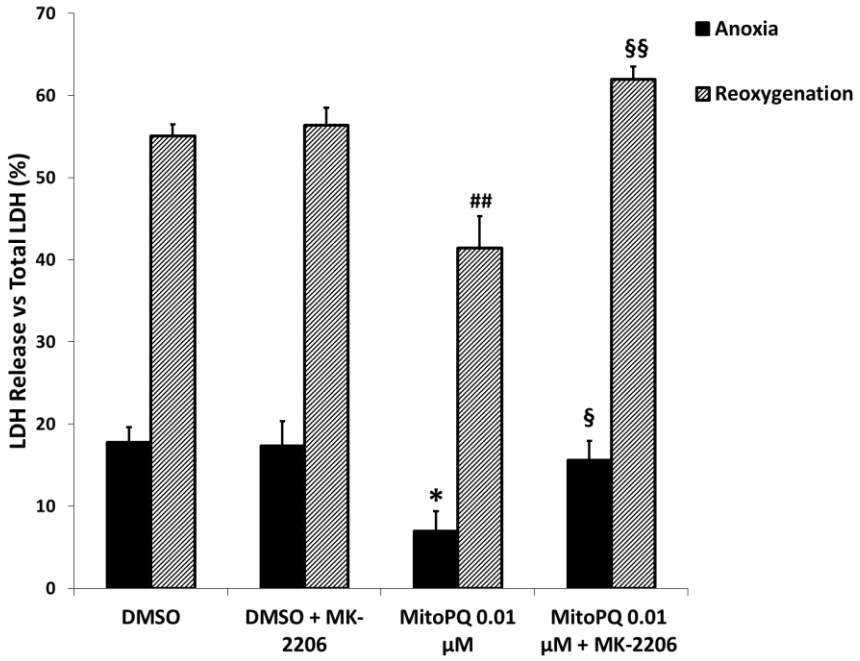

Figure 40. <u>Effects of MitoPQ and AKT inhibition on NRVMs viability exposed to Anoxia/Reoxygenation protocol</u>. Cell death measured by LDH release from isolated NRVMs treated for 2 hours with 0.01 µM MitoPQ, with or without 0.05 µM MK-2206. Cells were exposed to 12 h of Anoxia and 1 h of reoxygenation. *p < 0.05 vs DMSO Anoxia, ##p < 0.001 vs DMSO Reoxygenation, §p < 0.05, §§p < 0.01 vs MitoPQ. *DMSO*: Dimethyl Sulfoxide, *LDH*: Lactate Dehydrogenase, *MitoPQ*: Mitochondrial Paraquat, *NRVMs*: Neonatal Rat Ventricular Myocytes

Similarly to ROS removal by MPG, AKT inhibition abolished the protective efficacy of low doses of MitoPQ (**Figure 40**).

The results obtained with low doses of MitoPQ provide a very strong support to the beneficial effects of slight increase in mitochondrial ROS formation demonstrated in the MCU OE experiments. Altogether, a sequence of events can be described whereby a primary increase in mitochondrial ROS formation, that can also be the consequence of an increased mitochondrial Ca^{2+} uptake, activates pro-survival kinase AKT eventually increasing the tolerance to A/R injury.

8 DISCUSSION AND CONCLUSIONS

This study demonstrates that a primary formation of mitochondrial ROS induces a wide array of intracellular changes that vary from protection to injury in a clear dose-dependent manner. This evidence has been obtained by using either a cellular or a mitochondrial source of ROS. This latter protocol exploited the innovative compound MitoPQ to investigate the role of a primary mitochondrial ROS increase on mitochondrial function, $[Ca^{2+}]_I$ homeostasis and cell viability.

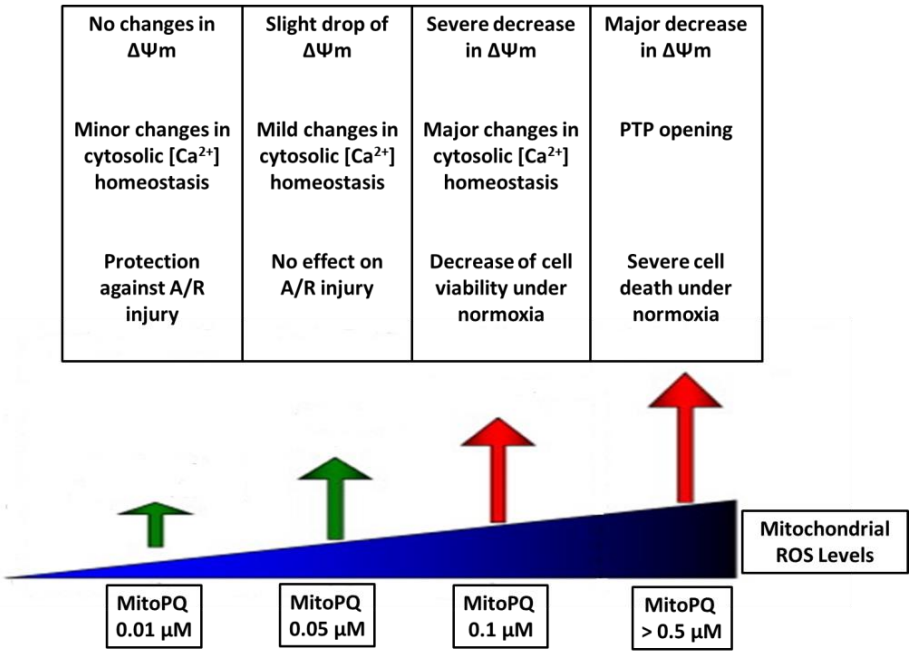

Figure 41. Dose-dependency curve of MitoPQ and relative effects on mitochondrial and cell function.

In a dose dependent fashion, MitoPQ elicits specific effects that are characterized by an increase degree of mitochondrial injury, and that at higher doses spread to the rest of the cell. The profound collapse of ΔΨm associated with PTP opening elicited by ROS induced by MitoPQ doses ≥ 0.5 µM eventually results in a loss of cell viability.

Interestingly, most of the effects induced by MitoPQ are contributed by MAO activity, providing a clear evidence of an amplification pathway [232] whereby ROS produced by these mitochondrial flavoenzymes are those responsible for mitochondrial abnormalities. Nevertheless, at the highest MitoPQ levels, MAO contribution becomes negligible. Further studies are necessary to clarify how an initial oxidative stress can trigger an increase in MAO activity. This process could result from the release of MAO

substrates from intracellular compartments that in cardiac myocytes have not yet been identified.

We showed that moderate levels of ROS can impact on cytosolic [Ca^{2+}] homeostasis in Min6 β-cells with a slightly positive effect since oscillations are more frequent. The interest possibility is that dynamic control of ROS levels contributes to shaping physiological Ca^{2+} oscillations.[210] ROS are known to target components of Ca^{2+} signaling both in cardiac and in pancreatic cells, and the mathematical model supports the idea that ROS are particularly involved in the regulation of SERCA and PMCA activity. Therefore future studies will aim to clarify which proteins and which residues undergo oxidation when mitochondrial ROS formation is elevated.

Besides detrimental effects of mitochondrial ROS, results obtained with both MitoPQ and MCU OE concur in demonstrating that low levels of mitochondrial ROS protects against A/R injury. The link between mitochondrial ROS generation and decreased cell death appears to be represented by AKT activation. This kinase is not directly modulated by oxidation, therefore the redox element upstream of AKT activation has to be identified. This could be one of the phosphatases controlling the phosphorylation state of AKT, such as PP2A and PTEN.[263, 264] Several protein phosphatases are inhibited by oxidation that eventually results in an increased phosphorylation of downstream targets including AKT.

An additional issue that has to be clarified is whether the mechanism of protection is restricted to mitochondria or involves cytosolic processes. For instance AKT has been described to be present also in mitochondria [203] so that H_2O_2 generated in these organelles could target the mitochondrial pool of this protective kinase with the final result of mitochondrial and cell protection. In this respect several processes have been identified downstream of AKT activation that could be responsible for the increased tolerance to the ischemic injury. However, the recent identification of the F_0F_1 ATP Synthase as the main constituent of the PTP [178] prompts revision of previous works to investigate whether phosphorylation events might modulate the pore forming function of the F_0F_1 ATP Synthase.

Last but not least, while we have determined the doses of MitoPQ associated with the various effects in mitochondrial and in intact cells, the actual concentration of ROS

required for cardiomyocytes injury and protection remains to be established. It is clear that a threshold exists between beneficial and detrimental ROS. It will be worth to investigate whether this threshold is modified by cell conditions associated with various diseases. For instance the protective efficacy of iPC is lost in aging or in diabetic hearts. [191] It is tempting to hypothesize that under those conditions adaptive mechanisms cause a slight increase in ROS formation to maintain cell viability that cannot be further increased when the ischemic event occurs. Alternatively, protection under diseased conditions requires an increase of ROS formation that cannot be produced by endogenous sources. This could imply that not only antioxidants are expected to fail, but also that low levels of oxidants could rescue self-endogenous mechanisms. Only the quantitative definition of the threshold will allow to determine whether an increase or a decrease of beneficial ROS is required to maintain cell viability for each pathophysiological condition.

9 REFERENCES

1. Bers, D.M., *Cardiac excitation-contraction coupling.* Nature, 2002. **415**(6868): p. 198-205.
2. Eisner, D.A., et al., *Calcium and Excitation-Contraction Coupling in the Heart.* Circ Res, 2017. **121**(2): p. 181-195.
3. Delbridge, L.M., J.W. Bassani, and D.M. Bers, *Steady-state twitch Ca2+ fluxes and cytosolic Ca2+ buffering in rabbit ventricular myocytes.* Am J Physiol, 1996. **270**(1 Pt 1): p. C192-9.
4. Dibb, K.M., et al., *Characterization of an extensive transverse tubular network in sheep atrial myocytes and its depletion in heart failure.* Circ Heart Fail, 2009. **2**(5): p. 482-9.
5. Lyon, A.R., et al., *Loss of T-tubules and other changes to surface topography in ventricular myocytes from failing human and rat heart.* Proc Natl Acad Sci U S A, 2009. **106**(16): p. 6854-9.
6. Zuhlke, R.D., et al., *Calmodulin supports both inactivation and facilitation of L-type calcium channels.* Nature, 1999. **399**(6732): p. 159-62.
7. Bers, D.M., *Excitation-Contraction Coupling and Cardiac Contractile Force.* 2001, Kluwer Academy: Dordrecht, Netherlands. p. 427.
8. Santulli, G. and A.R. Marks, *Essential Roles of Intracellular Calcium Release Channels in Muscle, Brain, Metabolism, and Aging.* Curr Mol Pharmacol, 2015. **8**(2): p. 206-22.
9. Bers, D.M., *Calcium cycling and signaling in cardiac myocytes.* Annu Rev Physiol, 2008. **70**: p. 23-49.
10. Berlin, J.R., J.W. Bassani, and D.M. Bers, *Intrinsic cytosolic calcium buffering properties of single rat cardiac myocytes.* Biophys J, 1994. **67**(4): p. 1775-87.
11. Hinken, A.C. and R.J. Solaro, *A dominant role of cardiac molecular motors in the intrinsic regulation of ventricular ejection and relaxation.* Physiology (Bethesda), 2007. **22**: p. 73-80.
12. Periasamy, M. and S. Huke, *SERCA pump level is a critical determinant of Ca(2+)homeostasis and cardiac contractility.* J Mol Cell Cardiol, 2001. **33**(6): p. 1053-63.
13. Periasamy, M., P. Bhupathy, and G.J. Babu, *Regulation of sarcoplasmic reticulum Ca2+ ATPase pump expression and its relevance to cardiac muscle physiology and pathology.* Cardiovasc Res, 2008. **77**(2): p. 265-73.
14. Lipskaia, L., et al., *Sarcoplasmic reticulum Ca(2+) ATPase as a therapeutic target for heart failure.* Expert Opin Biol Ther, 2010. **10**(1): p. 29-41.
15. Arai, M., et al., *Alterations in sarcoplasmic reticulum gene expression in human heart failure. A possible mechanism for alterations in systolic and diastolic properties of the failing myocardium.* Circ Res, 1993. **72**(2): p. 463-9.
16. Schwinger, R.H., et al., *Unchanged protein levels of SERCA II and phospholamban but reduced Ca2+ uptake and Ca(2+)-ATPase activity of cardiac sarcoplasmic reticulum from dilated cardiomyopathy patients compared with patients with nonfailing hearts.* Circulation, 1995. **92**(11): p. 3220-8.
17. Lancel, S., et al., *Oxidative posttranslational modifications mediate decreased SERCA activity and myocyte dysfunction in Galphaq-overexpressing mice.* Circ Res, 2010. **107**(2): p. 228-32.

18. MacLennan, D.H. and E.G. Kranias, *Phospholamban: a crucial regulator of cardiac contractility.* Nat Rev Mol Cell Biol, 2003. **4**(7): p. 566-77.

19. Li, L., et al., *Phosphorylation of phospholamban and troponin I in beta-adrenergic-induced acceleration of cardiac relaxation.* Am J Physiol Heart Circ Physiol, 2000. **278**(3): p. H769-79.

20. Territo, P.R., et al., *Ca(2+) activation of heart mitochondrial oxidative phosphorylation: role of the F(0)/F(1)-ATPase.* Am J Physiol Cell Physiol, 2000. **278**(2): p. C423-35.

21. De Stefani, D., et al., *A forty-kilodalton protein of the inner membrane is the mitochondrial calcium uniporter.* Nature, 2011. **476**(7360): p. 336-40.

22. Baughman, J.M., et al., *Integrative genomics identifies MCU as an essential component of the mitochondrial calcium uniporter.* Nature, 2011. **476**(7360): p. 341-5.

23. Raffaello, A., et al., *The mitochondrial calcium uniporter is a multimer that can include a dominant-negative pore-forming subunit.* EMBO J, 2013. **32**(17): p. 2362-76.

24. Trollinger, D.R., W.E. Cascio, and J.J. Lemasters, *Selective loading of Rhod 2 into mitochondria shows mitochondrial Ca2+ transients during the contractile cycle in adult rabbit cardiac myocytes.* Biochem Biophys Res Commun, 1997. **236**(3): p. 738-42.

25. Williams, G.S., et al., *Mitochondrial calcium uptake.* Proc Natl Acad Sci U S A, 2013. **110**(26): p. 10479-86.

26. Drago, I., et al., *Mitochondrial Ca2+ uptake contributes to buffering cytoplasmic Ca2+ peaks in cardiomyocytes.* Proc Natl Acad Sci U S A, 2012. **109**(32): p. 12986-91.

27. Maack, C., et al., *Elevated cytosolic Na+ decreases mitochondrial Ca2+ uptake during excitation-contraction coupling and impairs energetic adaptation in cardiac myocytes.* Circ Res, 2006. **99**(2): p. 172-82.

28. Rizzuto, R., et al., *Close contacts with the endoplasmic reticulum as determinants of mitochondrial Ca2+ responses.* Science, 1998. **280**(5370): p. 1763-6.

29. Hajnoczky, G., et al., *The machinery of local Ca2+ signalling between sarco-endoplasmic reticulum and mitochondria.* J Physiol, 2000. **529 Pt 1**: p. 69-81.

30. Boyman, L., et al., *Calcium movement in cardiac mitochondria.* Biophys J, 2014. **107**(6): p. 1289-301.

31. Boyman, L., et al., *NCLX: the mitochondrial sodium calcium exchanger.* J Mol Cell Cardiol, 2013. **59**: p. 205-13.

32. Bernardi, P. and F. Di Lisa, *The mitochondrial permeability transition pore: molecular nature and role as a target in cardioprotection.* J Mol Cell Cardiol, 2015. **78**: p. 100-6.

33. Bernardi, P., et al., *The Mitochondrial Permeability Transition Pore: Channel Formation by F-ATP Synthase, Integration in Signal Transduction, and Role in Pathophysiology.* Physiol Rev, 2015. **95**(4): p. 1111-55.

34. De Stefani, D., M. Patron, and R. Rizzuto, *Structure and function of the mitochondrial calcium uniporter complex.* Biochim Biophys Acta, 2015. **1853**(9): p. 2006-11.

35. Turrens, J.F., *Mitochondrial formation of reactive oxygen species.* J Physiol, 2003. **552**(Pt 2): p. 335-44.

36. Balaban, R.S., S. Nemoto, and T. Finkel, *Mitochondria, oxidants, and aging.* Cell, 2005. **120**(4): p. 483-95.

37. Murphy, M.P., *How mitochondria produce reactive oxygen species.* Biochem J, 2009. **417**(1): p. 1-13.

38. Giordano, F.J., *Oxygen, oxidative stress, hypoxia, and heart failure.* J Clin Invest, 2005. **115**(3): p. 500-8.

39. Murphy, M.P., *Mitochondrial thiols in antioxidant protection and redox signaling: distinct roles for glutathionylation and other thiol modifications.* Antioxid Redox Signal, 2012. **16**(6): p. 476-95.

40. Forman, H.J., F. Ursini, and M. Maiorino, *An overview of mechanisms of redox signaling.* J Mol Cell Cardiol, 2014. **73**: p. 2-9.

41. Chalmers, S., et al., *Selective uncoupling of individual mitochondria within a cell using a mitochondria-targeted photoactivated protonophore.* J Am Chem Soc, 2012. **134**(2): p. 758-61.

42. Galluzzi, L., et al., *Guidelines for the use and interpretation of assays for monitoring cell death in higher eukaryotes.* Cell Death Differ, 2009. **16**(8): p. 1093-107.

43. Anderson, E.J., et al., *Monoamine oxidase is a major determinant of redox balance in human atrial myocardium and is associated with postoperative atrial fibrillation.* J Am Heart Assoc, 2014. **3**(1): p. e000713.

44. Bianchi, P., et al., *Oxidative stress by monoamine oxidase mediates receptor-independent cardiomyocyte apoptosis by serotonin and postischemic myocardial injury.* Circulation, 2005. **112**(21): p. 3297-305.

45. Kaludercic, N., et al., *Monoamine oxidases (MAO) in the pathogenesis of heart failure and ischemia/reperfusion injury.* Biochim Biophys Acta, 2011. **1813**(7): p. 1323-32.

46. Ago, T., et al., *The NADPH oxidase Nox4 and aging in the heart.* Aging (Albany NY), 2010. **2**(12): p. 1012-6.

47. Ago, T., et al., *Upregulation of Nox4 by hypertrophic stimuli promotes apoptosis and mitochondrial dysfunction in cardiac myocytes.* Circ Res, 2010. **106**(7): p. 1253-64.

48. Hirschhauser, C., et al., *NOX4 in Mitochondria: Yeast Two-Hybrid-Based Interaction with Complex I Without Relevance for Basal Reactive Oxygen Species?* Antioxid Redox Signal, 2015. **23**(14): p. 1106-12.

49. Di Lisa, F. and L. Scorrano, *Mitochondrial Morphology and Function*, in *Muscle - Fundamental biology and mechanisms of disease*, J.A. Hill and E.N. Olson, Editors. 2012, Elsevier Inc. p. 217-229.

50. Sazanov, L.A., *A giant molecular proton pump: structure and mechanism of respiratory complex I.* Nat Rev Mol Cell Biol, 2015. **16**(6): p. 375-88.

51. Murphy, E., et al., *Mitochondrial Function, Biology, and Role in Disease: A Scientific Statement From the American Heart Association.* Circ Res, 2016. **118**(12): p. 1960-91.

52. Chouchani, E.T., et al., *Ischaemic accumulation of succinate controls reperfusion injury through mitochondrial ROS.* Nature, 2014. **515**(7527): p. 431-435.

53. Fridovich, I., *Superoxide radical and superoxide dismutases.* Annu Rev Biochem, 1995. **64**: p. 97-112.

54. Chen, Q., et al., *Ischemic defects in the electron transport chain increase the production of reactive oxygen species from isolated rat heart mitochondria.* Am J Physiol Cell Physiol, 2008. **294**(2): p. C460-6.

55. Drose, S., U. Brandt, and I. Wittig, *Mitochondrial respiratory chain complexes as sources and targets of thiol-based redox-regulation.* Biochim Biophys Acta, 2014. **1844**(8): p. 1344-54.

56. Kaludercic, N., et al., *Monoamine oxidase B prompts mitochondrial and cardiac dysfunction in pressure overloaded hearts.* Antioxid Redox Signal, 2014. **20**(2): p. 267-80.

57. Dorn, G.W., 2nd, *Mitochondrial dynamism and heart disease: changing shape and shaping change.* EMBO Mol Med, 2015. **7**(7): p. 865-77.

58. Kaludercic, N., et al., *Monoamine oxidases as sources of oxidants in the heart.* J Mol Cell Cardiol, 2014. **73**: p. 34-42.

59. Abell, C.W. and S.W. Kwan, *Molecular characterization of monoamine oxidases A and B.* Prog Nucleic Acid Res Mol Biol, 2001. **65**: p. 129-56.

60. Edmondson, D.E., et al., *Structure and mechanism of monoamine oxidase.* Curr Med Chem, 2004. **11**(15): p. 1983-93.

61. Di Lisa, F., et al., *Mitochondrial pathways for ROS formation and myocardial injury: the relevance of p66(Shc) and monoamine oxidase.* Basic Res Cardiol, 2009. **104**(2): p. 131-9.

62. Lairez, O., et al., *Genetic deletion of MAO-A promotes serotonin-dependent ventricular hypertrophy by pressure overload.* J Mol Cell Cardiol, 2009. **46**(4): p. 587-95.

63. Pchejetski, D., et al., *Oxidative stress-dependent sphingosine kinase-1 inhibition mediates monoamine oxidase A-associated cardiac cell apoptosis.* Circ Res, 2007. **100**(1): p. 41-9.

64. Kaludercic, N., et al., *Monoamine oxidase A-mediated enhanced catabolism of norepinephrine contributes to adverse remodeling and pump failure in hearts with pressure overload.* Circ Res, 2010. **106**(1): p. 193-202.

65. Carpi, A., et al., *The cardioprotective effects elicited by p66(Shc) ablation demonstrate the crucial role of mitochondrial ROS formation in ischemia/reperfusion injury.* Biochim Biophys Acta, 2009. **1787**(7): p. 774-80.

66. Villeneuve, C., et al., *p53-PGC-1alpha pathway mediates oxidative mitochondrial damage and cardiomyocyte necrosis induced by monoamine oxidase-A upregulation: role in chronic left ventricular dysfunction in mice.* Antioxid Redox Signal, 2013. **18**(1): p. 5-18.

67. Santin, Y., et al., *Oxidative Stress by Monoamine Oxidase-A Impairs Transcription Factor EB Activation and Autophagosome Clearance, Leading to Cardiomyocyte Necrosis and Heart Failure.* Antioxid Redox Signal, 2016. **25**(1): p. 10-27.

68. Deshwal, S., et al., *Emerging role of monoamine oxidase as a therapeutic target for cardiovascular disease.* Curr Opin Pharmacol, 2017. **33**: p. 64-69.

69. Di Lisa, F., et al., *New aspects of p66Shc in ischemia reperfusion injury and cardiovascular diseases.* Br J Pharmacol, 2016.

70. Cosentino, F., et al., *Final common molecular pathways of aging and cardiovascular disease: role of the p66Shc protein.* Arterioscler Thromb Vasc Biol, 2008. **28**(4): p. 622-8.

71. Di Lisa, F., et al., *New aspects of p66Shc in ischaemia reperfusion injury and other cardiovascular diseases.* Br J Pharmacol, 2017. **174**(12): p. 1690-1703.

72. Orsini, F., et al., *Regulatory effects of the mitochondrial energetic status on mitochondrial p66Shc.* Biol Chem, 2006. **387**(10-11): p. 1405-10.

73. Giorgio, M., et al., *Electron transfer between cytochrome c and p66Shc generates reactive oxygen species that trigger mitochondrial apoptosis.* Cell, 2005. **122**(2): p. 221-33.

74. Yang, M., et al., *Reversible blockade of complex I or inhibition of PKCbeta reduces activation and mitochondria translocation of p66Shc to preserve cardiac function after ischemia.* PLoS One, 2014. **9**(12): p. e113534.

75. Fujio, Y., et al., *Akt promotes survival of cardiomyocytes in vitro and protects against ischemia-reperfusion injury in mouse heart.* Circulation, 2000. **101**(6): p. 660-7.

76. Tong, H., et al., *Ischemic preconditioning activates phosphatidylinositol-3-kinase upstream of protein kinase C.* Circ Res, 2000. **87**(4): p. 309-15.

77. Frijhoff, J., et al., *The mitochondrial reactive oxygen species regulator p66Shc controls PDGF-induced signaling and migration through protein tyrosine phosphatase oxidation.* Free Radic Biol Med, 2014. **68**: p. 268-77.

78. Gorlach, A., et al., *Calcium and ROS: A mutual interplay.* Redox Biol, 2015. **6**: p. 260-71.

79. Gordeeva, A.V., R.A. Zvyagilskaya, and Y.A. Labas, *Cross-talk between reactive oxygen species and calcium in living cells.* Biochemistry (Mosc), 2003. **68**(10): p. 1077-80.

80. Zhang, L., et al., *Oxidative modifications of mitochondria complex II.* Methods Mol Biol, 2013. **1005**: p. 143-56.

81. Yan, Y., et al., *Bidirectional regulation of Ca2+ sparks by mitochondria-derived reactive oxygen species in cardiac myocytes.* Cardiovasc Res, 2008. **77**(2): p. 432-41.

82. Petry, A., M. Weitnauer, and A. Gorlach, *Receptor activation of NADPH oxidases.* Antioxid Redox Signal, 2010. **13**(4): p. 467-87.

83. Gorlach, A., P. Klappa, and T. Kietzmann, *The endoplasmic reticulum: folding, calcium homeostasis, signaling, and redox control.* Antioxid Redox Signal, 2006. **8**(9-10): p. 1391-418.

84. Gonzalez, D.R., et al., *NADPH oxidase-2 inhibition restores contractility and intracellular calcium handling and reduces arrhythmogenicity in dystrophic cardiomyopathy.* Am J Physiol Heart Circ Physiol, 2014. **307**(5): p. H710-21.

85. Sanchez, G., et al., *Tachycardia increases NADPH oxidase activity and RyR2 S-glutathionylation in ventricular muscle.* J Mol Cell Cardiol, 2005. **39**(6): p. 982-91.

86. Brookes, P.S., et al., *Calcium, ATP, and ROS: a mitochondrial love-hate triangle.* Am J Physiol Cell Physiol, 2004. **287**(4): p. C817-33.

87. Adam-Vizi, V. and A.A. Starkov, *Calcium and mitochondrial reactive oxygen species generation: how to read the facts.* J Alzheimers Dis, 2010. **20 Suppl 2**: p. S413-26.

88. Di Lisa, F., *Mitochondria in Myocardial Ischemia*. The Encyclopedia of Biological Chemistry, ed. L.W.J.a.L. M.D. Vol. 3. 2013, Waltham, MA: Academic Press. 108-112.

89. Hudasek, K., S.T. Brown, and I.M. Fearon, *H2O2 regulates recombinant Ca2+ channel alpha1C subunits but does not mediate their sensitivity to acute hypoxia.* Biochem Biophys Res Commun, 2004. **318**(1): p. 135-41.

90. Hool, L.C., *Evidence for the regulation of L-type Ca2+ channels in the heart by reactive oxygen species: mechanism for mediating pathology.* Clin Exp Pharmacol Physiol, 2008. **35**(2): p. 229-34.

91. Sag, C.M., S. Wagner, and L.S. Maier, *Role of oxidants on calcium and sodium movement in healthy and diseased cardiac myocytes.* Free Radic Biol Med, 2013. **63**: p. 338-49.

92. Meissner, G., *Regulation of Ryanodine Receptor Ion Channels Through Posttranslational Modifications.* Curr Top Membr, 2010. **66**: p. 91-113.

93. Terentyev, D., et al., *Redox modification of ryanodine receptors contributes to sarcoplasmic reticulum Ca2+ leak in chronic heart failure.* Circ Res, 2008. **103**(12): p. 1466-72.

94. Zima, A.V. and L.A. Blatter, *Redox regulation of cardiac calcium channels and transporters.* Cardiovasc Res, 2006. **71**(2): p. 310-21.

95. Bovo, E., S.L. Lipsius, and A.V. Zima, *Reactive oxygen species contribute to the development of arrhythmogenic Ca(2)(+) waves during beta-adrenergic receptor stimulation in rabbit cardiomyocytes.* J Physiol, 2012. **590**(14): p. 3291-304.

96. Ho, H.T., et al., *Arrhythmogenic adverse effects of cardiac glycosides are mediated by redox modification of ryanodine receptors.* J Physiol, 2011. **589**(Pt 19): p. 4697-708.

97. Sharov, V.S., et al., *Quantitative mapping of oxidation-sensitive cysteine residues in SERCA in vivo and in vitro by HPLC-electrospray-tandem MS: selective protein oxidation during biological aging.* Biochem J, 2006. **394**(Pt 3): p. 605-15.

98. Anderson, M.E., J.H. Brown, and D.M. Bers, *CaMKII in myocardial hypertrophy and heart failure.* J Mol Cell Cardiol, 2011. **51**(4): p. 468-73.

99. Brown, D.I. and K.K. Griendling, *Regulation of signal transduction by reactive oxygen species in the cardiovascular system.* Circ Res, 2015. **116**(3): p. 531-49.

100. Erickson, J.R., et al., *A dynamic pathway for calcium-independent activation of CaMKII by methionine oxidation.* Cell, 2008. **133**(3): p. 462-74.

101. Chen, Y.R. and J.L. Zweier, *Cardiac mitochondria and reactive oxygen species generation.* Circ Res, 2014. **114**(3): p. 524-37.

102. Bugger, H. and E.D. Abel, *Mitochondria in the diabetic heart.* Cardiovasc Res, 2010. **88**(2): p. 229-40.

103. Sena, L.A. and N.S. Chandel, *Physiological roles of mitochondrial reactive oxygen species.* Mol Cell, 2012. **48**(2): p. 158-67.

104. Collins, Y., et al., *Mitochondrial redox signalling at a glance.* J Cell Sci, 2012. **125**(Pt 4): p. 801-6.

105. Janssen-Heininger, Y.M., et al., *Redox-based regulation of signal transduction: principles, pitfalls, and promises.* Free Radic Biol Med, 2008. **45**(1): p. 1-17.

106. Finkel, T., *From sulfenylation to sulfhydration: what a thiolate needs to tolerate.* Sci Signal, 2012. **5**(215): p. pe10.

107. Tonks, N.K., *Redox redux: revisiting PTPs and the control of cell signaling.* Cell, 2005. **121**(5): p. 667-70.

108. Gorlach, A. and T. Kietzmann, *Superoxide and derived reactive oxygen species in the regulation of hypoxia-inducible factors.* Methods Enzymol, 2007. **435**: p. 421-46.

109. Semenza, G.L., *Hypoxia-inducible factor 1 and cardiovascular disease.* Annu Rev Physiol, 2014. **76**: p. 39-56.

110. Hayes, J.D. and A.T. Dinkova-Kostova, *The Nrf2 regulatory network provides an interface between redox and intermediary metabolism.* Trends Biochem Sci, 2014. **39**(4): p. 199-218.

111. Finkel, T., *Oxygen radicals and signaling.* Curr Opin Cell Biol, 1998. **10**(2): p. 248-53.

112. Sauer, H., et al., *Role of reactive oxygen species and phosphatidylinositol 3-kinase in cardiomyocyte differentiation of embryonic stem cells.* FEBS Lett, 2000. **476**(3): p. 218-23.

113. Scherz-Shouval, R., et al., *Reactive oxygen species are essential for autophagy and specifically regulate the activity of Atg4.* EMBO J, 2007. **26**(7): p. 1749-60.

114. Forbes, R.A., C. Steenbergen, and E. Murphy, *Diazoxide-induced cardioprotection requires signaling through a redox-sensitive mechanism.* Circ Res, 2001. **88**(8): p. 802-9.

115. Robin, E., et al., *Oxidant stress during simulated ischemia primes cardiomyocytes for cell death during reperfusion.* J Biol Chem, 2007. **282**(26): p. 19133-43.

116. Akhmedov, A., et al., *Genetic deletion of the adaptor protein p66Shc increases susceptibility to short-term ischaemic myocardial injury via intracellular salvage pathways.* Eur Heart J, 2015. **36**(8): p. 516-26a.

117. Spindel, O.N. and B.C. Berk, *Redox redux: protecting the ischemic myocardium.* J Clin Invest, 2012. **122**(1): p. 30-2.

118. Pain, T., et al., *Opening of mitochondrial K(ATP) channels triggers the preconditioned state by generating free radicals.* Circ Res, 2000. **87**(6): p. 460-6.

119. Harman, D., *The biologic clock: the mitochondria?* J Am Geriatr Soc, 1972. **20**(4): p. 145-7.

120. Ristow, M. and K. Zarse, *How increased oxidative stress promotes longevity and metabolic health: The concept of mitochondrial hormesis (mitohormesis).* Exp Gerontol, 2010. **45**(6): p. 410-8.

121. Tapia, P.C., *Sublethal mitochondrial stress with an attendant stoichiometric augmentation of reactive oxygen species may precipitate many of the beneficial alterations in cellular physiology produced by caloric restriction, intermittent fasting, exercise and dietary phytonutrients: "Mitohormesis" for health and vitality.* Med Hypotheses, 2006. **66**(4): p. 832-43.

122. Ristow, M. and K. Schmeisser, *Mitohormesis: Promoting Health and Lifespan by Increased Levels of Reactive Oxygen Species (ROS).* Dose Response, 2014. **12**(2): p. 288-341.

123. Cnop, M., et al., *Mechanisms of pancreatic beta-cell death in type 1 and type 2 diabetes: many differences, few similarities.* Diabetes, 2005. **54 Suppl 2**: p. S97-107.

124. Atkinson, M.A. and G.S. Eisenbarth, *Type 1 diabetes: new perspectives on disease pathogenesis and treatment.* Lancet, 2001. **358**(9277): p. 221-9.

125. Kloppel, G., et al., *Islet pathology and the pathogenesis of type 1 and type 2 diabetes mellitus revisited.* Surv Synth Pathol Res, 1985. **4**(2): p. 110-25.

126. Kahn, S.E., *The relative contributions of insulin resistance and beta-cell dysfunction to the pathophysiology of Type 2 diabetes.* Diabetologia, 2003. **46**(1): p. 3-19.

127. Rhodes, C.J., *Type 2 diabetes-a matter of beta-cell life and death?* Science, 2005. **307**(5708): p. 380-4.

128. Kahn, S.E., M.E. Cooper, and S. Del Prato, *Pathophysiology and treatment of type 2 diabetes: perspectives on the past, present, and future.* Lancet, 2014. **383**(9922): p. 1068-83.

129. Rosen, P., et al., *The role of oxidative stress in the onset and progression of diabetes and its complications: a summary of a Congress Series sponsored by UNESCO-MCBN, the American Diabetes Association and the German Diabetes Society.* Diabetes Metab Res Rev, 2001. **17**(3): p. 189-212.

130. Brownlee, M., *Biochemistry and molecular cell biology of diabetic complications.* Nature, 2001. **414**(6865): p. 813-20.

131. Forbes, J.M. and M.E. Cooper, *Mechanisms of diabetic complications.* Physiol Rev, 2013. **93**(1): p. 137-88.

132. Pi, J., et al., *ROS signaling, oxidative stress and Nrf2 in pancreatic beta-cell function.* Toxicol Appl Pharmacol, 2010. **244**(1): p. 77-83.

133. Schmidt, K.N., et al., *Identification of hydrogen peroxide as the relevant messenger in the activation pathway of transcription factor NF-kappaB.* Adv Exp Med Biol, 1996. **387**: p. 63-8.

134. Anderson, E.J., et al., *Substrate-specific derangements in mitochondrial metabolism and redox balance in the atrium of the type 2 diabetic human heart.* J Am Coll Cardiol, 2009. **54**(20): p. 1891-8.

135. Boudina, S., et al., *Contribution of impaired myocardial insulin signaling to mitochondrial dysfunction and oxidative stress in the heart.* Circulation, 2009. **119**(9): p. 1272-83.

136. Shen, X., et al., *Cardiac mitochondrial damage and biogenesis in a chronic model of type 1 diabetes.* Am J Physiol Endocrinol Metab, 2004. **287**(5): p. E896-905.

137. Boudina, S., et al., *Reduced mitochondrial oxidative capacity and increased mitochondrial uncoupling impair myocardial energetics in obesity.* Circulation, 2005. **112**(17): p. 2686-95.

138. Skelin, M., M. Rupnik, and A. Cencic, *Pancreatic beta cell lines and their applications in diabetes mellitus research.* ALTEX, 2010. **27**(2): p. 105-13.

139. Stanfield, C.L., et al., *Principles of human physiology (6th ed.)*. 2009, San Francisco: Pearson/Benjamin Cummings.

140. Aguilar-Bryan, L., et al., *Toward understanding the assembly and structure of KATP channels.* Physiol Rev, 1998. **78**(1): p. 227-45.

141. Caicedo, A., *Paracrine and autocrine interactions in the human islet: more than meets the eye.* Semin Cell Dev Biol, 2013. **24**(1): p. 11-21.

142. De Leon, D.D. and C.A. Stanley, *Mechanisms of Disease: advances in diagnosis and treatment of hyperinsulinism in neonates.* Nat Clin Pract Endocrinol Metab, 2007. **3**(1): p. 57-68.

143. Tarasov, A.I., et al., *The mitochondrial Ca2+ uniporter MCU is essential for glucose-induced ATP increases in pancreatic beta-cells.* PLoS One, 2012. **7**(7): p. e39722.

144. Kennedy, E.D. and C.B. Wollheim, *Role of mitochondrial calcium in metabolism-secretion coupling in nutrient-stimulated insulin release.* Diabetes Metab, 1998. **24**(1): p. 15-24.

145. Antinozzi, P.A., et al., *Mitochondrial metabolism sets the maximal limit of fuel-stimulated insulin secretion in a model pancreatic beta cell: a survey of four fuel secretagogues.* J Biol Chem, 2002. **277**(14): p. 11746-55.

146. Nishikawa, T., et al., *Normalizing mitochondrial superoxide production blocks three pathways of hyperglycaemic damage.* Nature, 2000. **404**(6779): p. 787-90.

147. Pi, J., et al., *Reactive oxygen species as a signal in glucose-stimulated insulin secretion.* Diabetes, 2007. **56**(7): p. 1783-91.

148. Li, L.X., et al., *Uncoupling protein-2 participates in cellular defense against oxidative stress in clonal beta-cells.* Biochem Biophys Res Commun, 2001. **282**(1): p. 273-7.

149. Produit-Zengaffinen, N., et al., *Increasing uncoupling protein-2 in pancreatic beta cells does not alter glucose-induced insulin secretion but decreases production of reactive oxygen species.* Diabetologia, 2007. **50**(1): p. 84-93.

150. Li, N., S. Stojanovski, and P. Maechler, *Mitochondrial hormesis in pancreatic beta cells: does uncoupling protein 2 play a role?* Oxid Med Cell Longev, 2012. **2012**: p. 740849.

151. Schannwell, C.M., et al., *Left ventricular diastolic dysfunction as an early manifestation of diabetic cardiomyopathy.* Cardiology, 2002. **98**(1-2): p. 33-9.

152. Maharaj, R., *Diastolic dysfunction and heart failure with a preserved ejection fraction: Relevance in critical illness and anaesthesia.* J Saudi Heart Assoc, 2012. **24**(2): p. 99-121.

153. Michalski, B., et al., *The differences in the relationship between diastolic dysfunction, selected biomarkers and collagen turn-over in heart failure patients with preserved and reduced ejection fraction.* Cardiol J, 2016.

154. Alpert, M.A., J. Omran, and B.P. Bostick, *Effects of Obesity on Cardiovascular Hemodynamics, Cardiac Morphology, and Ventricular Function.* Curr Obes Rep, 2016.

155. Smiseth, O.A., *Assessment of ventricular diastolic function.* Can J Cardiol, 2001. **17**(11): p. 1167-76.

156. Chan, E., et al., *Exercise training in heart failure patients with preserved ejection fraction: a systematic review and meta-analysis.* Monaldi Arch Chest Dis, 2016. **86**(1-2): p. 759.

157. Bugger, H. and E.D. Abel, *Molecular mechanisms of diabetic cardiomyopathy.* Diabetologia, 2014. **57**(4): p. 660-71.

158. Roul, D. and F.A. Recchia, *Metabolic alterations induce oxidative stress in diabetic and failing hearts: different pathways, same outcome.* Antioxid Redox Signal, 2015. **22**(17): p. 1502-14.

159. Bonnefont-Rousselot, D., *Glucose and reactive oxygen species.* Curr Opin Clin Nutr Metab Care, 2002. **5**(5): p. 561-8.

160. Boudina, S., et al., *Mitochondrial energetics in the heart in obesity-related diabetes: direct evidence for increased uncoupled respiration and activation of uncoupling proteins.* Diabetes, 2007. **56**(10): p. 2457-66.

161. Shen, X., et al., *Protection of cardiac mitochondria by overexpression of MnSOD reduces diabetic cardiomyopathy.* Diabetes, 2006. **55**(3): p. 798-805.

162. Belke, D.D. and W.H. Dillmann, *Altered cardiac calcium handling in diabetes.* Curr Hypertens Rep, 2004. **6**(6): p. 424-9.

163. Dong, F., et al., *Impaired cardiac contractile function in ventricular myocytes from leptin-deficient ob/ob obese mice.* J Endocrinol, 2006. **188**(1): p. 25-36.

164. Belke, D.D., E.A. Swanson, and W.H. Dillmann, *Decreased sarcoplasmic reticulum activity and contractility in diabetic db/db mouse heart.* Diabetes, 2004. **53**(12): p. 3201-8.

165. Bhamra, G.S., et al., *Metformin protects the ischemic heart by the Akt-mediated inhibition of mitochondrial permeability transition pore opening.* Basic Res Cardiol, 2008. **103**(3): p. 274-84.

166. Williamson, C.L., et al., *Enhanced apoptotic propensity in diabetic cardiac mitochondria: influence of subcellular spatial location.* Am J Physiol Heart Circ Physiol, 2010. **298**(2): p. H633-42.

167. Baines, C.P., *The mitochondrial permeability transition pore and the cardiac necrotic program.* Pediatr Cardiol, 2011. **32**(3): p. 258-62.

168. Halestrap, A.P., *A pore way to die: the role of mitochondria in reperfusion injury and cardioprotection.* Biochem Soc Trans, 2010. **38**(4): p. 841-60.

169. Di Lisa, F. and P. Bernardi, *Mitochondria and ischemia-reperfusion injury of the heart: fixing a hole.* Cardiovasc Res, 2006. **70**(2): p. 191-9.

170. Di Lisa, F., et al., *The role of mitochondria in the salvage and the injury of the ischemic myocardium.* Biochim Biophys Acta, 1998. **1366**(1-2): p. 69-78.

171. Perrelli, M.G., P. Pagliaro, and C. Penna, *Ischemia/reperfusion injury and cardioprotective mechanisms: Role of mitochondria and reactive oxygen species.* World J Cardiol, 2011. **3**(6): p. 186-200.

172. Downey, J.M., *Free radicals and their involvement during long-term myocardial ischemia and reperfusion.* Annu Rev Physiol, 1990. **52**: p. 487-504.

173. Murphy, E. and C. Steenbergen, *Preconditioning: the mitochondrial connection.* Annu Rev Physiol, 2007. **69**: p. 51-67.

174. Murphy, E., et al., *Unresolved questions from the analysis of mice lacking MCU expression.* Biochem Biophys Res Commun, 2014. **449**(4): p. 384-5.

175. Kwong, J.Q., et al., *The Mitochondrial Calcium Uniporter Selectively Matches Metabolic Output to Acute Contractile Stress in the Heart.* Cell Rep, 2015. **12**(1): p. 15-22.

176. Bernardi, P., *The mitochondrial permeability transition pore: a mystery solved?* Front Physiol, 2013. **4**: p. 95.

177. Giorgio, V., et al., *Cyclophilin D modulates mitochondrial F0F1-ATP synthase by interacting with the lateral stalk of the complex.* J Biol Chem, 2009. **284**(49): p. 33982-8.

178. Giorgio, V., et al., *Dimers of mitochondrial ATP synthase form the permeability transition pore.* Proc Natl Acad Sci U S A, 2013. **110**(15): p. 5887-92.

179. Alavian, K.N., et al., *An uncoupling channel within the c-subunit ring of the F1FO ATP synthase is the mitochondrial permeability transition pore.* Proc Natl Acad Sci U S A, 2014. **111**(29): p. 10580-5.

180. Bonora, M., et al., *Role of the c subunit of the FO ATP synthase in mitochondrial permeability transition.* Cell Cycle, 2013. **12**(4): p. 674-83.

181. Di Lisa, F. and P. Bernardi, *Modulation of Mitochondrial Permeability Transition in Ischemia-Reperfusion Injury of the Heart. Advantages and Limitations.* Curr Med Chem, 2015. **22**(20): p. 2480-7.

182. Di Lisa, F., et al., *Mitochondria and reperfusion injury. The role of permeability transition.* Basic Res Cardiol, 2003. **98**(4): p. 235-41.

183. Bernardi, P., et al., *The mitochondrial permeability transition from in vitro artifact to disease target.* FEBS J, 2006. **273**(10): p. 2077-99.

184. Di Lisa, F. and P. Bernardi, *A CaPful of mechanisms regulating the mitochondrial permeability transition.* J Mol Cell Cardiol, 2009. **46**(6): p. 775-80.

185. Hausenloy, D.J., E.A. Boston-Griffiths, and D.M. Yellon, *Cyclosporin A and cardioprotection: from investigative tool to therapeutic agent.* Br J Pharmacol, 2012. **165**(5): p. 1235-45.

186. Morel, O., et al., *Pharmacological approaches to reperfusion therapy.* Cardiovasc Res, 2012. **94**(2): p. 246-52.

187. Ruiz-Meana, M., et al., *The role of mitochondrial permeability transition in reperfusion-induced cardiomyocyte death depends on the duration of ischemia.* Basic Res Cardiol, 2011. **106**(6): p. 1259-68.

188. Piot, C., et al., *Effect of cyclosporine on reperfusion injury in acute myocardial infarction.* N Engl J Med, 2008. **359**(5): p. 473-81.

189. Bernardi, P. and F. Di Lisa, *Cyclosporine before PCI in Acute Myocardial Infarction.* N Engl J Med, 2016. **374**(1): p. 89-90.

190. Murry, C.E., R.B. Jennings, and K.A. Reimer, *Preconditioning with ischemia: a delay of lethal cell injury in ischemic myocardium.* Circulation, 1986. **74**(5): p. 1124-36.

191. Hausenloy, D.J., et al., *Ischaemic conditioning and targeting reperfusion injury: a 30 year voyage of discovery.* Basic Res Cardiol, 2016. **111**(6): p. 70.

192. Miura, T. and M. Tanno, *The mPTP and its regulatory proteins: final common targets of signalling pathways for protection against necrosis.* Cardiovasc Res, 2012. **94**(2): p. 181-9.

193. Nishihara, M., et al., *Modulation of the mitochondrial permeability transition pore complex in GSK-3beta-mediated myocardial protection.* J Mol Cell Cardiol, 2007. **43**(5): p. 564-70.

194. Qiu, Y., et al., *Direct evidence that protein kinase C plays an essential role in the development of late preconditioning against myocardial stunning in conscious rabbits and that epsilon is the isoform involved.* J Clin Invest, 1998. **101**(10): p. 2182-98.

195. Baxter, G.F., et al., *Adenosine receptor involvement in a delayed phase of myocardial protection 24 hours after ischemic preconditioning.* Circulation, 1994. **90**(6): p. 2993-3000.

196. Xu, M., et al., *Calcium preconditioning inhibits mitochondrial permeability transition and apoptosis.* Am J Physiol Heart Circ Physiol, 2001. **280**(2): p. H899-908.

197. Yaguchi, Y., et al., *Protective effects of hydrogen peroxide against ischemia/reperfusion injury in perfused rat hearts.* Circ J, 2003. **67**(3): p. 253-8.

198. Miura, T., M. Tanno, and T. Sato, *Mitochondrial kinase signalling pathways in myocardial protection from ischaemia/reperfusion-induced necrosis.* Cardiovasc Res, 2010. **88**(1): p. 7-15.

199. Catalucci, D., et al., *Akt increases sarcoplasmic reticulum Ca2+ cycling by direct phosphorylation of phospholamban at Thr17.* J Biol Chem, 2009. **284**(41): p. 28180-7.

200. Ong, S.B., et al., *Akt protects the heart against ischaemia-reperfusion injury by modulating mitochondrial morphology.* Thromb Haemost, 2015. **113**(3): p. 513-21.

201. Zhang, J., et al., *ROS and ROS-Mediated Cellular Signaling.* Oxid Med Cell Longev, 2016. **2016**: p. 4350965.

202. Leslie, N.R. and C.P. Downes, *PTEN: The down side of PI 3-kinase signalling.* Cell Signal, 2002. **14**(4): p. 285-95.

203. Bijur, G.N. and R.S. Jope, *Rapid accumulation of Akt in mitochondria following phosphatidylinositol 3-kinase activation.* J Neurochem, 2003. **87**(6): p. 1427-35.

204. Ishihara, H., et al., *Pancreatic beta cell line MIN6 exhibits characteristics of glucose metabolism and glucose-stimulated insulin secretion similar to those of normal islets.* Diabetologia, 1993. **36**(11): p. 1139-45.

205. Landa, L.R., Jr., et al., *Interplay of Ca2+ and cAMP signaling in the insulin-secreting MIN6 beta-cell line.* J Biol Chem, 2005. **280**(35): p. 31294-302.

206. Robb, E.L., et al., *Selective superoxide generation within mitochondria by the targeted redox cycler MitoParaquat.* Free Radic Biol Med, 2015. **89**: p. 883-94.

207. Menazza, S., et al., *Oxidative stress by monoamine oxidases is causally involved in myofiber damage in muscular dystrophy.* Hum Mol Genet, 2010. **19**(21): p. 4207-15.

208. Di Lisa, F., et al., *Opening of the mitochondrial permeability transition pore causes depletion of mitochondrial and cytosolic NAD+ and is a causative event in the death of myocytes in postischemic reperfusion of the heart.* J Biol Chem, 2001. **276**(4): p. 2571-5.

209. Cali, B., et al., *Critical role of gap junction communication, calcium and nitric oxide signaling in bystander responses to focal photodynamic injury.* Oncotarget, 2015. **6**(12): p. 10161-74.

210. Antonucci, S., A. Tagliavini, and M.G. Pedersen, *Reactive oxygen and nitrogen species disturb Ca(2+) oscillations in insulin-secreting MIN6 beta-cells.* Islets, 2015. **7**(4): p. e1107255.

211. Schindelin, J., et al., *Fiji: an open-source platform for biological-image analysis.* Nat Methods, 2012. **9**(7): p. 676-82.

212. Belousov, V.V., et al., *Genetically encoded fluorescent indicator for intracellular hydrogen peroxide.* Nat Methods, 2006. **3**(4): p. 281-6.

213. Choi, H., et al., *Structural basis of the redox switch in the OxyR transcription factor.* Cell, 2001. **105**(1): p. 103-13.

214. Bilan, D.S. and V.V. Belousov, *HyPer Family Probes: State of the Art.* Antioxid Redox Signal, 2016. **24**(13): p. 731-51.

215. Inoue, M., et al., *Role of ATP decrease in secretion induced by mitochondrial dysfunction in guinea-pig adrenal chromaffin cells.* J Physiol, 2002. **539**(Pt 1): p. 145-55.

216. Canton, M., et al., *PUVA-induced apoptosis involves mitochondrial dysfunction caused by the opening of the permeability transition pore.* FEBS Lett, 2002. **522**(1-3): p. 168-72.

217. Petronilli, V., et al., *Transient and long-lasting openings of the mitochondrial permeability transition pore can be monitored directly in intact cells by changes in mitochondrial calcein fluorescence.* Biophys J, 1999. **76**(2): p. 725-34.

218. Wallach, D.F. and T.L. Steck, *Fluorescence Techniques in Microdetermination of Metals in Biological Materials. Ii. An Improved Method for Direct Complexometric Titration of Calcium in Small Serum Samples.* Anal Biochem, 1963. **6**: p. 176-80.

219. Chen, T.W., et al., *Ultrasensitive fluorescent proteins for imaging neuronal activity.* Nature, 2013. **499**(7458): p. 295-300.

220. Bond, J.M., B. Herman, and J.J. Lemasters, *Protection by acidotic pH against anoxia/reoxygenation injury to rat neonatal cardiac myocytes.* Biochem Biophys Res Commun, 1991. **179**(2): p. 798-803.

221. Matsuoka, R., et al., *Characteristics of death of neonatal rat cardiomyocytes following hypoxia or hypoxia-reoxygenation: the association of apoptosis and cell membrane disintegrity.* Heart Vessels, 2002. **16**(6): p. 241-8.

222. Bergmeyer, H.U. and E. Bernt, *Methods of Enzymatic Analysis*. 1974, Verlag Chemie, Weinheim, Germany. 607-612.

223. Bertram, R. and A. Sherman, *A calcium-based phantom bursting model for pancreatic islets.* Bull Math Biol, 2004. **66**(5): p. 1313-44.

224. Li, J., et al., *Oscillations of sub-membrane ATP in glucose-stimulated beta cells depend on negative feedback from Ca(2+).* Diabetologia, 2013. **56**(7): p. 1577-86.

225. Varadi, A. and G.A. Rutter, *Dynamic imaging of endoplasmic reticulum Ca2+ concentration in insulin-secreting MIN6 Cells using recombinant targeted cameleons: roles of sarco(endo)plasmic reticulum Ca2+-ATPase (SERCA)-2 and ryanodine receptors.* Diabetes, 2002. **51 Suppl 1**: p. S190-201.

226. Ermentrout, B., *Simulating, Analyzing, and Animating Dynamical Systems: A Guide to XPPAUT for Researchers and Students.* 2002, Philadelphia: SIAM Books.

227. Saybasili, H., et al., *Effect of mitochondrial electron transport chain inhibitors on superoxide radical generation in rat hippocampal and striatal slices.* Antioxid Redox Signal, 2001. **3**(6): p. 1099-104.

228. Rhee, S.G., *Cell signaling. H2O2, a necessary evil for cell signaling.* Science, 2006. **312**(5782): p. 1882-3.

229. Hassan, H.M., *Exacerbation of superoxide radical formation by paraquat.* Methods Enzymol, 1984. **105**: p. 523-32.

230. Birrell, J.A., M.S. King, and J. Hirst, *A ternary mechanism for NADH oxidation by positively charged electron acceptors, catalyzed at the flavin site in respiratory complex I.* FEBS Lett, 2011. **585**(14): p. 2318-22.

231. Buckman, J.F., et al., *MitoTracker labeling in primary neuronal and astrocytic cultures: influence of mitochondrial membrane potential and oxidants.* J Neurosci Methods, 2001. **104**(2): p. 165-76.

232. Zorov, D.B., M. Juhaszova, and S.J. Sollott, *Mitochondrial reactive oxygen species (ROS) and ROS-induced ROS release.* Physiol Rev, 2014. **94**(3): p. 909-50.

233. Rolo, A.P. and C.M. Palmeira, *Diabetes and mitochondrial function: role of hyperglycemia and oxidative stress.* Toxicol Appl Pharmacol, 2006. **212**(2): p. 167-78.

234. Di Lisa, F., et al., *Mitochondrial injury and protection in ischemic pre- and postconditioning.* Antioxid Redox Signal, 2011. **14**(5): p. 881-91.

235. Kokoszka, J., et al., *Increased mitochondrial oxidative stress in the Sod2 (+/-) mouse results in the age-related decline of mitochondrial function culminating in increased apoptosis.* Proc Natl Acad Sci U S A, 2001. **98**(5): p. 2278-2283.

236. Fauconnier, J., et al., *Effects of palmitate on Ca(2+) handling in adult control and ob/ob cardiomyocytes: impact of mitochondrial reactive oxygen species.* Diabetes, 2007. **56**(4): p. 1136-42.

237. Nguyen, T.T., et al., *Cysteine 203 of cyclophilin D is critical for cyclophilin D activation of the mitochondrial permeability transition pore.* J Biol Chem, 2011. **286**(46): p. 40184-92.

238. Wang, S.B., et al., *Redox regulation of mitochondrial ATP synthase.* Trends Cardiovasc Med, 2013. **23**(1): p. 14-8.

239. Bernardi, P., *Modulation of the mitochondrial cyclosporin A-sensitive permeability transition pore by the proton electrochemical gradient. Evidence that the pore can be opened by membrane depolarization.* J Biol Chem, 1992. **267**(13): p. 8834-9.

240. Petronilli, V., et al., *Physiological effectors modify voltage sensing by the cyclosporin A-sensitive permeability transition pore of mitochondria.* J Biol Chem, 1993. **268**(29): p. 21939-45.

241. Zorov, D.B., et al., *Reactive oxygen species (ROS)-induced ROS release: a new phenomenon accompanying induction of the mitochondrial permeability transition in cardiac myocytes.* J Exp Med, 2000. **192**(7): p. 1001-14.

242. Huser, J., C.E. Rechenmacher, and L.A. Blatter, *Imaging the permeability pore transition in single mitochondria.* Biophys J, 1998. **74**(4): p. 2129-37.

243. Dietel, M., et al., *Secondary combined resistance to the multidrug-resistance-reversing activity of cyclosporin A in the cell line F4-6RADR-CsA.* J Cancer Res Clin Oncol, 1994. **120**(5): p. 263-71.

244. Eisner, D., *Calcium in the heart: from physiology to disease.* Exp Physiol, 2014. **99**(10): p. 1273-82.

245. Fearnley, C.J., H.L. Roderick, and M.D. Bootman, *Calcium signaling in cardiac myocytes.* Cold Spring Harb Perspect Biol, 2011. **3**(11): p. a004242.

246. Yancey, D.M., et al., *Cardiomyocyte mitochondrial oxidative stress and cytoskeletal breakdown in the heart with a primary volume overload.* Am J Physiol Heart Circ Physiol, 2015. **308**(6): p. H651-63.

247. Bernardi, P., et al., *A mitochondrial perspective on cell death.* Trends Biochem Sci, 2001. **26**(2): p. 112-7.

248. Di Lisa, F., et al., *Mitochondria and vascular pathology.* Pharmacol Rep, 2009. **61**(1): p. 123-30.

249. Baynes, J.W., *Role of oxidative stress in development of complications in diabetes.* Diabetes, 1991. **40**(4): p. 405-12.

250. Kaludercic, N., S. Deshwal, and F. Di Lisa, *Reactive oxygen species and redox compartmentalization.* Front Physiol, 2014. **5**: p. 285.

251. Frustaci, A., et al., *Myocardial cell death in human diabetes.* Circ Res, 2000. **87**(12): p. 1123-32.

252. Dinarello, C.A., M.Y. Donath, and T. Mandrup-Poulsen, *Role of IL-1beta in type 2 diabetes.* Curr Opin Endocrinol Diabetes Obes, 2010. **17**(4): p. 314-21.

253. Mandrup-Poulsen, T., L. Pickersgill, and M.Y. Donath, *Blockade of interleukin 1 in type 1 diabetes mellitus.* Nat Rev Endocrinol, 2010. **6**(3): p. 158-66.

254. Yu, T., J.L. Robotham, and Y. Yoon, *Increased production of reactive oxygen species in hyperglycemic conditions requires dynamic change of mitochondrial morphology.* Proc Natl Acad Sci U S A, 2006. **103**(8): p. 2653-8.

255. Lagadic-Gossmann, D., et al., *Altered Ca2+ handling in ventricular myocytes isolated from diabetic rats.* Am J Physiol, 1996. **270**(5 Pt 2): p. H1529-37.

256. Daneman, D., *Type 1 diabetes.* Lancet, 2006. **367**(9513): p. 847-58.

257. Ning, G., *Decade in review-type 2 diabetes mellitus: At the centre of things.* Nat Rev Endocrinol, 2015. **11**(11): p. 636-8.

258. Tengholm, A. and E. Gylfe, *Oscillatory control of insulin secretion.* Mol Cell Endocrinol, 2009. **297**(1-2): p. 58-72.

259. Rosenthal, I., *Phthalocyanines as photodynamic sensitizers.* Photochem Photobiol, 1991. **53**(6): p. 859-70.

260. Hidalgo, C. and P. Donoso, *Crosstalk between calcium and redox signaling: from molecular mechanisms to health implications.* Antioxid Redox Signal, 2008. **10**(7): p. 1275-312.

261. Hausenloy, D., et al., *Transient mitochondrial permeability transition pore opening mediates preconditioning-induced protection.* Circulation, 2004. **109**(14): p. 1714-7.

262. Ramanathan, R.K., et al., *Phase 2 study of MK-2206, an allosteric inhibitor of AKT, as second-line therapy for advanced gastric and gastroesophageal junction cancer: A SWOG cooperative group trial (S1005).* Cancer, 2015. **121**(13): p. 2193-7.

263. Padmanabhan, S., et al., *A PP2A regulatory subunit regulates C. elegans insulin/IGF-1 signaling by modulating AKT-1 phosphorylation.* Cell, 2009. **136**(5): p. 939-51.

264. Ruan, H., et al., *Inducible and cardiac specific PTEN inactivation protects ischemia/reperfusion injury.* J Mol Cell Cardiol, 2009. **46**(2): p. 193-200.